The Dissertation Committee for Kristen Marie Koenig Certifies that this is the approved version of the following dissertation:

COMPLEX EYE FORMATION IN THE SQUID *DORYTEUTHIS PEALEII* AND ITS EVOLUTIONARY IMPLICATIONS

Committee:

Edward M. Marcotte, Supervisor

Jeffrey M. Gross, Co-Supervisor

Thomas Juenger

Harold Zakon

David Stein

COMPLEX EYE FORMATION IN THE SQUID *DORYTEUTHIS PEALEII* AND ITS EVOLUTIONARY IMPLICATIONS

by

Kristen Marie Koenig, B.A.

Dissertation

Presented to the Faculty of the Graduate School of

The University of Texas at Austin

in Partial Fulfillment

of the Requirements

for the Degree of

Doctor of Philosophy

The University of Texas at Austin

December 2015

Acknowledgements

There are so many I need to thank. I have been given so much, so freely, by so many during this process.

I would like to acknowledge the University of Texas, the Grass Foundation and the Marine Biological Labs for many funding opportunities. I need to acknowledge all the members of the Gross lab. You have been my teachers, my support and my friends throughout my graduate career. I would like to thank Eli Meyer for all his work on the generating sequencing libraries and guiding me into the world or bioinformatics. I would like to thank Peter Sun, an undergraduate who contributed to this work. You worked hard and stayed curious. I am indebted to the Developmental Biology community at the University of Texas, the members of which have been engaged and endlessly supportive of my work. I would like to thank Dr. Hans Hofmann for his support and mentorship.

I have been lucky to have an excellent committee: Dr. Edward Marcotte, Dr. David Stein, Dr. Tom Juenger, and Dr. Harold Zakon. They have all been generous with their time, their support and their ideas.

I would like to thank my advisor, Dr. Jeffrey Gross who has been interminably patient, trusting, kind and supportive of me.

I would like to thank my family, my friends and Trey. I would be lost without you all.

Thank you.

COMPLEX EYE FORMATION IN THE SQUID *DORYTEUTHIS PEALEII* AND ITS EVOLUTIONARY IMPLICATIONS

Kristen Marie Koenig, Ph.D.

The University of Texas at Austin, 2015

Supervisor: Edward M. Marcotte

Co-Supervisor: Jeffrey M. Gross

Photoreception is a ubiquitous sensory ability found across the Metazoa, and photoreceptive organs are intricate and diverse in their structure. While the morphology of the compound eye in *Drosophila* and the single-chambered eye in vertebrates have elaborated independently, the amount of conservation within the "eye" gene regulatory network remains controversial with few taxa studied. To better understand the evolution of photoreceptive organs, we established the cephalopod, *Doryteuthis pealeii,* as a Lophotrochozoan model for eye development. Utilizing histological, transcriptomic and molecular assays we characterize eye formation in *Doryteuthis pealeii*. Through lineage tracing and gene expression analyses, we demonstrate that cells expressing Pax and Six genes incorporate into the lens, cornea and iris. Functional assays demonstrate that Notch signaling is required for photoreceptor cell formation and retina organization. This comparative approach places the canon of eye research in traditional models into perspective, highlighting complexity as a result of conserved or convergent mechanisms.

Table of Contents

List of Tables

List of Figures

Chapter 1: Introduction to eye evolution and development in the Metazoa

1.1: PHOTORECEPTIVE ORGAN DIVERSITY

In *On the Origin of Species*, Darwin marveled at the capacity of natural selection to produce the eye as an "organ of extreme perfection and complication." It is the exacting intricacy of photoreceptive organs that provides an elegant system to study the emergence of complex systems, both molecularly and morphologically. The capacity for photoreception is a sensory tool that evolved early in the Metazoa (Schnitzler, 2012). The extent of this capacity ranges from single photoreceptor cells, pigmented eyespots and cups, to complicated organs that focus, reflect and absorb light to resolve images (Land and Fernald, 1992). In the Bilateria, high-resolution vision is known to have evolved in only a few animal groups including vertebrates, arthropods and cephalopods (Nilsson, 2013). The arthropod eye is a compound eye composed of many individual ommatidial units containing multiple photoreceptor cells and a lens. Both the vertebrate and the cephalopod eye are single-chambered, with a single lens at the anterior of the eye and a cup shaped retina in the posterior. Despite the use of a homologous optical strategy, these two eye structures have independently evolved (Fernald, 2006).

There are multiple types of optics exist within the Metazoa. These optical strategies can be broken into two main categories: the chambered eyes and the compound eyes (Fernald, 2006). Examples of the three chambered-eyes include the nautilus pit-eye, the lens containing chambered eyes of cephalopods and vertebrates, and finally the mirror-containing eye of scallops. The four compound-type eyes can be seen in the

simple compound eye of the bivalve mollusks, the apposition compound eye of many arthropods including *Drosophila*, the reflecting superposition eye (found in moths) or the refracting superposition eye (found in lobster).

To construct these complex image-forming eyes, three specific tissues are functioning together to form an operative photoreceptive organ: the photoreceptor cell, the pigment cell and the lens.

1.1.1: Photoreceptor cells

Many types of light responsive photo pigments and molecular response mechanisms have been discovered. These light-responsive mechanisms have been found both contained within photoreceptive organs as well as found diffusely and dispersed across an organism's body, presumably for a non-directional light sensitivity (Oakley, 2015). The field of non-visual photo pigments is recently garnering momentum, but the most understood light responsive mechanism within photoreceptive organs remains the opsin photo pigments and their associated signal transduction.

Two primary opsin types are found in the Metazoa, ciliary and rhabdomeric. These two opsins are associated with two types of photoreceptor cell types with different strategies to expand their cell membrane (Fain, 2010). Photoreceptor cells require an expanded membrane to house their abundance of membrane bound photo pigments. This expansion is accomplished by either modifying the cilium or by microvilli. These two photoreceptor types and photo-pigments are homologous, but diversified before the Urbilaterian ancestor. The signal transduction cascade downstream of these opsin families also differs. Both opsins and photoreceptor cell types are found in protostomes

and Deuterostomes. Rod and cone photoreceptors found in the vertebrate retina are of the ciliary type and express C-opsins. At the same time, a subset of retinal ganglion cells found in the vertebrate retina express the rhabdomeric opsin, melanopsin. The *Drosophila* eye is comprised of rhabdomeric photoreceptor cells but the annelid worm *Platynereis drumerii* has both ciliary and rhabdomeric photoreceptor cells.

The only photoreceptor cell type identified in the cephalopod is rhabdomeric expressing a rhodopsin. However, recent studies have identified a ciliary opsin in transcriptomic sequence in the species *Idiosepius paradoxus*. Furthermore, alternate photosensitive pigments such as retinochrome have been identified and their protein expression has been detected in the adult retina of the squid *Doryteuthis pealeii* (Yoshida, 2015; Kingston, 2015).

1.1.2: Pigment cells

For a simple opsin-expressing cell to sense directionality of a light source, an accompanying dark pigment must be present (Vopalensky, 2009). These screening pigments are essential to the functionality of all complex eyes. In the vertebrate retina, this pigment is found in the Retinal Pigmented Epithelium, which surrounds the photoreceptor cell layer with apical extensions containing melanin filled melanosomes. Cnidarian photoreceptive organs also use melanin. In *Drosophila,* each ommatidium contains several pigment cells that express both ommachrome and pterin. In the Lophotrochozoa, both melanin and ommachrome are found in photoreceptive organs, but ommachrome is the only pigment found in the cephalopod retina to date. These pigment generation pathways are very ancient but because of the diversity of pigments used in

photoreceptive organs across the Metazoa, they appear to have been associated with photoreception independently (Oakley, 2015).

1.1.3: The lens

Eyespots and cups abound in the animal kingdom but are only able to convey very basic information. One of the unique features of complex image-forming eyes is the lens. The lens enables the collection of a larger amount of visual information and better resolution of an image. The vertebrate lens is generated from a placode of surface ectodermal tissue. The placode cells thicken, generate a vesicle, eventually these cells elongate and form onion-like layers, stretching anterior to the posterior of the lens. Lens cells ultimately degrade their nuclei and the majority of their organelles and become packed with high concentrations of Crystallin proteins (Bibliowicz, 2011). The *Drosophila* lens is generated from the eye imaginal disc tissue. After the photoreceptor cells of the ommatidia differentiate, four lens secreting cells or cone cells differentiate. The *Drosophila* lens is secreted through microvillar projections of the cone cells. The lens is acellular and filled with Crystallin (Charlton-Perkins, 2011).

The Crystallin group of proteins are polyphyletic and often have other functions in the animal outside of the lens. **α**-Crystallin expressed in all vertebrate lenses is a small heat shock protein while **ε**-Crystallin expressed in only birds and crocodiles is a lactate dehydrogenase (Piatigorsky, 2007). Crystalins in the cubazoan jellyfish eye are homologs to saposin and Crystallins in the Cephalopod lens are glutathione S-transferase homologs. All these metabolic enzymes and stress proteins share the feature that they are highly soluble and will remain in solution at high concentrations. Solubility is essential to

maintain consistency, which enables a reduction of light scatter and a gain in refractive power (Piatigorsky, 2003). Overall, similar to the pigment type found in the pigment cells, these lens-associated proteins have also been wedded to photoreceptive organs independently.

1.2: RETINA DETERMINATION NETWORK

The incredible diversity in eye shape and photoreceptor cell structure in animals led Salvini-Plawen and Mayr to originally conclude that the eye had evolved independently 40 to 65 times (Salvini-Palwen and Mayr, 1977). With the expansion of molecular tools, however, extensive genetic analysis in *Drosophila* and vertebrates has shown that many orthologous genes and signaling pathways are necessary for eye formation. The Pax-Six-Eya-Dach network (Retina Determination Network or RDN) has been extensively discussed as occupying the nexus of this genetic homology. *Eyeless*, *twin of eyeless* (Pax6 ortholog), *sine oculis* (Six1 and Six2 ortholog), *eya*, and *dac* (Dach ortholog) are all necessary for eye development in *Drosophila* (reviewed in Kumar, 2010). They each can also induce ectopic eye formation when mis-expressed in the antennal imaginal disk. In vertebrates, Pax6, Six3 and Six6 (*optix* homologs), Eya1, Eya2, Eya3 and Dach1 are each known to play a role in eye development. Among these, Pax6, Six3 and Eya3 can also induce ectopic retina and lens formation when mis-expressed in vertebrates (Reviewed in Tomarev, 1997; Arendt, 2003; Nilsson, 2004; Kumar, 2010; Wagner, 2014).

1.3: *DROSOPHILA* EYE DEVELOPMENT

As described above, the *Drosophila* retina is composed of about 750-800 individual ommatidial units. These units are identical to the others, each containing 8 photoreceptor cells (R1-R8), and 12 lens-secreting cone cells and pigment cells. All the ommatidia are hexagonal and arrayed in a crystalline lattice. The *Drosophila* eye forms from the eye imaginal disk in the larvae of the fly. The disk remains undifferentiated until the final instar larval stage when pattern formation is initiated.

Differentiation follows the passing of the morphogenetic furrow, a constriction of the imaginal disk epithelium, that moves in a wave across the disk. The furrow starts on the posterior side of the disk, sweeping to the anterior, leading to the sequential differentiation of the individual photoreceptor cells starting with R8, followed by R5 and R2 differentiating together, then followed by R3 and R4 together, R1 and R6 together, and ending in R7. After photoreceptor differentiation, pigment and cone cells differentiate and the structure of the ommatidia elongates to its final form (Kumar, 2010). As the furrow is moving through the disk, four different states of differentiation exist in the disk. Cells far anterior of the furrow are completely undifferentiated, proliferative and expressing *Wingless* (Bao, 2010). Cells just anterior to the furrow are pre-proneural and are beginning to express RDN genes such as *Eya*, *So* and *Dach*. Cells in the furrow are proneural and express the marker *Atonal*. Finally, cells posterior to the furrow are differentiated and expressing photoreceptor cell markers including *Spitz* and assembling into ommatidia.

1.4: VERTEBRATE EYE DEVELOPMENT

The vertebrate retina is composed of five neural cell types (photoreceptor cells, bipolar cells, amacrine cells, horizontal cells, and retinal ganglion cells) and one glial cell type (Müller glia). The posterior retina is surrounded by the Retinal Pigmented Epithelium and the anterior segment of the eye contains the lens, cornea and iris tissue. The vertebrate eye arises from the developing forebrain shortly after neurulation. The developing diencephalon evaginates to form the two optic vesicles (Lamb, 2007). Each of these vesicles invaginate to form optic cups. A gap is formed on the ventral side of the optic cup and the two sides of the developing neural retina must fuse at the choroid fissure.

The optic cup undergoes waves of cell differentiation to form the layers of the retina. The first cells to differentiate are the retinal ganglion cells. These cells are the most anterior layer in the retina and their axons exit the retina in a bundle and form the optic nerve, synapsing on the optic tectum in fish and amphibians, and parts of Lateral Geniculate Nucleus and then visual cortex in mammals. The next wave of differentiation leads to the cone photoreceptors, horizontal cells and most of the amacrine cells. The last cells to differentiate are the bipolar cells, the Müller glia and the rod photoreceptor cells (Basset, 2012).

As mentioned above, the lens is formed from surface ectodermal tissue abutting the optic vesicle after forebrain evagination. The vesicle sends inductive signals to the surface ectoderm, leading to lens placode formation. In turn, the lens placode induces neural differentiation in the retina. In mammals, the lens placode cells elongate and invaginate to form the lens pit. The sides of the pit fuse and form the lens vesicle and the new overlying surface ectoderm and presumptive cornea tissue (Gunhaga, 2011).

1.5: THE MOLECULAR UNDERPINNINGS OF EYE FORMATION

Pax and Six underlie the gene regulatory network at the initiation of eye development, but they also serve additional roles in the eye during later stages of eye formation. For example, during optic cup formation in vertebrates, Pax6 and Pax2 establish opposing territories between proximal (optic stalk) and distal (retinal) aspects of the optic vesicle (Schwarz, 2000). Pax6 and Six3 function in lens placode induction in vertebrates (Reviewed in Oingo, 2012; Cvekl, 2014). Pax6 and Prox1 (*Pros* homolog) are involved in fiber cell elongation and Crystallin regulation in the vertebrate lens (Dyer, 2003). Prox1 also plays a role in promoting horizontal cell formation and regulating cell proliferation in the retina. In *Drosophila*, *dPax2* and *Pros* are required for specification of lens-forming cells and for *Crystallin* expression (Charlton-Perkins, 2011). *Pros* also dictates R7/R8 photoreceptor cell fate in the *Drosophila* retina (Cook, 2003). Pax, Six and Prospero orthologous genes function in many cell types and contexts even within retina and lens development across species. It also appears that in some cases these genes have evolved a convergent function.

The Notch signaling pathway also plays multiple essential roles during retina and lens formation in vertebrates and *Drosophila*. Notch is necessary for regulating cell cycle progression within retina and lens progenitor cells, and regulation of Notch activity is necessary for maintenance of progenitor populations (Livesey, 2001; Charlton-Perkins, 2011). In vertebrates, retinal progenitor cells deficient in Notch signaling prematurely exit the cell cycle which results in a smaller retina and a higher proportion of early born cell types (Tomita, 1996; Dorsky et al., 1997). In *Drosophila*, the loss of Notch signaling

reduces antennal disk proliferation and can lead to loss of the eye (Go, 1998). Notch also regulates photoreceptor cell fate and ommatidia polarity (Blair, 1999).

1.6: SUMMARY

When we look at the diversity in the structure, details of cell type and developmental mechanism, the eye appears independently evolved across the Metazoa. However, the extensive amount of molecular similarity has led many to conclude that all photoreceptive organs have a shared ancestry (Halder, 1995; Gehring, 1996,1999, 2005; Tomarev, 1997). Conversely, others suggest that despite the inclusion of the same gene families, the regulatory networks underlying eye development in vertebrates and *Drosophila* are fundamentally different in their connectivity, and are therefore likely to have evolved independently (Wagner, 2014). To address the homology of photoreceptive organs in the Bilateria and to better recognize the novelty found in each of these systems it is necessary to understand the regulatory and transcriptional relationship of genes within these networks in taxa beyond *Drosophila* and a few, select vertebrate models. The Lophotrochozoa can shed light on shared molecular mechanisms during organ formation and illuminate the conservation of shared regulatory modules. The Lophotrochozoa also show greater genomic conservation relative to vertebrates and therefore can be more enlightening in regards to the Urbilaterian ancestor relative to the most widely studied Ecdysozoan species (Simakov, 2013). To better understand the evolution of complexity in the visual system across the Bilateria, we propose the squid *Doryteuthis pealeii* as a model for complex eye development in the Lophotrochozoa. The following work is an in depth description of eye development in the squid using multiple

methodological approaches. Furthermore, this work expands on its descriptive foundation to test functional hypotheses regarding gene regulatory network evolution and cell signaling and cell behavior.

Chapter 2: Morphogenesis, growth and pattering of the cephalopod eye

2.1: THE SQUID *DORYTEUTHIS PEALEII* AS A MODEL FOR EMBRYOLOGY

The cephalopod has long been the interest of researchers for their amazing behaviors, complex neuroanatomy, unusual body plan and interesting taxon specific novelties. To date, the cephalopod research community has suffered from the inability to raise species in the lab with any practicality, limiting the molecular and genetic potential and leading most researchers to study local species. For our work, we have chosen the squid *Doryteuthis (Loligo) pealeii*. *Doryteuthis pealeii* is widely available on the Eastern seaboard of the United States and is fished commercially. Embryos are available during the summer months when the adults migrate close to shore. The Marine Biological Labs provide extensive access to marine species from off the coast of Massachusetts for the research community. The MBL has been a consistent source for *Doryteuthis* embryos throughout my dissertation work.

Doryteuthis pealeii eggs are fertilized externally by males who place sperm packets in the female mantle (Jacobson, 2005). Females store sperm resulting in single egg sacks with multiple paternity. Females lay eggs in egg sacks, also referred to colloquially as fingers, containing 100-250 embryos per sack. Each embryo resides in a chorion and wrapped in a string of coiled mucus inside the sack. Females lay eggs over the course of multiple weeks and will die shortly after reproducing. Many individual females lay egg sacks in the same location at the same time resulting in a multi-egg-sack pile, referred to as a mop. Tens of thousands of embryos can be in any such mop. At the time of oviposition, all embryos are synchronous in their development.

2.2: INTRODUCTION TO CEPHALOPOD DEVELOPMENT AND ORGANOGENESIS

Cephalopods have the largest and most complex invertebrate nervous system known and *Doryteuthis pealeii* has long been the subject of neurobiology and neurophysiology research (e.g. Hodgkin, 1949,1952a, 1952b, 1952; Vale, 1985a, 1985b; Brady, 1982; Allen 1982). Adult neuroanatomy of multiple cephalopod species has been well detailed (Young, 1962a, 1962b, 1971; Nixon and Young, 2003). Despite these elegant studies, only a handful of investigations of gene expression patterns have been reported during development and detailed molecular and genomic analyses of cephalopod organogenesis are in their infancy (Hartmann, 2003; Lee, 2003; Baratte, 2007; Navet, 2009; Buresi, 2012; Peyer, 2014; Wollesen, 2014; Yoshida, 2014; Shigeno, 2015). The cephalopod eye is a single-chambered eye generated from an internalization of the optic placode (Gilbert, 1990). The single lens is produced by populations of specialized lentigenic cells and is located at the anterior of the eye; the retina, composed of rhabdomeric photoreceptor cells and a support cell layer, is located at the posterior of the eye (Zonana, 1961; West 1994, 1995). Photoreceptor outer segments are arrayed anteriorly and thus, are the first region of the retina to be exposed to light. This differs from the vertebrate retina where light must traverse through the retina prior to interacting with photoreceptors. In the cephalopod, as a result of this architecture, photoreceptor nuclei are located at the posterior of the retina, and photoreceptor axons form a plexiform layer at the posterior-most region of the retina, exiting the eye and synapsing directly on the optic lobe (Young, 1971). Several morphological descriptions of eye development in various cephalopod species have been documented, but an in-depth molecular and

cellular understanding of major morphogenetic and cell differentiation events is lacking (Arnold, 1965, 1966, 1967, 1976; Gilbert, 1990; Marthy, 1973; Yamamoto, 1985a, 1985b; Naef, 1928).

2.3: FLUORESCENT STAGING SERIES

To provide a foundation on which to build a molecular and cellular understanding of eye development in *D. pealeii*, it was first necessary to generate a detailed histological description of key events in eye formation. All staging nomenclature follows that originally described by John Arnold (Arnold, 1965) (Fig. 1). Eye development commences at Stage 16 with the eyes forming from bilateral placodes, or groups of condensed cells, shortly before epiboly is complete (Fig.1). These placodes are then internalized to form the optic vesicles (Fig. 2). Internalization initiates at Stage 18 when a lip of cells forms around the periphery of the placode, and the lip progressively extends over the placode, fusing centrally at Stage 21 (Gilbert, 1990; Marthy, 1973). At Stage 19 the medial and lateral are present and the placode tissue has organized into a pseudostratified neuroepithelium. Apical divisions are apparent at this stage. At Stage 21, vesicle fusion occurs and F-actin enrichment can be observed at the fusion site. Once the vesicle is closed, the eye continues to grow and the retina begins to curve. At Stage 23, cells at the anterior of the vesicle begin to differentiate into three distinct populations of lentigenic cells that project cellular processes forming the segmented extracellular lens (Arnold, 1967; West, 1995). These cells have a distinct nuclear architecture and are enriched in filamentous actin. The plexiform layer within the optic lobe tissue is also apparent at this stage. At Stage 25, the lens has formed into a teardrop shape and the

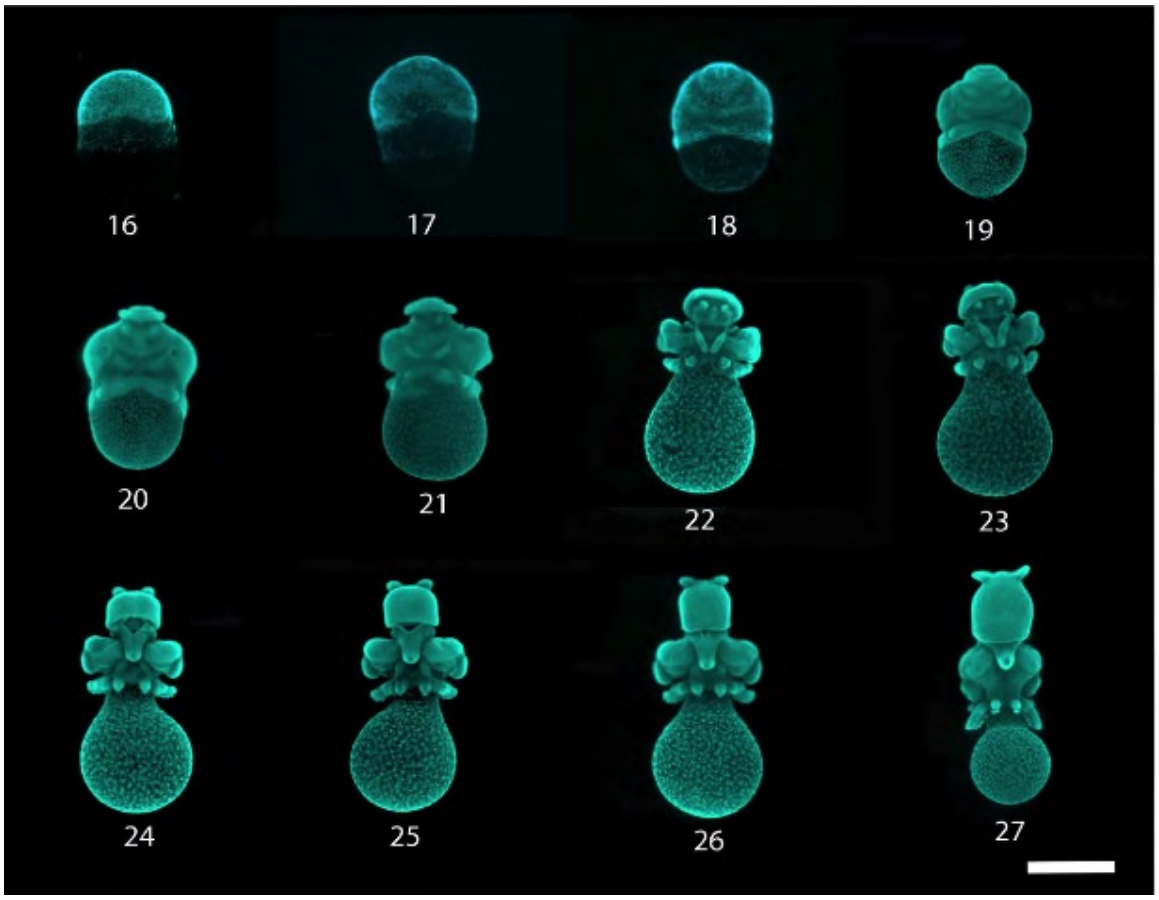

Figure 1: Embryonic Stages and Transcriptome
Sytox-Green stained *Doryteuthis pealeii* embryos from Stages 16-27 as defined by John Arnold (Arnold, 1965). Embryos are shown from the posterior. Each of these stages was sequenced to generate a whole-embryo transcriptome. Eye and optic lobe tissue were also dissected and sequenced at stages 19, 21, 23, 25, and 27. Scale bar = 1000um

lentigenic cells are obvious. F-actin enrichment in the apical side of the retina suggests outer-segment formation of the photoreceptor cells at this stage. At hatching (post-Stage 29), the retina is primarily composed of two cell types: photoreceptors and glial-like support cells (Young, 1971). Between Stage 18 and Stage 26, the neuroepithelium appears as a single layer with no obvious morphological distinction between photoreceptors and glial-like cells. However, at Stage 27 photoreceptor nuclei in the posterior retina begin to segregate to the basal side, behind the basal membrane (Yamamoto, 1985). Photoreceptors penetrate the basal membrane, extending through the support cell layer and forming outer segments on the apical side of the retina. Outer segments are prominently labeled with phalloidin, indicative of high concentrations of F-Actin. Photoreceptors synapse directly on the optic lobe, where visual processing takes place (Young, 1971). At these later Stages, 28 and 29, vasculature can also bee seen throughout the retina. At hatching (Stage 29 and 30), the eye is fully functional (Gilbert, 1990).

2.4: STAGED CELL PROLIFERATION SERIES

The apical side of the retinal neuroepithelium faces anteriorly, and progenitor cells consistently undergo mitosis on the apical side of the retina (Fig. 2, 3), similar to neuroepithelia in other organisms (Baye, 2008). We were curious if there was a pattern of progenitor cell cycle exit in the squid retina, as there is in vertebrates and *Drosophila*. Utilizing BrdU incorporation assays (three hour exposures and immediate fixation), we determined the pattern of proliferation and cell cycle exit during retina formation. All cells of the Stage 19 to Stage 25 retina incorporate BrdU (Fig. 4). At Stage 25, it is

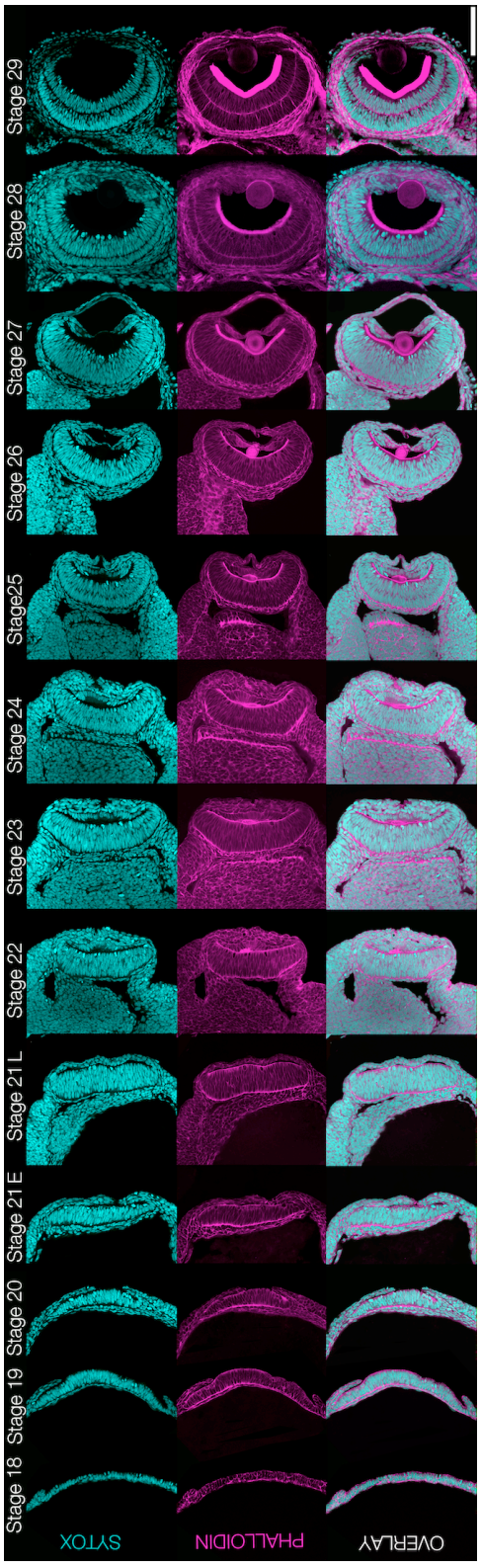

Figure 2: Staging Series of Eye Development

Morphogenesis of the developing eye, stages 18-29 in cross-section, stained for DNA (Sytox-Green) and F-Actin (Phalloidin). Anterior of the animal is up. Stage 18: The placode has formed and the lateral edge of the lip is present. Stage 19: The medial and lateral sides of the lip are present and the placode neuroepithelium has formed. Stage 20: The lips of the placode are close to fusing and apical cell divisions are obvious in the retina. Stage 21 Early: The placode lips fuse forming the optic vesicle. F-actin enrichment is observed at the fusion site. Stage 21 Late: The optic lobe is apparent and the pseudostratified epithelium of the retina has grown along the apical-basal axis. Stage 22: The retina begins to curve and the first evidence of the lens is apparent. Stage 23: The plexiform layer in the optic lobe is apparent. Stage 24: Lentigenic cell morphology becomes obvious. Stage 25: The lens has grown and is teardrop shaped, the cornea is apparent and F-Actin enrichment on the apical side of the retina suggests the initiation of outer segment formation from the photoreceptor cells. Stage 26: F-Actin accumulation in the lentigenic cells, and the anterior and posterior lens segments are obvious. Stage 27: The basal membrane in the retina begins to form and the photoreceptor nuclei segregate themselves at the posterior of the retina. Stage 28: The basal membrane spans the width of the retina and a layer of photoreceptor cell nuclei line the entire posterior retina. Vasculature is also present. Stage 29: The lens is round and the photoreceptor cell layer has grown significantly. Photoreceptor outer segments are substantial and highly enriched with F-Actin. The eye is functional at hatching (stage 29 or 30). Scale bar = 50um

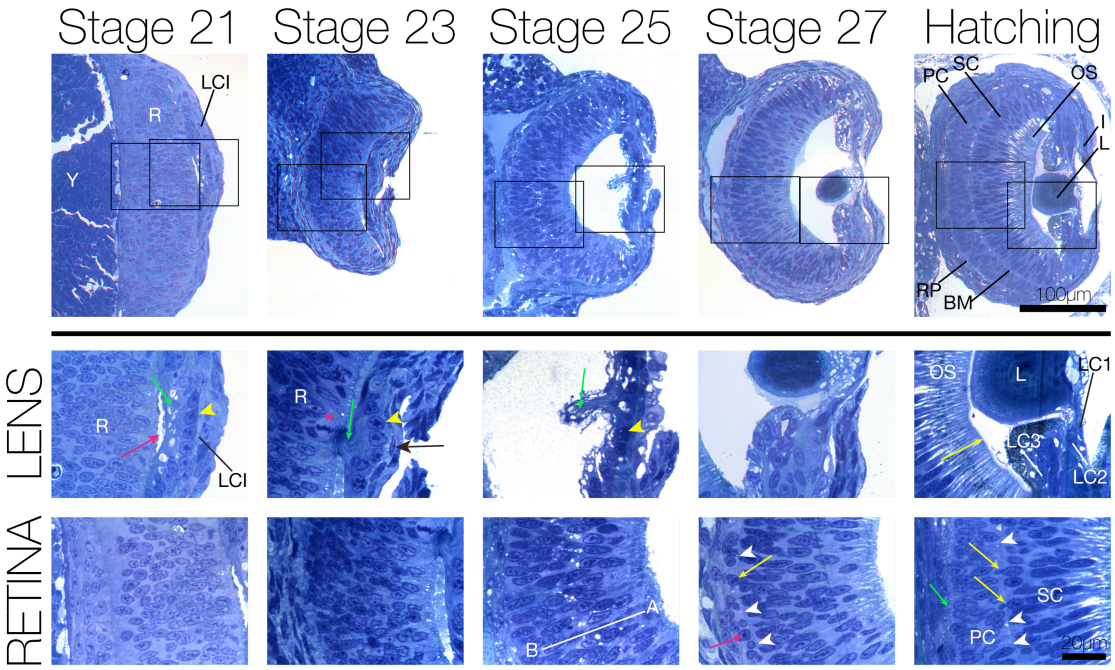

Figure 3: Histological Staging Series
Toluidine blue stained staging series. Boxed regions are high-magnification images of developing lens and retina shown below each stage. Stage 21 Lens: Yellow Arrowhead: Lentigenic cells, Green Arrow: Lentigenic cell processes, Pink Arrow: Formation of vitreous cavity. Stage 23 Lens: Pink Asterisk: Mitotic cell on the apical side of the retina, Black Arrow: Primary lentigenic cells, Yellow Arrowhead: Secondary lentigenic cells, Green Arrow: Lentigenic cell processes. Stage 25 Lens: Yellow Arrowhead: Secondary lentigenic cells, Green Arrow: Lentigenic cell processes and developing lens. Stage 25 Retina: Apical (A) and Basal (B) axis is labeled. Stage 27 Retina: Pink Arrow: Newly born photoreceptor cell nuclei, White Arrowheads: Basal membrane, Yellow Arrow: Nucleus crossing the basal membrane. Hatching Lens: Yellow Arrow: Limiting membrane. Hatching Retina: White Arrowheads: Basal membrane, Yellow Arrows: Nuclei crossing the basal membrane, Green Arrow: Retina Plexiform Layer. *A: Apical side of the neuroepithelium, B: Basal side of the neuroepithelium, BM: Basal membrane, I: Iris, L: Lens, LC1: Primary lentigenic cells, LC2: Secondary lentigenic cells, LC3: Tertiary lentigenic cells, LCI: Lens, Cornea and Iris, OS: Outer segment (also known as Distal Segment) containing photoreceptor cell outer-segment and support cell layer cellular extensions, PC: Photoreceptor cell nuclear layer, R: Retina, SC: Support Cell layer, Y: Yolk.* Scale on low magnification images = 100um, Scale on high magnification images = 20 um

apparent that labeled cells are segregated either apically or basally, supporting the idea that cells are going through S phase basally and migrating swiftly to the apical side to go through M phase. At Stage 27, once photoreceptor nuclei have migrated to the posterior retina behind the basal membrane, they no longer incorporate BrdU, suggesting that they are no longer proliferative (Fig. 4). Interestingly, the support cell layer continues to incorporate BrdU until at least two days post-hatching (Fig. 4). Nuclei are observed crossing from one side of the basal membrane to the other (Fig. 2); however, without *in vivo* tracking, it is unknown whether these nuclei move apical to basal across the basal membrane (i.e. from support cell layer to the photoreceptor cell layer) or vice versa. Given the lack of BrdU incorporation by nuclei on the photoreceptor side of this membrane, and the rapid growth of this layer, it is likely that newly generated photoreceptor cells that arise from the support cell layer may be crossing this membrane.

2.5: STAGED APOPTOSIS SERIES

Apoptosis is an important contributor in both vertebrate and *Drosophila* eye formation. In vertebrates, at early stages of optic cup formation, programmed cell death occurs in the ventral optic vesicle, cup and retina during morphogenesis (Lang, 1997). In the surface ectoderm program cell death occurs in the ventral lens placode and is also necessary for proper lens vesicle formation. Developing vasculature in the vertebrate retina undergoes apoptosis during refinement, and the vertebrate lens cells also show apoptotic markers as they degrade their nuclei and organelles to become optically clear.

In *Drosophila* cell death occurs in the developing imaginal disk at multiple stages. This process eliminates peripheral ommatidia as well as supernumerary cells that have

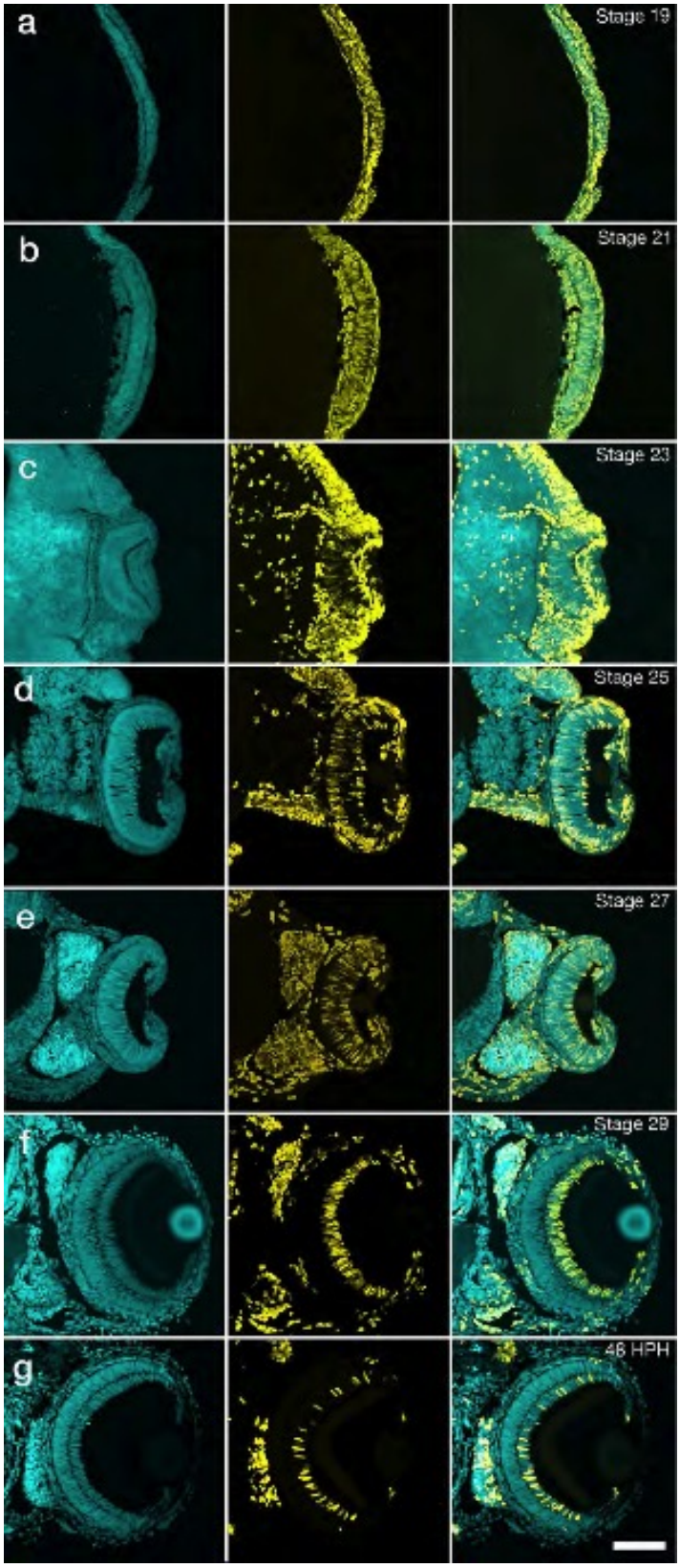

Figure 4:
BrdU Incorporation Assays Reveal Spatial Patterns of Cell Proliferation During Retina Development
Sytox-Green (DNA) left column, BrdU (yellow) middle column, overlay right column. Embryos were pulsed with BrdU for 3 hours and immediately fixed. A), B, C) BrdU incorporation is detected broadly throughout the entire retina at Stages 19, 21, and 23. D) BrdU incorporation begins to become segregated to the apical and basal sides of the epithelium. E) Photoreceptor cell nuclei located behind the basal membrane no longer incorporate BrdU. F) Support cells continue to incorporate BrdU. Cells within the lens and iris also incorporate BrdU. G) Two days post-hatching, the support cell layer continues to incorporate BrdU, as do the lentigenic cells. Scale = 50um

not been included into the ommatidial lattice (Bonini, 1997). The regulation of apoptotic signals is key during eye formation and mis-regulation can lead to widespread cell death or extra neural, pigment or cone cells distributed throughout the retina.

We were interested if cell death played a critical role in eye morphogenesis in the squid. We performed a staged study of apoptosis using TUNEL as a marker for cell death. Interestingly, these surveys for apoptosis do not reveal an appreciable level of apoptotic cells during cephalopod eye development (Fig. 5).

2.6: DISCUSSION

This is the most in-depth study of organogenesis in any Lophotrochozoan species to date and opens the door to new questions regarding the evolution of complexity and organ formation. We can see in our data that the eye is internalized and does not invaginate similar to placode development in other vertebrate species. We also have described the first pseudostratified neuroepithelium observed in the Lophotrochozoa. The existence of such a neuroepithelial tissue has previously been linked to the formation of neuro-complexity in vertebrates and specific to the vertebrate lineage. We now can address questions regarding the nature of neural differentiation in a neuroepithelium, asymmetric division and delamination in the cephalopod. Using the squid eye as an entry point into the complex nervous system of cephalopods, we can evaluate whether complexity relies upon the same mechanisms in across the Bilateria.

Furthermore, we have also identified new characters of the support cell layer in the cephalopod retina. Our data suggest that the support cell layer may be a proliferative

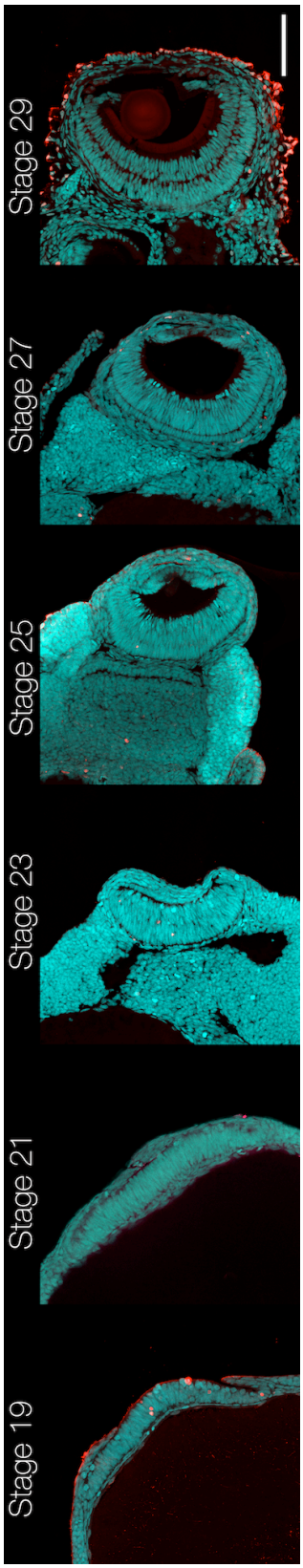

Figure 5: Staged TUNEL assays
Stages 19, 21, 23, 25, 27 and 29 TUNEL assay. Sytox-Green labeled DNA (cyan) and TUNEL (red) overlaid images. Few TUNEL^{+} cells are detected at any time point indicating that apoptosis does not likely play a significant role during eye morphogenesis. Red cells at Stage 29 are in the dermal tissue and this is likely background from the developing iridophores.

progenitor population that could be essential to the growth of the retina during the paralarval stage. Further experiments are necessary to truly determine whether support cells incorporate into the photoreceptor cell layer, however this discovery could have implications about regeneration in cephalopods and the maintenance of a retinal stem cell population.

Finally, we have identified morphological markers for development in a tightly timed series so that we can understand the process of cell differentiation and morphogenesis thoroughly. As we begin investigations that perturb these processes, it is necessary to have an in-depth understanding of what occurs in a wild-type case.

Chapter 3: Lineage tracing of the eye placode and surrounding tissue

Very little is known currently about the early cell fates in the cephalopod. No early cell lineage has been performed to date. We were interested in understanding the terminal fates of cells in the developing eye field at early stages. To better identify these cell fates, we performed a linage tracing study. These data will ultimately be used as a tool to better understand cell movement and morphogenesis, as well as properly interpret gene expression studies from these early stages. Such a cell lineage map is also necessary for any transplantation experiment and local transfection techniques.

3.1: Experimental Design

To perform this series of experiments we designed a lineage tracing study utilizing the fixable lipophilic dye, DiI (Fig. 6). We dissolved the dye in vegetable oil and labeled populations of cells at Stage 18. We labeled the placode in multiple regions as well as tissue surrounding the placode. We generated a map to ensure adequate coverage across the placode, labeling each of 10 delineated regions in at least 20 different individuals, with a total of 249 embryos labeled. These animals were allowed to grow until hatching stage, fixed and documented in whole-mount. After this documentation, these individuals were embedded and 75 individual were cryo-sectioned, counterstained with a nuclear dye and imaged using confocal microscopy.

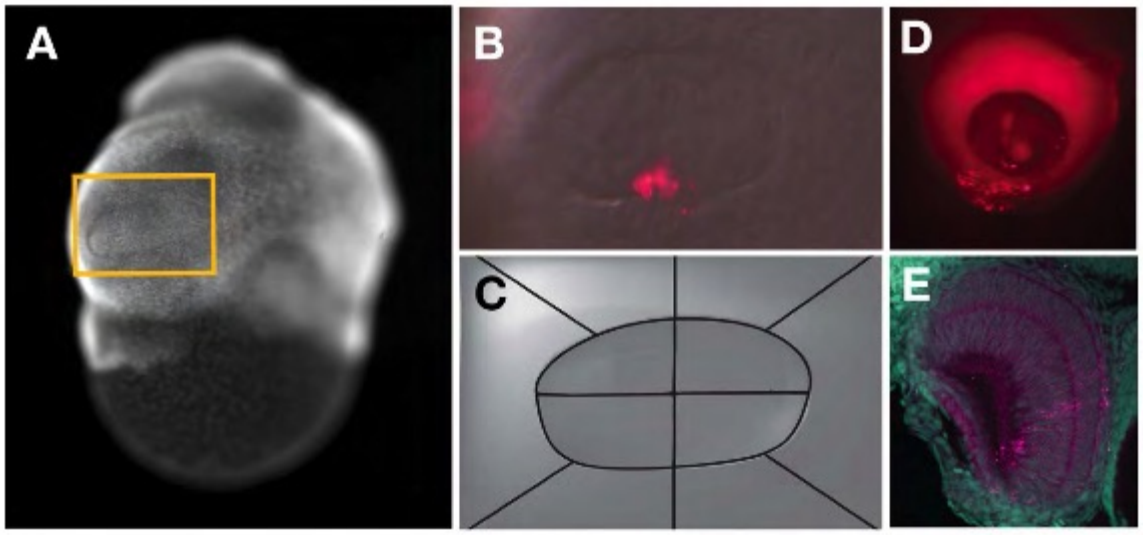

Figure 6: DiI Lineage Tracing Experimental Design
A) Embryos at stage 18 were dissected from their egg sacks and chorions. The gold box indicates the eye placode. B) An example of DiI labeling of the Stage 18 placode. DiI, dissolved in vegetable oil, was held to groups of cells either in the placode or the surrounding region until cells were labeled. C) Labeled cells were documented on a gridded map of the placode region. To ensure equal coverage across the placode and surrounding tissue, at least 20 embryos were labeled in each of the 10 regions on the map. D) An example of a labeled embryo at hatching stage. Embryos were allowed to grow until hatching stage, fixed and documented in whole mount. In this example, a lateral view of the eye is shown with labeled cells in the retina. E) Embryos were cryosectioned into serial 12um sections, counterstained with the DNA stain Sytox-Green, and documented using confocal microscopy. In this example of a placode-labeled embryo, DiI label is detected in both the support cell layer and the photoreceptor layer of the retina.

3.2: LINEAGE MAP

The results of this lineage tracing experiment can be seen in Figure 7 and a summary of these data, in conjunction with gene expression data can be seen in Figure 24. The following is a description of each of the identified primordial regions that contributed to specific tissues of the hatching stage embryo.

3.2.1: Cerebral ganglia, Buccal mass & ganglia

The Cerebral ganglia is also known as the central brain in cephalopods. It is the center of learning and memory and higher functioning (Grasso, 2014). The Buccal mass is the beginning of the digestive tract and the Buccal ganglia sits upon the Buccal mass and controls the Buccal mass and tongue (Boycott, 1961). Cells medial and ventral to the placode incorporated into the cerebral ganglion. Cells labeled medial but dorsal to the placode were still found all the way ventral to the Buccal mass and ganglion. DiI labeling was typically not found to cross the midline of the animal.

3.2.2: Optic lobe

The optic lobe is the center of all visual processing and the largest part of the cephalopod brain. The animal contains bilateral optic lobes that reside directly adjacent to the eyes. Cells labeled dorsal to the placode and lateral to the placode all incorporated into the optic lobe. Interestingly, the more medial part of this region also incorporated

into the anterior chamber organ (ACO). No specific cells only incorporated into the ACO, all cells labeled in the more medial region incorporated DiI in both the optic lobe and ACO at hatching. As discussed further below, this placement of optic lobe progenitors is interesting because it is in a drastically different location than previously described from fixed tissue (Yamamoto, 2003).

One other cell population that incorporated into the optic lobe at hatching was the placode proper. When cells in the placode were labeled, the majority of the DiI was found in the retina, however, some DiI was detected in the optic lobe. The location of this DiI was specific and found in and around the optic lobe outer plexiform layer. The incorporation of DiI in the optic lobe was greatly reduced when the placode was labeled, as compared to when the tissue dorsal to the placode was labeled. All together, this type of DiI incorporation suggested that we might be detecting axons from photoreceptor cells synapsing in the optic lobe, rather than optic lobe cells. Our data do not distinguish between these two possibilities.

3.2.3: Pedal ganglia

The Pedal ganglia innervate the arms and the funnel of the animal (Boycott, 1961). Cells labeled lateral and ventral to the placode incorporated into the subesophageal mass and a subsection of the pedal ganglia. The terminal location of this labeling was not incorporated broadly but rather restricted to a subpopulation of the subesophageal mass, more closely located toward the eye. The previously identified primordia for the pedal ganglia was not so close to the placode tissue and in the previous map this region had been suggested as part of the optic lobe (Yamamoto, 2003).

3.2.4: Retina

Cells labeled in the placode proper were the only cells that incorporated into the retina. This suggests that all the cells in the retina are derived from only the placode tissue itself, or cells that are migrating a great distance that were not labeled in this series of experiments. We labeled the retina in four quadrants. This polarity in the labeling was maintained, however the placode appeared to rotate medially, moving the quadrants a quarter turn at hatching. We could not identify any specific location where support cells were derived versus photoreceptor cells. Both cell layers incorporated DiI in all individuals with placode cells labeled.

3.2.5: Lens, cornea and iris

I also labeled the group of cells surrounding the placode, the placode lip. This tissue grows to internalize the placode, fuse in the center and form the optic vesicle. This tissue when labeled with DiI consistently incorporated in to lens, iris and cornea tissue at hatching. DiI extensively labeled iris tissue and we often found DiI puncta in the lens itself. These data suggested that the lentigenic cells were derived from the placode lip cells and that these cells formed on all sides of the lip, they were not generated in any detectable polarized fashion.

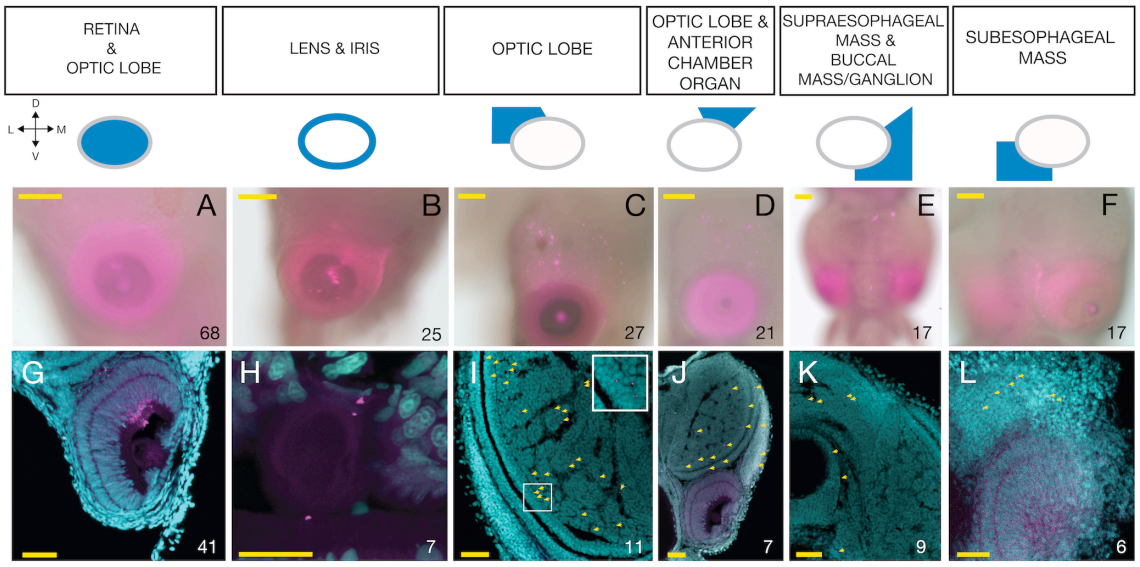

Figure 7: DiI Lineage Tracing Results

Representative examples of the progenitor domains identified in the placode stage (Stage 18) lineage tracing experiment. Cartoons at the top of the figure show the Stage 18 location of cells. The orientation of the cartoon is shown in the key: Dorsal, Ventral, Medial, Lateral. Below each cartoon is whole-mount documentation (A-F) and sectioned examples of the dataset (G-L). Sectioned data are counter stained with the DNA marker Sytox-Green. Yellow arrows highlight DiI puncta. Inset in I show a high magnification image of these puncta. Replicate numbers are shown in the bottom right corner of each image. Fate mapping revealed several progenitor regions. A,G) Cells within the placode are the only cells found to incorporate into the retina. B,H) The lip surrounding the placode generates the lens and iris. C,D,E,F, I,J,K,L) Regions surrounding the placode and placode lip incorporate into specific brain regions. Scale bar = 100um in whole-mount images, 50um in sectioned images, with the exception of the lens and iris image where the scale bar is 25um.

3.3: SUMMARY OF DATA AND DISCUSSION

3.3.1: Redrawing the cephalopod neural primordia map

We have confirmed with our lineage tracing that the retina in *Doryuteuthis* arises from the eye placode and that the lens, cornea and iris is derived from the placode lip (Arnold, 1965; Marthy, 1973; Naef, 1928). We do not see cells incorporating into the eye from any other region, suggesting that all eye tissue is solely derived from the placode and placode lip.

Previous work has used histology to identify ganglionic anlagen in the developing cephalopod nervous system (Yamamoto, 2003). Our fate map confirms and expands the region of cells contributing to the cerebral ganglia, as well as the region of cells contributing to the pedal ganglia. Interestingly, our fate map identifies the population of optic lobe progenitor cells in a drastically different location than the previously identified optic lobe primordia (Naef, 1928; Yamamoto, 2003). Our data demonstrate that optic lobe progenitors lie dorsal to the placode, while previously optic lobe primordia had been placed ventral to the placode. This new placement of the optic lobe progenitors displaces the previously identified palliovisceral primordia, suggesting the location of this progenitor pool is likely dorsal to the optic lobe progenitors. The implication of this finding is that it is possible that neuroprogenitor cells delaminate from the neuroepithelium and migrate to generate the presumptive ganglia. This mechanism would not be that dissimilar to studies performed in polychaete annelids (Meyer, 2009).

These results are exciting because they now enable us to accurately map gene expression profiles from placode stage embryos onto later fates within the eye and CNS. These correlations suggest possible functions for gene products and necessarily dictate a reinterpretation of previous gene expression studies in other cephalopod species. Furthermore, this dataset will be essential to the community for any local transfection or transplantation experiments. A final summary of this data in conjunction with gene expression can be seen in Figure 24.

Chapter 4: Cephalopod transcriptomics and RNA-seq analysis

To better understand the molecular underpinnings of eye development in the cephalopod *Doryteuthis pealeii* it was necessary to better understand when and where key transcription factors and candidate genes were expressed. Enabling this work, we built an embryonic sequencing resource for the squid *Doryteuthis pealeii*.

4.1: EMBRYONIC TRANSCRIPTOMICS

Transcriptomic databases are beginning to emerge from the Cephalopod community, and recently the cephalopod genomic infrastructure has greatly improved with the publication of the *Octopus bimaculoides* genome and a number of deep sequencing transcriptomes from adult tissues in *Doryteuthis pealeii*. Despite these recent efforts, the genomic infrastructure for studies in cephalopods and more broadly in Lophotrochozoa are severely lacking, and these resources are needed in diverse taxa for targeted molecular and evolutionary studies to be performed. With this in mind, and our goal of identifying the genes and regulatory networks that facilitate eye development in *Doryteuthis pealeii,* it was necessary to establish a transcriptome and gene expression database for embryogenesis and eye morphogenesis in *D. pealeii*. To achieve this, a pooled embryonic transcriptome of twelve stages of development (Stages 16-27) was sequenced, assembled *de novo* and annotated, and additional RNA-seq data from dissected eye and optic lobe tissues were generated from five developmental stages (19, 21, 23, 25, 27), each developmental stage was sequenced in biological triplicate (see

Materials and methods for details).

4.1.1: Whole-Embryo Library Preparation

Our embryonic transcriptome library was generated from individuals from a single squid egg sack or "finger" to minimize polymorphism to aide in assembly. Two individuals for each stage between Stages 16 and Stage 27 were pooled in a final library (Fig. 1). This library was generated with aide of Dr. Eli Meyer according to the protocol generated by Dr. Meyer and Dr. Misha Matz at the University of Texas at Austin (Meyer, 2013). The library was normalized and sequenced using 454 Next Generation Sequencing technology.

Once sequenced, the raw data was processed. Concatenated primer sequence and low quality reads were removed using custom Perl scripts. The final transcriptome was *de novo* assembled using the Newbler software package. Statistics associated with this assembly can be seen in Figure 8. After assembly, the transcriptome was annotated using the Uniprot database.

4.2: EYE PLACODE AND EYE & OPIC LOBE TIME-COURSE RNA-SEQ

The eye is unique because it contains cell types with conserved function, such as photoreceptor cells, in the context of a complex and independently evolved organ. As a result, we would expect to find both conserved molecular markers in our tissue specific RNA-seq as well as many genes previously unassociated with photoreceptive organs. Assembly of this transcriptome allowed us to assess the presence of candidate eye genes

A

Raw Data	
# of 50 bp reads	144198926
# of 100 bp reads	202235835
# of 454 reads	1539740

Assemby Statistics	
Contigs	86,462
Isotigs	80,403
Isogroups	72,591
Singletons	78,974
Average lengh	714
maximum length	17,061
n50	1,178
size of assembly in bp	57,447,061

B

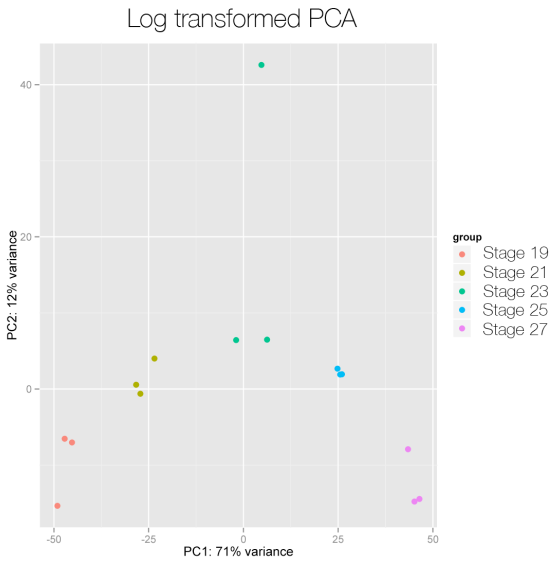

Figure 8: Sequencing raw data and assembly and RNA-seq statistics

Raw read counts and statistical analysis of the whole-embryo transcriptome. (B) Log transformed Principal Component Analysis graph of time-course RNA-seq data.

as a first step to determine homoplasy or conserved functionality in cell and tissue identity networks, while the time-course RNA-Seq data provided a quantitative assessment of gene expression over time to identify genes that displayed interesting changes throughout eye and optic lobe development.

We needed to first assess quality of the dataset before analyzing changes in gene expression. When plotting sample distances, replicates showed greater similarity to each other than across stage, which suggested that we had a consistent and robust dataset. We also generated a principal component analysis of our 15 libraries and we can see our time points grouping together with one Stage 23 replicate as a minor outlier. These transcriptome data confirm recent findings by Albertin et al. that reported an expansion of protocadherin genes in octopus (Albertin, 2015). Furthermore, we were able to identify organ specific gene family expansions including the S-crystallin gene family in *D. pealeii*.

4.2.1: Transcription factor expression

Our interest is to better understand key regulators during development in the eye and optic lobe of the squid *Doryteuthis pealeii*. Key regulators of this process will be members of transcriptional cascades, signaling pathways and gene regulatory networks. With this interest in mind, we specifically analyzed transcription factors whose expression varied in a statistically significant manner between Stage 19 and Stage 27. The heat map of these genes is presented in Figure 9.

Looking closely at two clusters in the heatmap, genes known to be involved in eye development in other systems are represented. For example, both Lim factors and

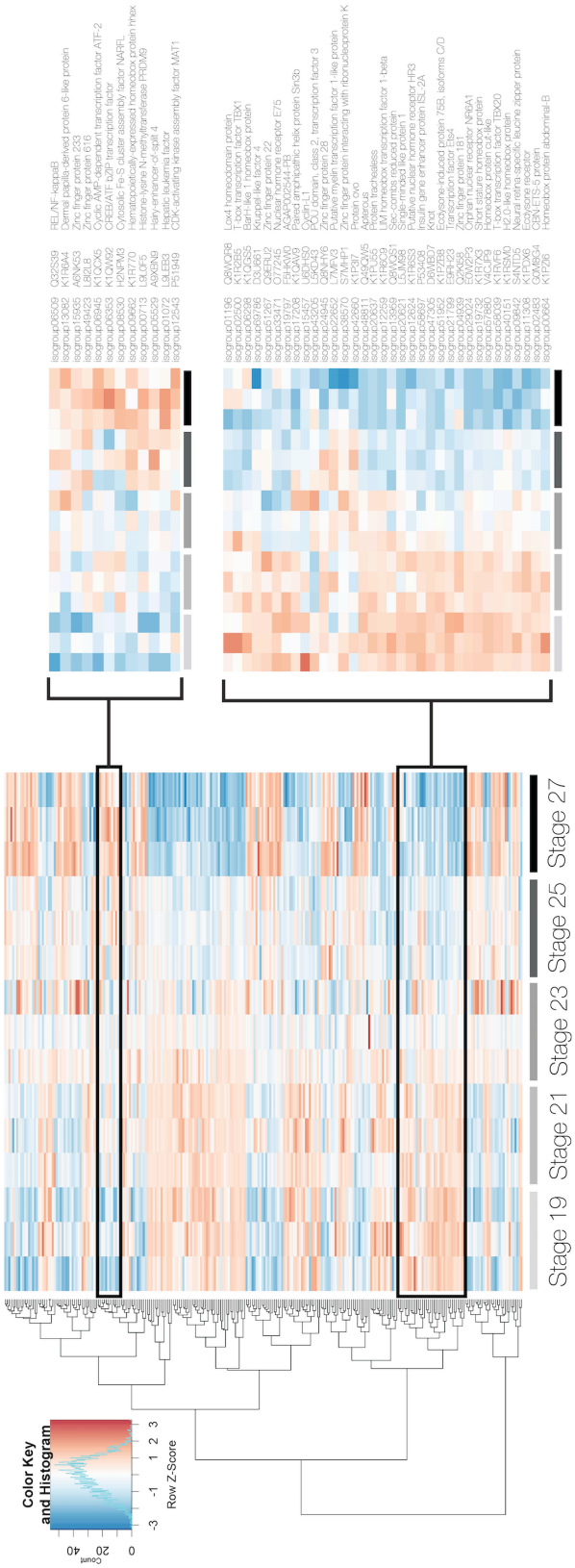

Figure 9: Transcription-Factor-specific Hierarchical Clustering of Time-Course RNA-seq Data from the Eye and Optic Lobe

Only statistically significant differentially expressed genes comparing Stage 19 to Stage 25 (FDR 0.1) are included. Upper right: A cluster of genes that are more represented in the dataset later in development. Lower right: A cluster of genes that are more represented in the dataset early in development.

Pou family of transcription factors as well as *BarH* are known to be essential in neurodevelopmental contexts and are important in both vertebrate and *Drosophila* eye development (Hobert, 2000; Rosenfeld, 1991; Reig, 2007). *Cut* is necessary for proper cone cell differentiation and lens formation in *Drosophila* and Neural retina-specific leucine zipper protein is necessary in vertebrate retina cell differentiation (Mears, 2001; Nepveu, 2001). Interestingly, the transcription factor *Ovo*, found enriched early in development in our dataset, has also been identified as a necessary player in eye regeneration in planaria (Lapan, 2012). Despite the occurrence of many transcription factors necessary for eye development in other systems, our RNA-seq also identifies a number of transcription factors that are as yet unexplored in the visual system (i.e. Abdominal-B, Knot, Hhex, Hepatic leukemia factor). These genes may have evolved a novel function in the cephalopod eye or we are witnessing a cryptic function, previously unidentified in *Drosophila* and vertebrates. These transcriptome data also confirm recent findings by Albertin et al. that reported an expansion of protocadherin gene families in octopus and squid (Albertin, 2015), and they also suggest an interesting expansion of the S-crystallin gene family in *D. pealeii*.

4.2.2: Candidate gene expression

The eye has been such a classic case of deep homology, we were immediately interested in the expression of candidate genes that are known to play an important role in the visual system of other animals. To evaluate their presence or absence and variance over time, we generated a heatmap with eye specific candidate genes, including Pax6, Pax2, Six3, Six2, Prospero and Eya (Fig. 10). What we can see from this heat map is that

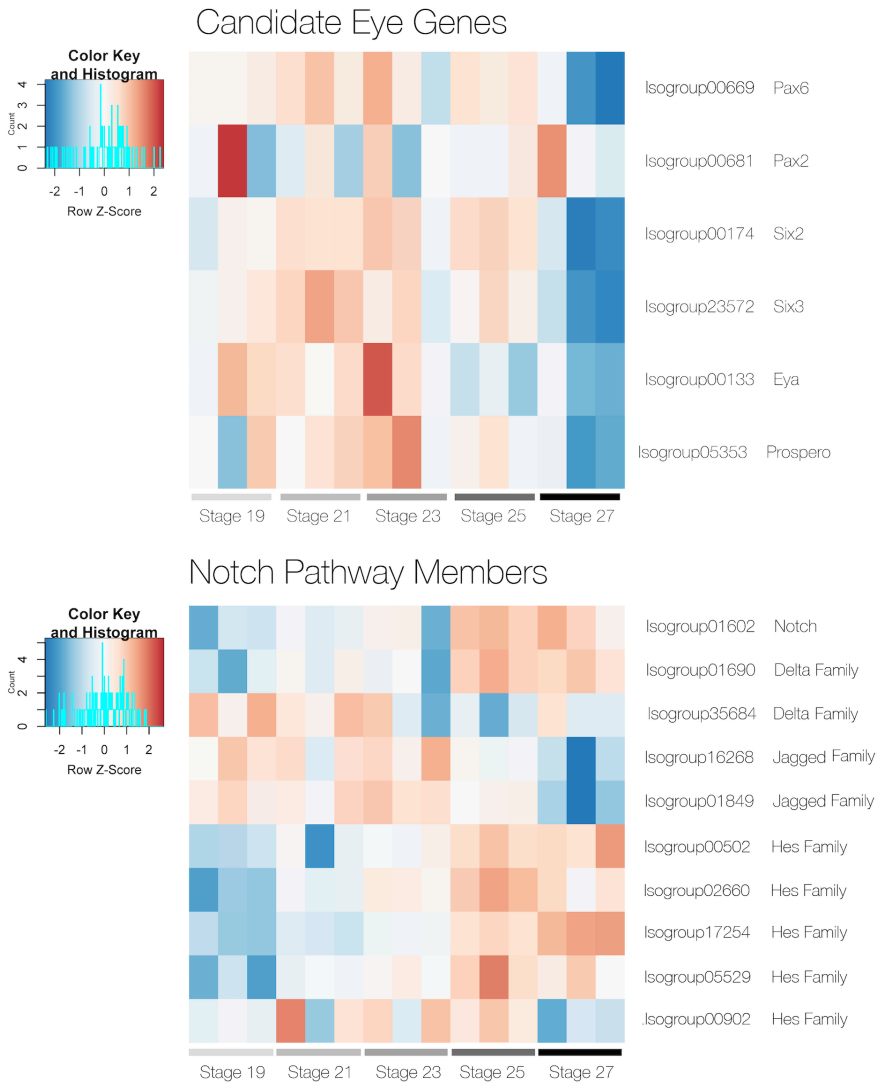

Figure 10: Candidate gene RNA-seq Heatmaps
Variance-stabilized transformed heatmaps for Retina Determination Network genes, eye candidate genes, and Notch Pathway members. Genes were identified by Uniprot annotation; sequences were then reciprocally blasted against *Drosophila* and *Mus musculus* non-redundant protein database to confirm annotation. Multiple Delta, Jagged, and Hes family members were identified. Phylogenetic trees were constructed for all eye candidate genes, Retina Determination Network Genes as well as Notch isogroup01602 and Hes family member isogroup00502 to confirm orthology (Figure S10-S15).

these genes are more highly represented in eye tissue in earlier stages rather than later stages and they are the most highly represented at Stage 21 and Stage 23, after vesicle closure but before photoreceptor cells have delaminated. Interestingly, Pax2 expression was the most variable across time and even between replicates.

Because of the interesting neuroanatomy of the cephalopod retina, and the formation of a pseudostratified epithelium, we were particularly interested in genes involved in neurogenesis. In particular, we focused on the Notch signaling pathways and pulled out pathway members to analyze their representation in the dataset over time. We generated a heatmap including Notch, two Delta family members, two Jagged family members and five Hes family members (Fig. 10). What we can see from our data is that Notch is expressed throughout development, however it appears to be more highly represented in later stages. More than one pattern of expression exists across this group of genes. We can see a similar pattern in one Delta family member as well as four of the five Hes family members. The second Delta family member, Jagged family member and the Isogroup00902 Hes family member are all down-regulated at Stage 27 when cells are differentiating. This suggests that Notch signaling may be functioning uniquely at different times in development. This is not surprising as Notch signaling performs multiple roles in the *Drosophila* and vertebrate retina at different points and in different cell types in the retina.

4.3: DISCUSSION

To begin our investigation of the molecular underpinnings of eye development in the squid, we needed the gene sequence for a number of candidate genes. With Next

Generation Sequencing technology, not only were we able to generate the most in-depth embryonic transcriptomic sequence library to date, we were also able to generate an organ specific time-course dataset. This dataset has not only been imperative to all the following work in this dissertation, this will provide a publically available resource that will can launch interesting hypothesis driven experimentation in the study of cephalopod eye development. This is the first transcriptomic analysis of organogenesis in any Lophotrochozoan and the temporal changes reveal how lacking single stage transcriptomics can be.

Chapter 5: Expression analysis of genes involved in Vertebrate and *Drosophila* eye development

Our transcriptomic databases provided a wealth of knowledge about gene expression, however, despite our organ-specific RNA-seq analysis, we still needed to identify and define specific expression in individual cells and tissue types in the developing eye. We used our new sequence libraries to further investigate specific genes of interest.

5.1: PLACODE STAGE EXPRESSION

As discussed in the previous chapter, this developmentally focused transcriptome dataset provided broad coverage of candidate transcription factors, transcriptional cascades and signaling pathways known to be involved in *Drosophila* and vertebrate eye development. Also discussed in Chapter 1, the Pax6 transcriptional cascade (Retinal Determination Network; RDN) and Notch signaling pathway both play critical roles during eye formation in other taxa. Furthermore, these RDN and Notch pathway members displayed interesting changes in expression over time (Fig. 10). Thus, we cloned eight candidate "eye" genes: *Pax6, Six3, Six2, Pax2, Eyes Absent, Notch, Hes* and *Prospero* and performed *in situ* hybridizations to identify spatial patterns of expression throughout eye development (Fig. 17-23, and 25). Primer sequences were designed based on transcriptomic sequence and are reported in the Table 1. To confirm the orthology of these genes, we sequenced them using Sanger sequencing and generated Maximum Likelihood trees (Fig. 11-16). More elaborated methods used in generating these trees

Figures 11-16: All trees are a consensus from 1000 bootstrapped ML trees. Bootstrap scores are indicated on the branches. *Doryteuthis pealeii* sequences are highlighted in magenta.

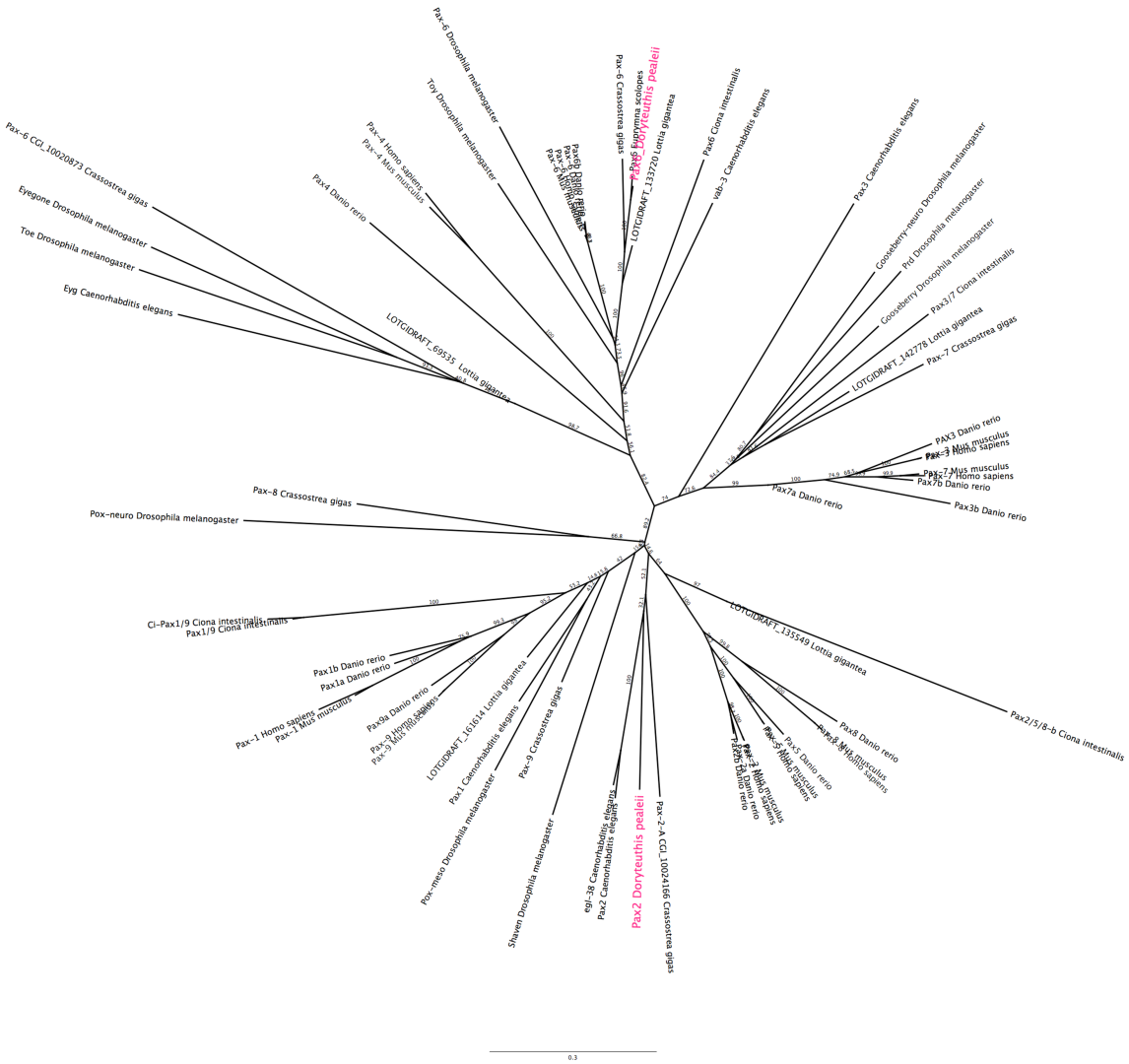

Figure 11: Maximum Likelihood Phylogenetic Analysis of Pax Genes

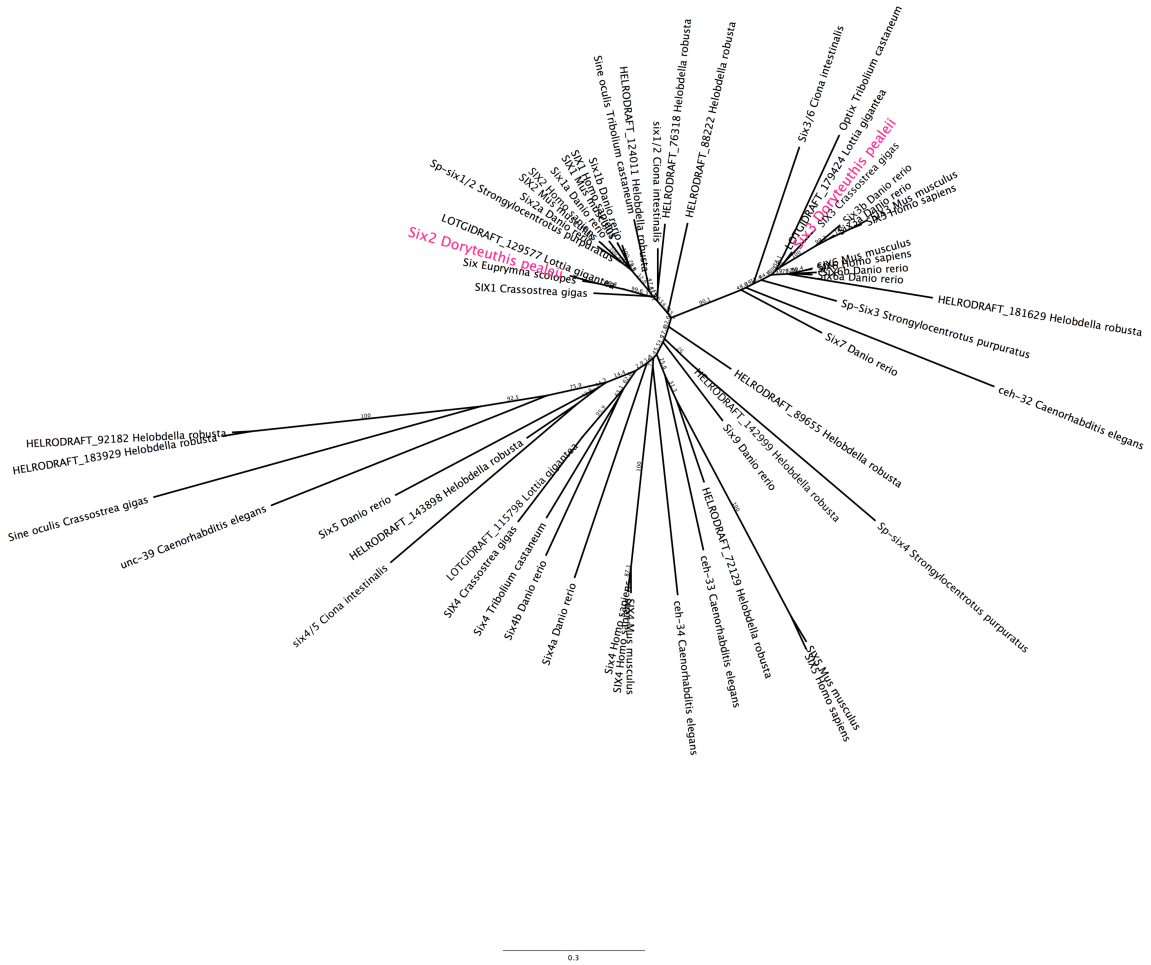

Figure 12: Maximum Likelihood Phylogenetic Analysis of Six Genes

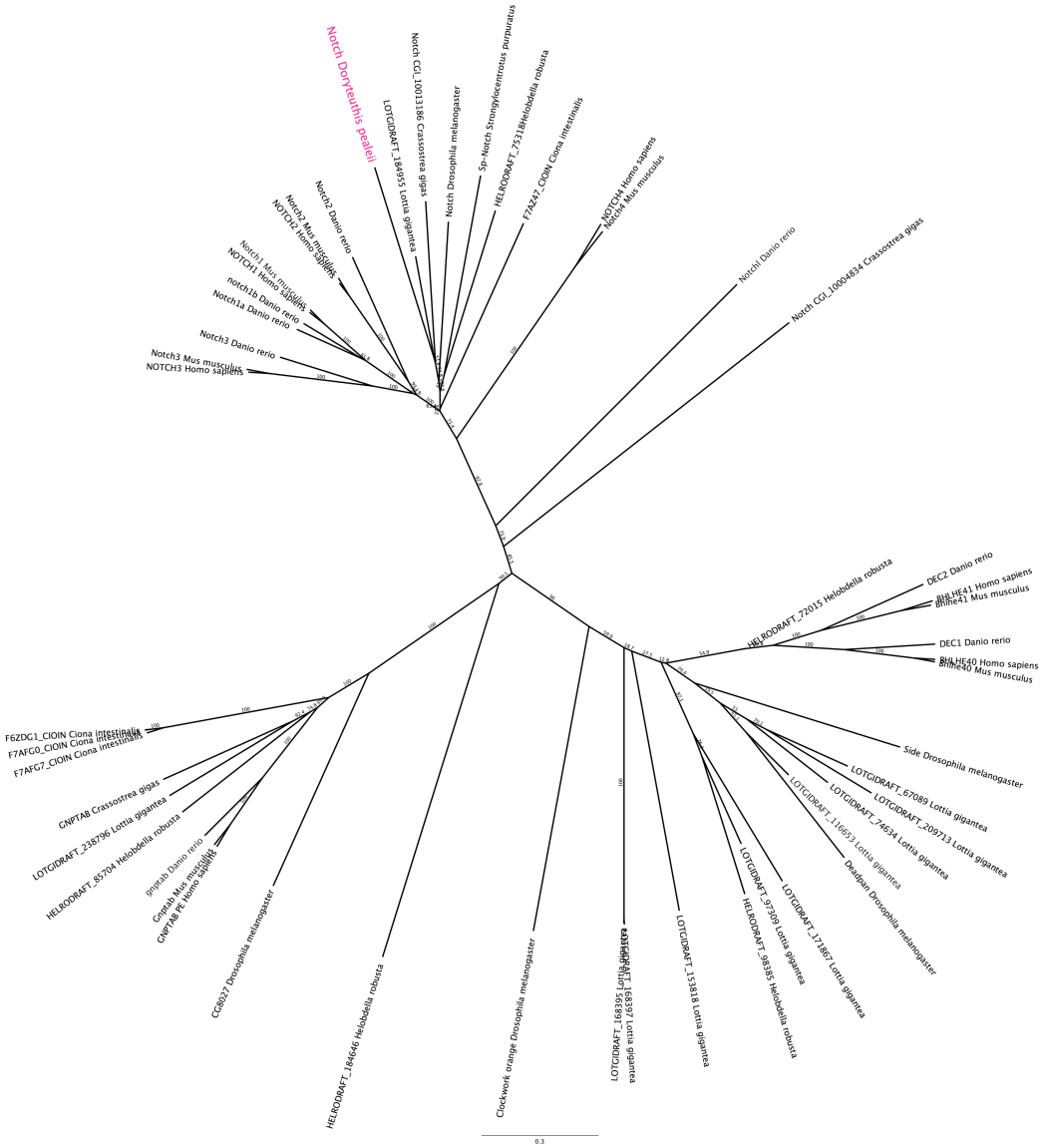

Figure 13: Maximum Likelihood Phylogenetic Analysis of Notch Genes

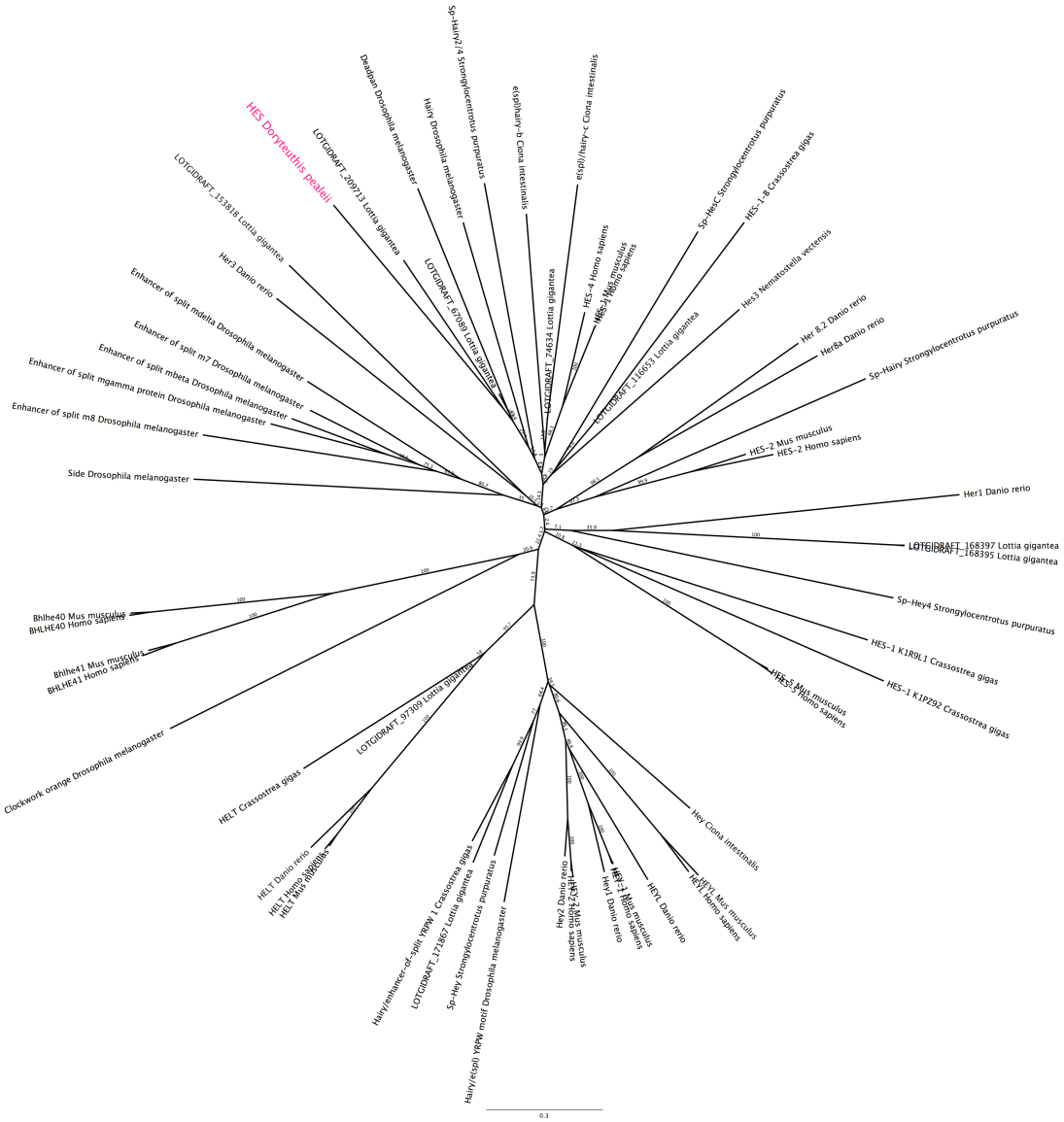

Figure 14: Maximum Likelihood Phylogenetic Analysis of Hes Genes

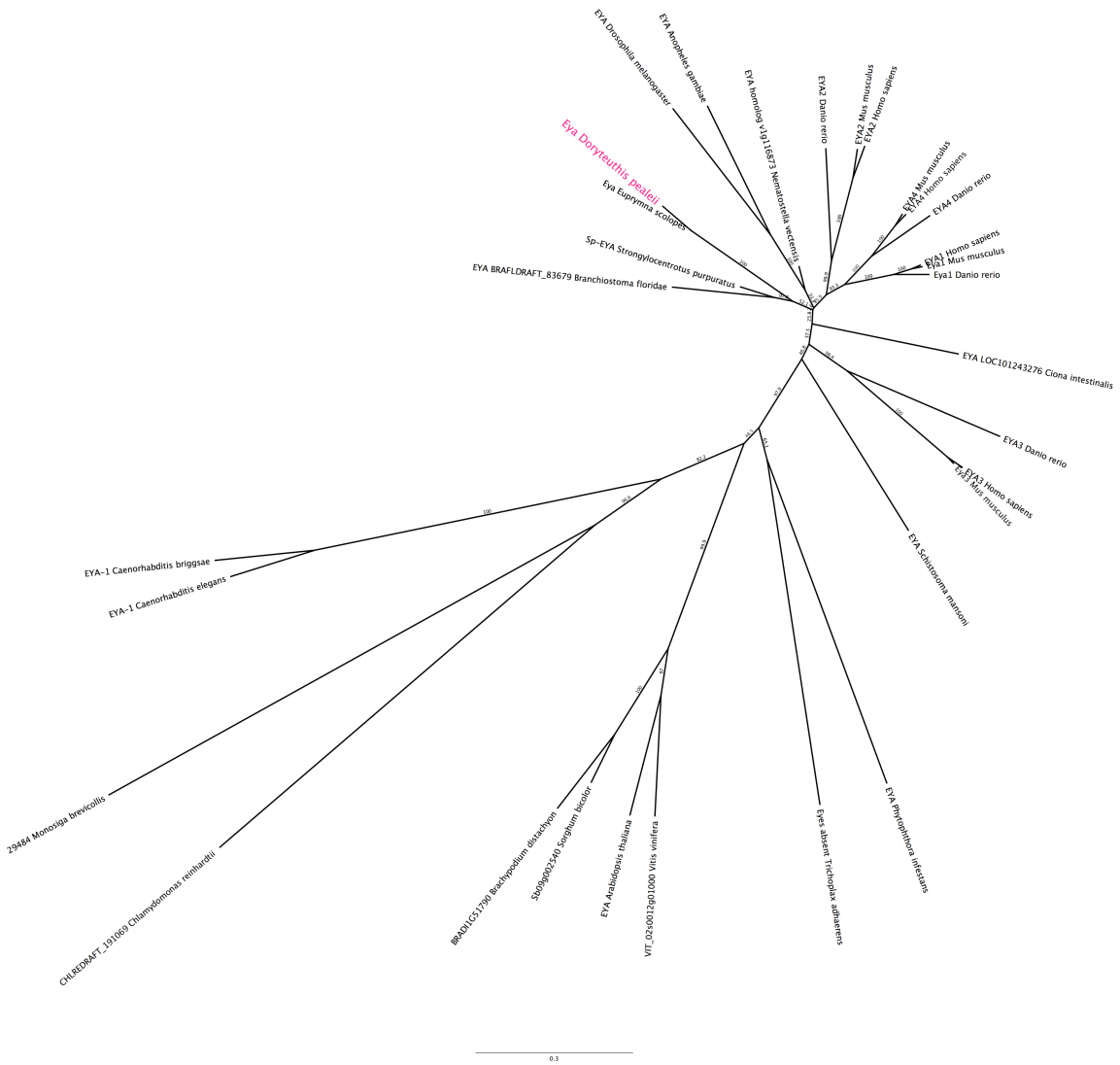

Figure 15: Maximum Likelihood Phylogenetic Analysis of Eya Genes

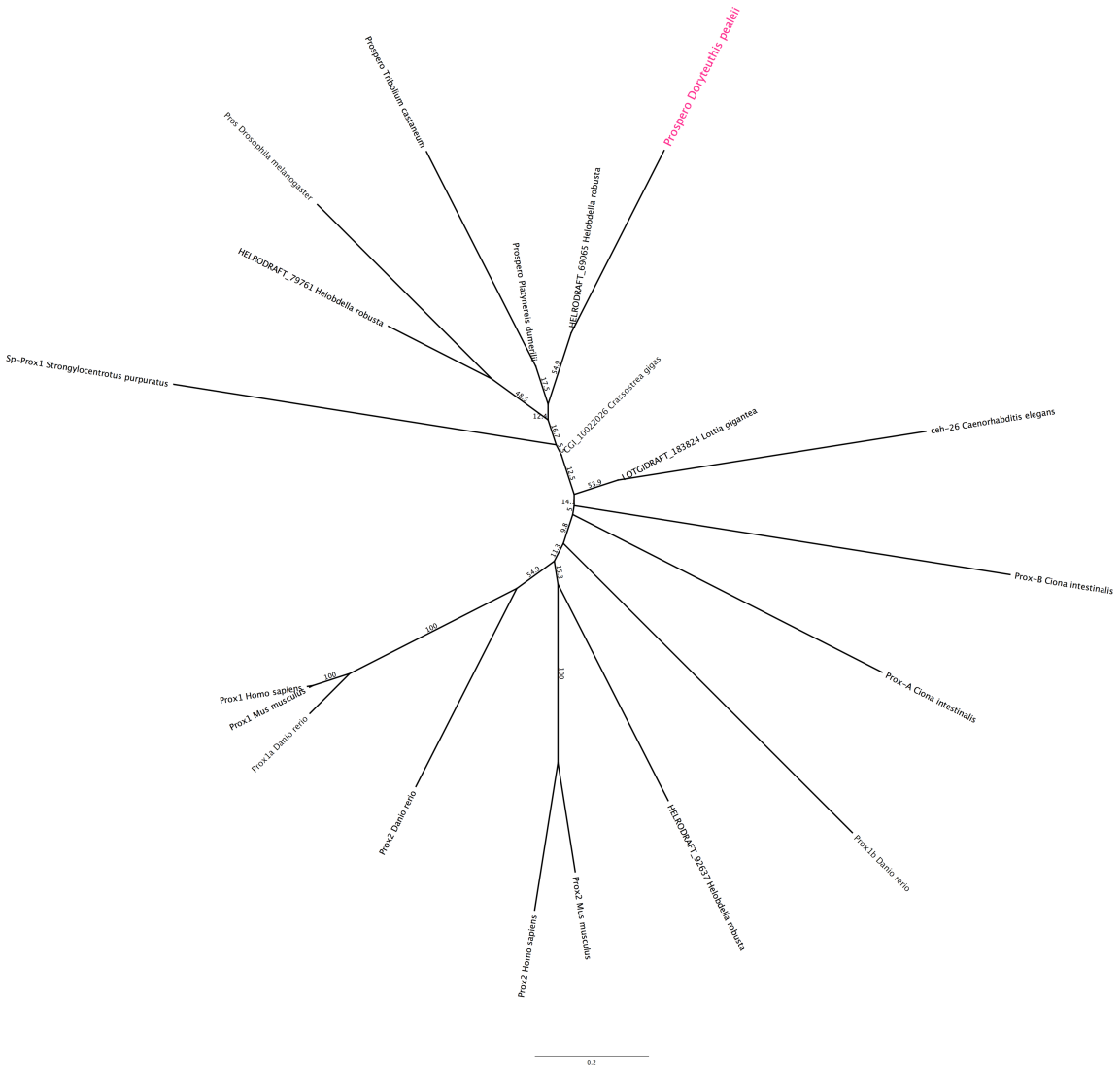

Figure 16: Maximum Likelihood Phylogenetic Analysis of Prospero Genes

can be found in the Appendix 6. We focused our preliminary analysis on the early placode Stage 18 with the understanding that cells at this stage may be in the process of specifying and are long before differentiation. Very few investigations in cephalopod gene expression have addressed these early stages.

5.1.1: Genes expressed within the placode

At Stage 18, *Notch*, *Hes*, *Prospero* and *Eyes Absent* were each expressed in cells of the placode, which give rise to the retina (Fig. 17). *Notch* expression was detected asymmetrically on the ventral side of the placode and also in the surrounding extra-ocular tissue. *Hes* expression was variable; at Stage 18, *Hes* was detected in only a portion of the placode, while at Stage 19, Hes is expressed throughout the entire placode (Fig. 17). *Hes* expression is detected in the retina through Stage 27 (Fig. 25). *Prospero* was expressed in a punctate pattern at the ventral edge of the placode. *Eyes Absent* is also expressed throughout the placode, but asymmetrically, with more signal detected on the ventral edge. *Eyes Absent* is also detected in tissue surrounding the placode.

5.1.2: Genes expressed outside the placode

Pax6, Pax2 and *Six3* are all expressed in the lip cells surrounding the placode, cells that give rise to the lens and iris (Fig. 17). *Pax6* expression is expanded dorsal and lateral to the placode, while *Six3* is expressed only medial to the placode. *Pax2* is expressed in cells of the lip as well as in distinct stripes dorsal to the placode. *Pax2* is also prominently expressed in the developing arms. Finally, *Six2* is expressed in the

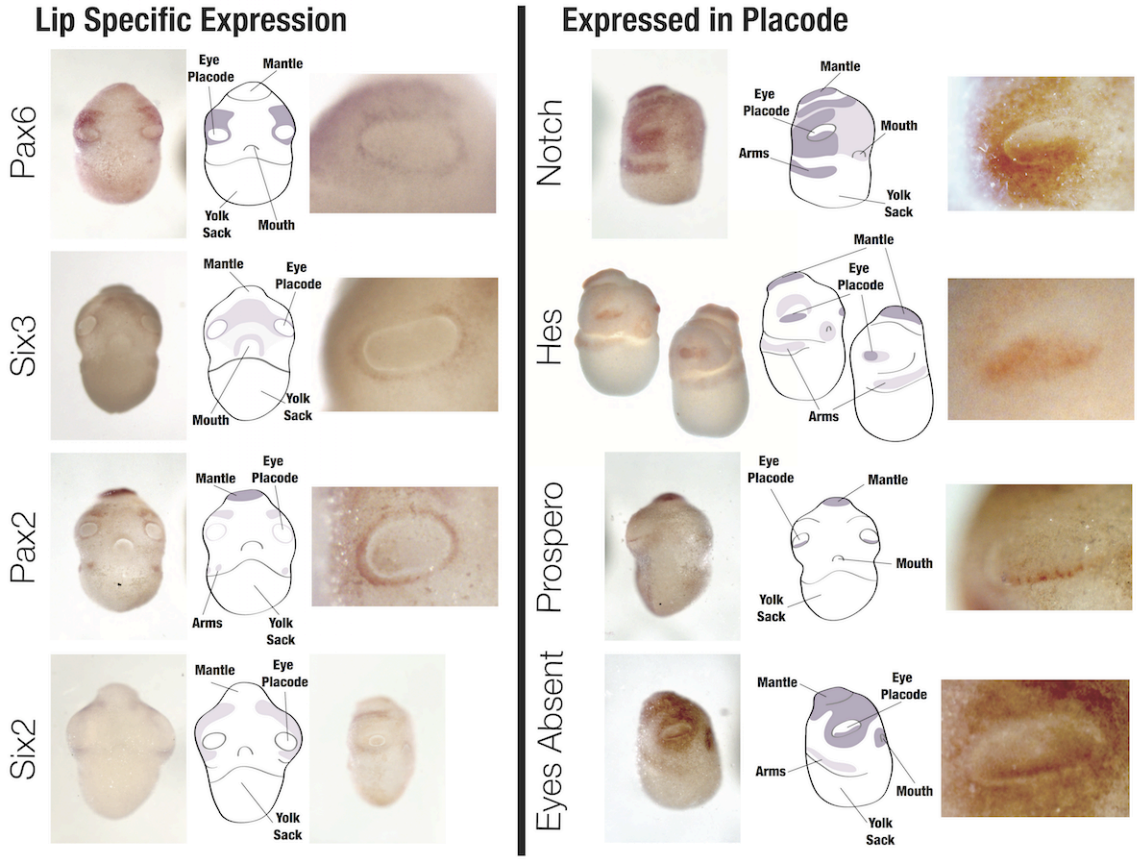

Figure 17: Expression Analysis of Candidate Eye Genes at Placode Stages

In situ hybridization for candidate genes involved in eye development in early stage embryos. Cartoon depictions of the expression patterns are located next to the whole embryo images. Higher magnification images are shown of the eye placode for all *in situs*, with the exception of *Six2*, where a lateral image of a Stage 20 embryo is shown. *Six2* expression is restricted from the eye at Stage 20. *Pax6, Six3, Pax2* and *Six2* are expressed in tissue surrounding the placode at Stage 18 and excluded from the placode proper. *Notch, Hes, Prospero* and *Eya* are all expressed in the placode at Stage 18. *Hes* expression is shown for both Stage 18 (left) and 19 (right). *Hes* expression changes quickly from the posterior half of the placode at Stage 18 to the entire placode at Stage 19. The high magnification image is of Stage 18.

tissue just ventral and lateral to the placode. Interestingly, while Pax and Six genes were expressed in the retina at later stages of development (Fig. 18-21), expression was not detected in the placode at Stage 18. At this time, we cannot rule out that they are expressed at levels below the threshold for detection.

5.2: GENE EXPRESSION AFTER PLACODE STAGE

Our primary interest was to better understand these genes during early eye formation but we extended our investigation of these genes to later time points as well. A summary of these data is discussed below.

5.2.1: Pax6 expression

Pax6 expression has been published in a number of cephalopod species and there is some evidence that Pax6 has multiple splice variants, contributing to complexity in the cephalopod (Fig. 18). Pax6 is expressed extensively in the optic lobe of the squid, arms and the eye. Expression is specifically excluded from the mantle.

5.2.2: Pax2 expression

Pax 2 expression is observed in the presumptive retina at Stage 21, as well as specifically in the arms and mantle (Fig. 19). This expression is then excluded from the retina but is maintained in the mantle and arms. We also observe the expression in the

tissue dorsal to the eye. This tissue may incorporate in the anterior chamber organ at later stages. At hatching, expression is diffuse.

5.2.3: Six2 expression

Six2 expression appears broad at all stages. Expression at Stage 21 appears localized to optic lobe and pedal ganglia (Fig. 21). At Stage 23, the retina appears enriched for Six2 as well as axonal projections into and out-of the optic lobe. At Stage 27, the retina also appears enriched with Six2 transcript but overall Six2 is diffuse in at this stage.

5.2.4: Six3 expression

The gene Six3 is expressed medial to the placode and this expression persists throughout development (Fig. 20). Once the cerebral ganglion is formed, Six3 is obviously restricted to this brain region. Interestingly, Six3 is a well-known marker for the anterior of the animal across the Bilateria. In this case, Six3 expression would suggest that the cerebral ganglia possesses the anterior identity of the animal. This would redefine the cephalopod body plan, unrooting the nomenclature cephalopod or "head foot," suggesting that the head is actually the central brain region.

5.2.5: Eya expression

At Stage 21 we can detect specific expression of Eya in cells surrounding the fusion site of the eye vesicle (Fig. 23). This expression suggests a function in lentigenic cells and lens formation. Eya is also observed in future optic lobe tissue as well as pedal ganglia tissue. Eya is also expressed in the mantle but is specifically excluded from the cerebral ganglia tissue. In Stage 23 and Stage 25, Eya expressing is expanded much more broadly. By Stage 27, expression is excluded for the mantle but still robust in the eye and brain regions.

5.2.6: Prosporo expression

Prospero expression is detected in the mantle, arms, retina and anterior to the retina at Stage 21 (Fig. 22). This expression continues at Stage 23 with robust expression in the retina arms and mantle. We also observe expression diffusely in the cerebral ganglia. At Stage 25, Pros expression is clear and segregated to a subset of cells in the arms. The retina, mantle and tissue dorsal to the retina are expressing the transcript. Finally at Stage 27 the expression is diffuse.

5.3: CORRELATING GENE EXPRESSION STUDIES WITH THE FATE MAP

Capitalizing on the fate map, we are able to superimpose gene expression patterns on this map and identify gene products whose expression correlates with late-stage ocular fates. *Pax6, Pax2,* and *Six3* are all co-expressed in the lip of the placode (Figure 17), and

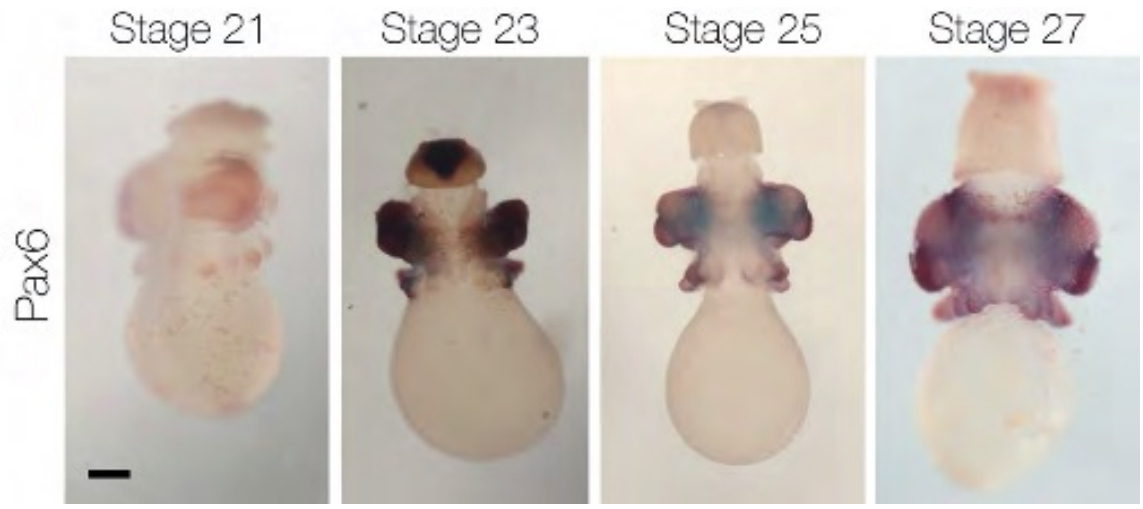

Figure 18: *In situ* hybridization for *Pax6*
In situ hybridization for *Pax6* expression at Stages 21, 23, 25 and 27. Expression in the eye and optic lobe tissue is apparent throughout development. Expression in the arms is also apparent. All embryos are shown from the anterior with the exception of Stage 21, which is shown from an anterolateral perspective. Scale = 100um

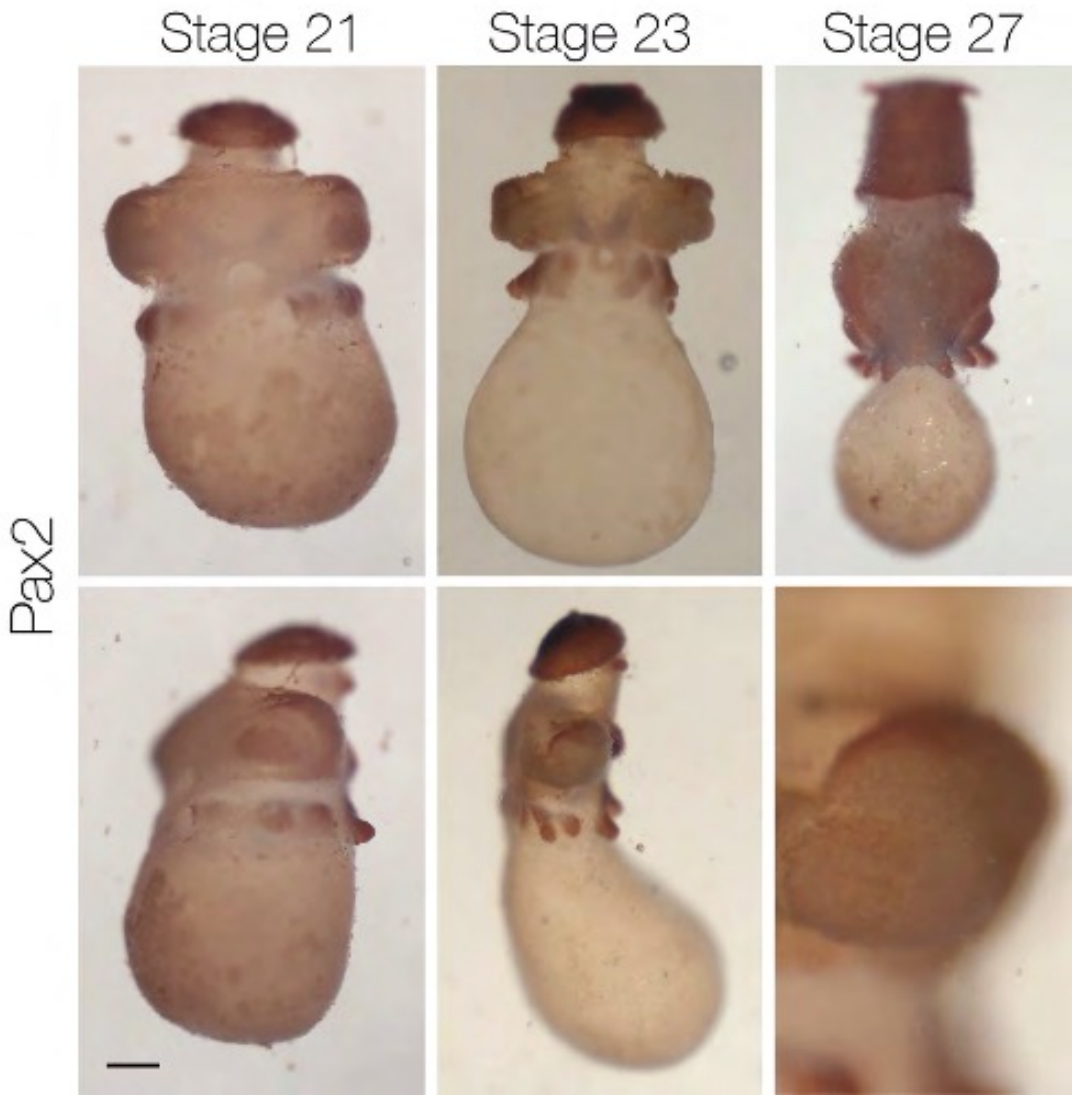

Figure 19: *In situ* hybridization for *Pax2*
In situ hybridizations for *Pax2* expression for Stages 21, 23 and 27. A,D) *Pax2* expression at Stage 21 is apparent in the mantle and developing eye and arms, as well as tissue incorporating into the developing optic lobe. A) is an anterior view and D) is a anterolateral view. B,E,F) Expression at Stage 23. Expression is apparent in the arms and in the tissue dorsal to the retina. This tissue may incorporate into the anterior chamber organ. B) Anterior view, E) lateral view, F) high magnification image of the eye in E). C) Diffuse expression at Stage 27. Scale for the low magnification images = 100um

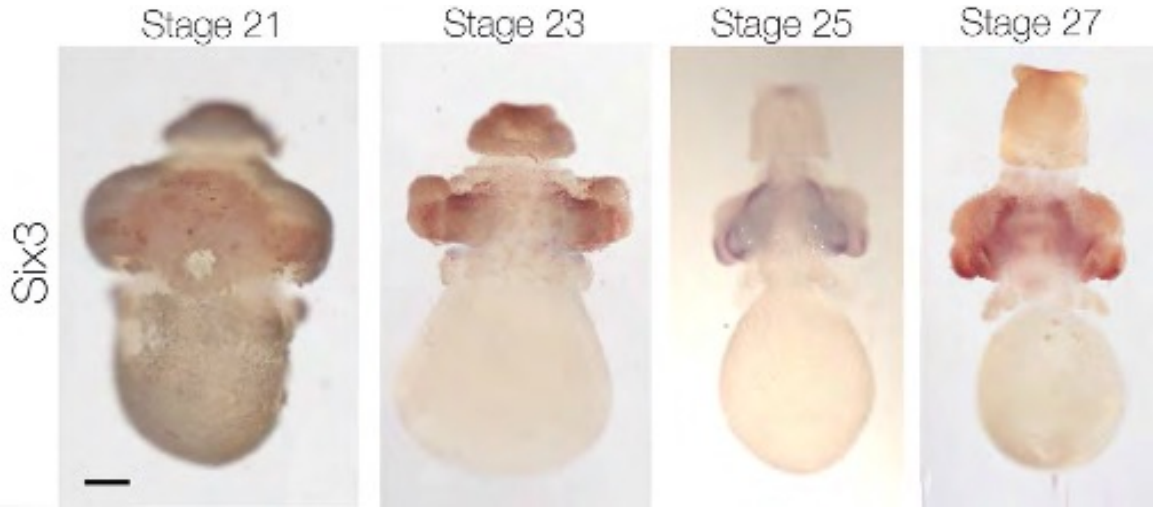

Figure 20: *In situ* hybridization for *Six3*
In situ hybridizations for *Six3* expression at Stages 21, 23, 25, and 27. Expression is in the developing cerebral ganglia tissue and parts of the developing eye. Expression in the eye is apparent at Stage 21 and 23. Lens and cornea and iris expression is apparent in at Stage 25. At Stage 27 this expression has expanded beyond the anterior of the eye. All embryos are shown from the anterior perspective. Scale = 100 um

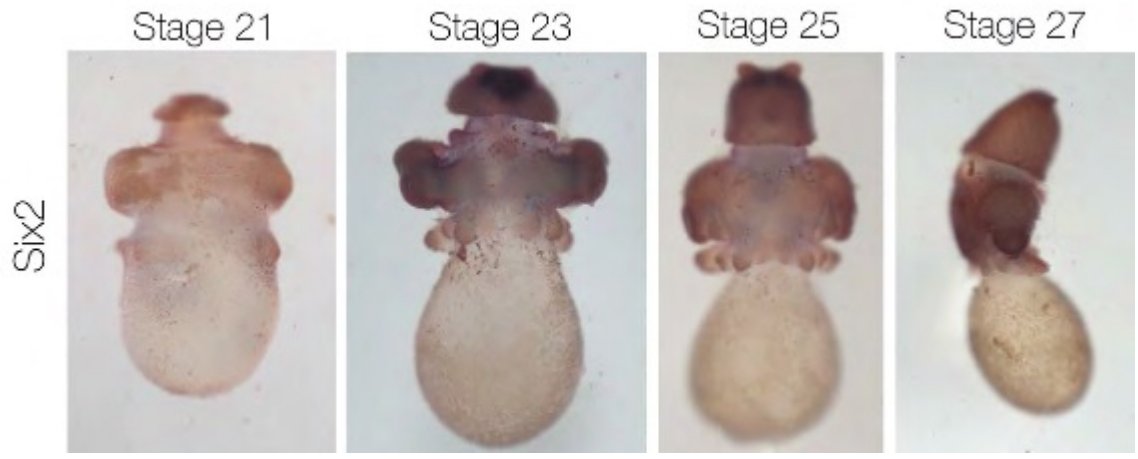

Figure 21: *In situ* hybridization for *Six2*
In situ hybridizations for *Six2* expression in Stages 21, 23, 25 and 27. Eye specific expression is apparent at later stages of development, noticeably at Stage 27. All embryos are shown from the anterior with the exception of Stage 27, which is a lateral view.

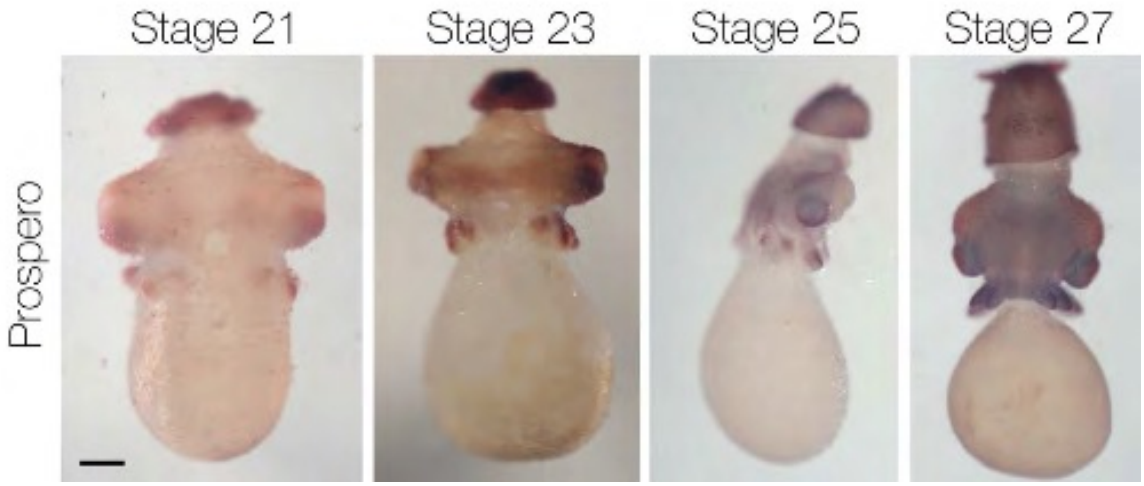

Figure 22: *In situ* hybridization for *Prospero*
In situ hybridization for *Prospero* expression in Stages 21, 23, 25, and 27. *Prospero* expression is apparent in the eye, mantle and developing arms at all stages. Expression in the cerebral ganglia is apparent at Stage 23 and Stage 25. Expression is diffuse at Stage 27. All embryos are shown from the anterior with the exception of Stage 25, which is a lateral view, anterior left. Scale = 100um

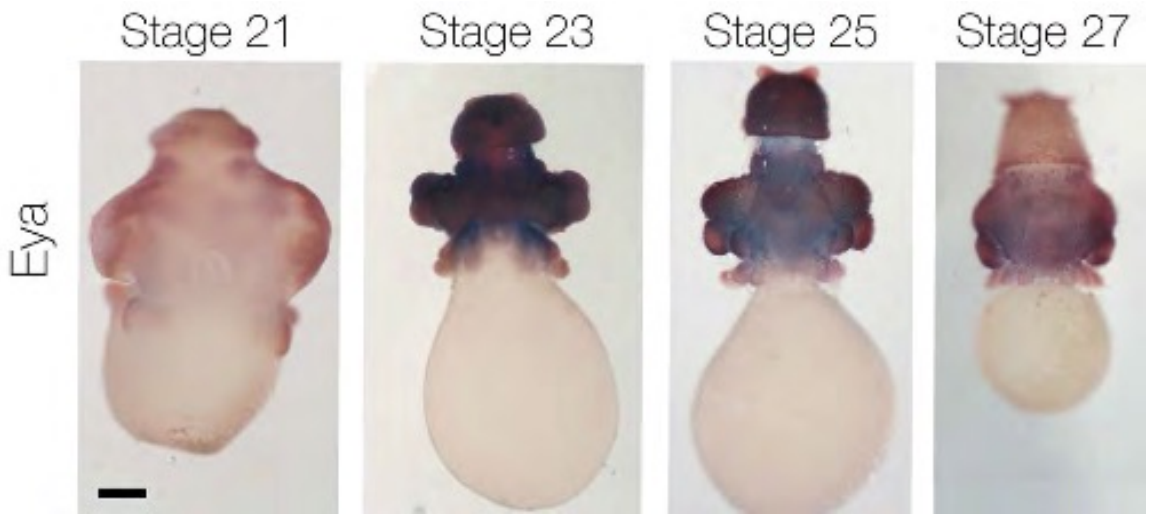

Figure 23: *In situ* hybridization for *Eya*
In situ hybridization for *Eya* expression in Stages 21, 23, 25 and 27. At Stage 21 expression is apparent in lens surrounding the developing lens tissue, as well as the optic lobe and palliovisceral primordial. Expression is also apparent in the developing arms and mantle but distinctly excluded from the cerebral ganglion region. Expression at Stage 23 and 25 is broad and robust. At Stage 27 expression decreases in the mantle. Scale = 100um

this region gives rise to the lens, cornea and iris (Figure 24). The lens, cornea and iris tissue are lineage specific novelties in the cephalopod, but interestingly, Pax6 and Six3 are required for lens induction in vertebrates. Currently little is known about any lens specific function of *eyeless* and *twin of eyeless* (Pax6 orthologs) in *Drosophila* but the same cells in the imaginal disc that give rise to the retina will also generate the lens. *eyeless* and *twin of eyeless* are expressed at the top of the RDN cascade in this tissue which may suggest a role in lens formation (Charlton-Perkins, 2011). *dPax2* is required for lens development in *Drosophila* but Pax2 does not play a known role in the vertebrate formation.

There are three interpretations of the redeployment of Pax and Six genes during lens formation. The first interpretation is that the tissue that generates the lens and the developmental origin of this tissue in *Drosophila*, vertebrates and cephalopods is homologous. This possibility would suppose that in the common ancestor this tissue expressed Pax and Six genes and elaborated into the lens tissue. In cephalopods and in Drosophila, the lens tissue is derived from the same cells as, or adjacent cells to, the retina and therefore this tissue homology is plausible. However, in vertebrates, the lens placode is derived from the surface ectoderm and therefore is unlikely a homologous tissue. The second possibility is the concept of the cell as a unit of homology. This would suggest that a lens cell program existed in the common ancestor and this program included Pax and Six genes and was redeployed in the Vertebrate surface ectoderm. This possibility is unlikely because Crystallin proteins, the refractive proteins that fill lens tissue, have evolved separately in each lineage, and therefore no such lens cell existed in the common ancestor (Oakley, 2015). Finally the most plausible possibility is that Pax and Six gene involvement is homoplastic and independently evolved. Interestingly, Pax genes have been consistently found to bind to regulatory sequences upstream of

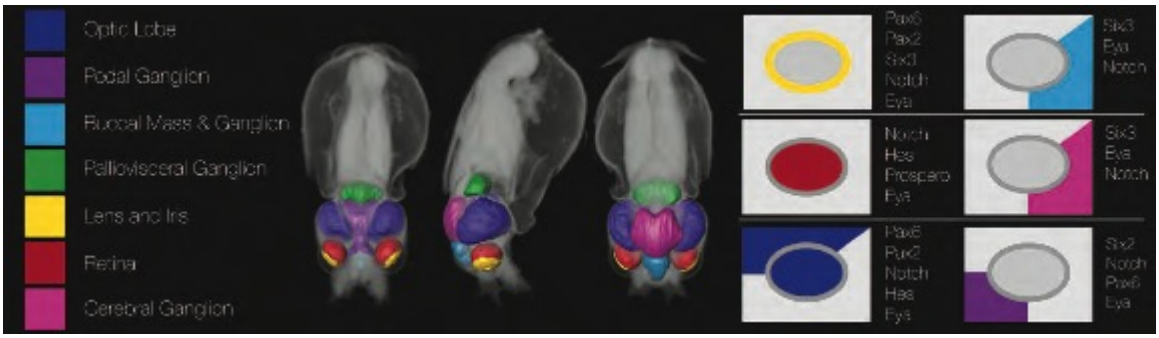

Figure 24: Summary of DiI Lineage Tracing and Gene Expression Analyses:
Summary of the placode stage fate map. The Stage 18 fate map is color-coded with corresponding cell fates highlighted on the hatchling stage model. The model was generated from segmented reconstructions of MicroCT scan data of a hatchling staged embryo. Placode stage gene expression profiles are correlated with the regions giving rise to distinct hatching stage eye and brain regions.

Crystallin genes not only in Vertebrates and *Drosophila* but in Scallops and Cnidarians (Piatigorsky, 2007). Pax involvement in lens formation in the cephalopod is one of many examples of this convergence. Currently, not enough is understood about the evolution of regulatory pathways to be able to answer the question of why similar, yet independently evolved, tissues require homologous gene regulation. Ultimately, the results of this study highlight the need for better characterization of gene regulatory networks across the Bilateria to address questions regarding how these networks elaborate and result in morphological complexity and diversity.

Beyond the placode lip, *Pax6* and *Pax2* are expressed in regions contributing to the optic lobe in the squid. *Pax6* expression also extends into the region contributing to the pedal ganglia. *Six3* is specifically expressed in the region contributing to the cerebral ganglia and *Six2* may play a role in pedal ganglia development. Interestingly, *Eya* has a very broad expression surrounding the retina, traversing all regions around the placode as well as including the placode proper.

In the squid, the gene *Prospero* is expressed in a subset of cells on the ventral side of the retina placode. Prox1, the vertebrate homolog of *pros*, is involved specification and differentiation of neurons within the retina as well as lens development. In the squid *Prospero* does not appear to be expressed in the early lens generating cells, but rather in the retina proper. This expression expands from a few cells to the entire retina later in development (Fig. 22). This specific punctate expression suggests a source of cell diversity in the retina. It's likely that the cephalopod retina is more heterogeneous than previously understood.

When we examine the localization of early expressed transcripts, it is not surprising that many of these genes are involved in brain development as well as eye development. This is consistent with what has been observed in other Bilaterian central

nervous systems. Interestingly, genes that may have overlapping expression patterns in the developing vertebrate nervous system such as *Pax6* and *Six3* in the forebrain don't overlap in the cephalopod brain. This suggests unique elaborations of the function of each of these genes in the cephalopod central nervous system.

Chapter 6: Notch signaling in the cephalopod retina

6.1: Introduction to Notch in Neurogenesis

Notch involvement in neurogenesis has been known for decades. One of the first contexts identifying Notch acting through lateral inhibition was studying photoreceptor cell differentiation in the *Drosophila* eye (Pan, 1997). This model was expanded in the vertebrate retina, where it was shown that lateral inhibition through Notch signaling was essential to vertebrate neurodevelopment as well (Austin, 1995). The retina has long been a model to understand Notch function in regard to neurodifferentiation. Our work is the first evaluation of Notch signaling in any Lophotrochozoan photoreceptive organ. This, in conjunction with a thorough developmental characterization, can speak to Notch's involvement in neurodifferentiation in the Bilateria more broadly.

It has been shown that Notch regulates differentiation in multiple Bilaterian species and that non-canonical Notch regulates neural differentiation in Cnidarians (Layden, 2014). Recent work has expanded on the classic Notch model of lateral inhibition to include aspects of interkinetic nuclear migration in the neuroepithelia of the vertebrate retina as essential for proper differentiation. A Notch gradient exposes the migrating nucleus to different amount of intra-cellular Notch, depending on where the cell is in the cell cycle (Del Bene, 2008). In both the classic model and in the new inclusion of nuclear migration, the loss of Notch signaling leads to the premature differentiation of neural cell types and the loss of neural progenitor populations. Non-canonical Notch has also been implicated in apicobasal polarity maintenance of the

murine cortex, leading to cell division throughout the epithelia and disorganization (Ohata, 2011).

We identified the cephalopod retina as a pseudostratified neuroepithelial tissue in Chapter 2, and we also identified expression of Notch signaling pathway members in the developing cephalopod retina in Chapter 3. We wanted to better understand Notch pathway involvement in retina formation and whether we could assess if Notch signaling was functioning comparably in a Lophotrochozoan.

6.2: NOTCH FAMILY MEMBER GENE EXPRESION

We have previously observed that Notch signaling pathway members were expressed in our RNA-seq dataset throughout development (Fig. 8). We also showed that at early placode Stage 18, Notch and Hes are expressed in the placode proper suggesting a role in retina formation. We were interested in whether Notch pathway members may continue expression throughout development (Fig. 17). Hes expression is maintained in the retina consistently from the earliest stage surveyed (Stage 18) until Stage 27, close to hatching (Fig. 25). Hes is often a useful readout for active Notch signaling suggesting that Notch may be playing an active role in retina formation at multiple stages.

6.3: NOTCH INHIBITION STUDY

To better characterize the role of Notch signaling in the developing retina, we wanted to perturb the pathway and analyze the consequences in the eye. If Notch is playing a role in progenitor cell maintenance, we would expect that cells would

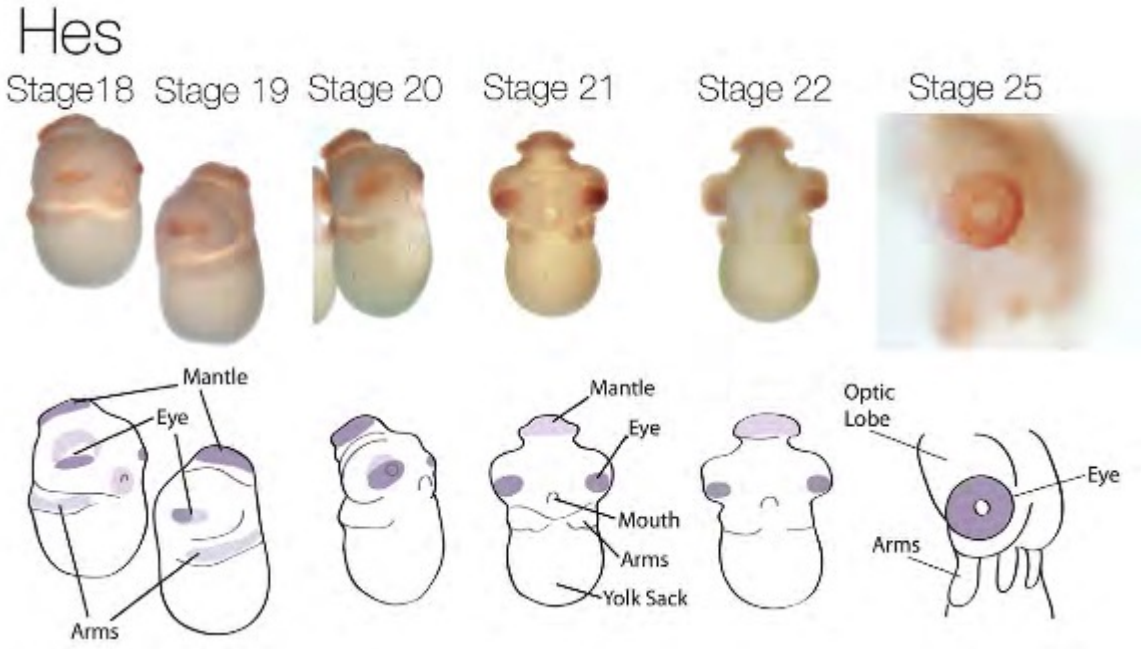

Figure 25: *In situ* hybridization for *Hes*
In situ hybridization for *Hes* expression for Stages 18, 19, 20, 21, 22, and 25. Expression is robust in the developing retina at all stages. Some expression is apparent in the developing mantle at early stages. Stage 18 and 20 are shown antrolaterally. Stage 19 is shown laterally, Stage 21 and Stage 22 are shown from the anterior and stage 25 is a lateral view.

prematurely differentiate into early born cell types, as is the case in *Drosophila* and vertebrates. We launched a series of experiments utilizing the pharmacological inhibitor DAPT, to disrupt the pathway. We bathed the animals in DMSO and DAPT and compared them to a DMSO control. Bathing occurred for 24 hours and washed out. The animals were allowed to recover until the control animal was at Stage 27. A more in depth description of these methods can be found in the Appendix.

6.3.1: Notch inhibited retinas

DAPT-treated embryos were microphthalmic, and lacked retina pigmentation (Fig. 26). In section we can see the retina is completely disorganized, the basal membrane is absent, morphologically distinct photoreceptor cells are not detectable and there is no defined photoreceptor layer as compared to DMSO treated controls (Figure 26B). Lentigenic cells and lens formation appeared to be normal, suggesting that the effects of blocking Notch pathway activity are specific to the retina. Apoptotic cells are observed in the retina after an extended recovery period, a result similar to the loss of Notch signaling in the vertebrate retina, but three hours after DAPT treatment apoptotic cell numbers do not differ from wild type (Fig. 27) (Tomita, 1996).

6.3.2: Notch involvement in progenitor cell maintenance

These data suggest that Notch signaling is required for photoreceptor cell differentiation in the developing squid retina. To further test this hypothesis we performed an *in situ* hybridization for the photoreceptor cell marker, *opsin*. In control

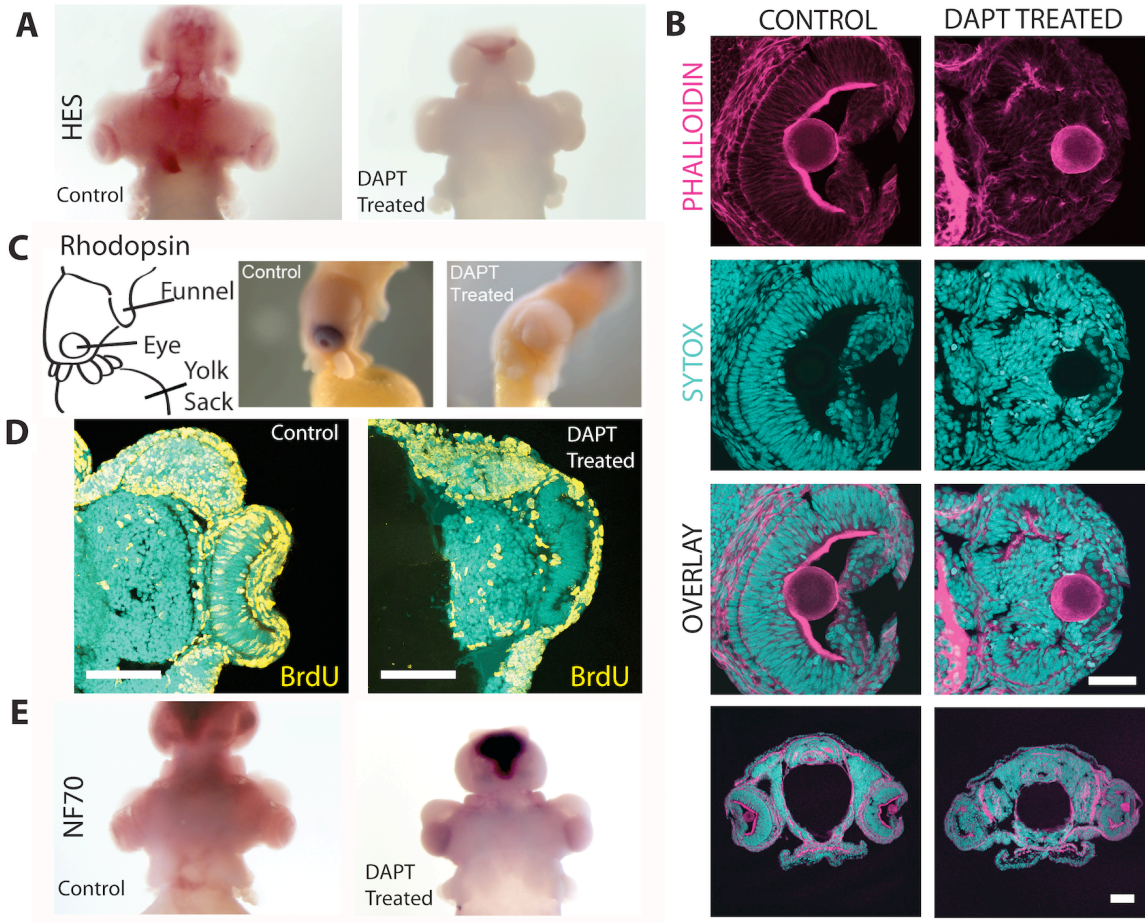

Figure 26: Notch Activity is Required to Maintain Progenitor Proliferation in the Squid Retina.

A) *Hes* expression is lost as a result of DAPT exposure (40uM). Anterior whole mount view of *in situ* hybridization at Stage 27 for *Hes* in both DMSO and DAPT treated embryos. The DIG positive region in the mantle in the treated embryo is a common background in cephalopods. B) DAPT treated embryos (20uM) show disorganization of the retina and defects in photoreceptor cell differentiation. Scale bar = 50um for high magnification images and 100um for low magnification images. C) DAPT treated retinas lack *rhodopsin* expression suggesting a loss of differentiated photoreceptor cells. Whole-mount, lateral view of DMSO and DAPT (20uM) treated embryos at Stage 27. D) DAPT treated embryos express the neural marker *NF70* in their retinas. Anterior whole mount view of DMSO and DAPT (20uM) treated embryos at Stage 27. E) DAPT treated retinas fail to incorporate BrdU into the retina. Cross-sections of DMSO and DAPT (20uM) treated embryos. Embryos were treated at Stage 21 for 24 hours, exposed to BrdU for 3 hours and fixed immediately thereafter. Scale bar = 50 um

embryos, *opsin* is robustly expressed in the retina. However, in DAPT treated animals, *opsin* expression is lost (Fig. 26D). Retina cells in DAPT-treated embryos could either remain in a progenitor-like, undifferentiated state or they could prematurely exit the cell cycle and differentiate into a cell other than an *opsin*-expressing photoreceptor cell. To distinguish between these possibilities, we performed BrdU incorporation assays, after DAPT exposure. While control embryos incorporated BrdU normally in proliferative populations of the developing retina, DAPT-treated embryos showed no $BrdU^{+}$ retinal cells (Fig. 26E). These data support a model in which photoreceptor cells prematurely exit the cell cycles and differentiate when Notch pathway activity is blocked. To determine if the prematurely differentiating retinal cells retained a neural fate, we performed *in situ* hybridization for the neural marker *Neural Filament 70* (*NF70*) (Szaro, 1991). Retinal cells in DAPT treated embryos were positive for *NF70* suggesting that, while not photoreceptors, they had differentiated into a neural cell type (Fig. 26C).

6.4: DISCUSSION

Our work shows that the cephalopod retina is also a pseudostratified epithelial tissue and that loss of Notch activity results in premature cell cycle exit. Our notch-inhibited retinas also show severe disorganization of the epithelial tissue and may be evidence of loss of apicobasal polarity in the epithelium. Both these scenarios support mechanisms of Notch signaling observed in neural tissues in other systems.

Interkinetic nuclear migration has been identified as a shared aspect of pseudostratified epithelia and has been seen in multiple tissues in vertebrates, in the Drosophila wing disc and in Nematostella, however this is the first description of

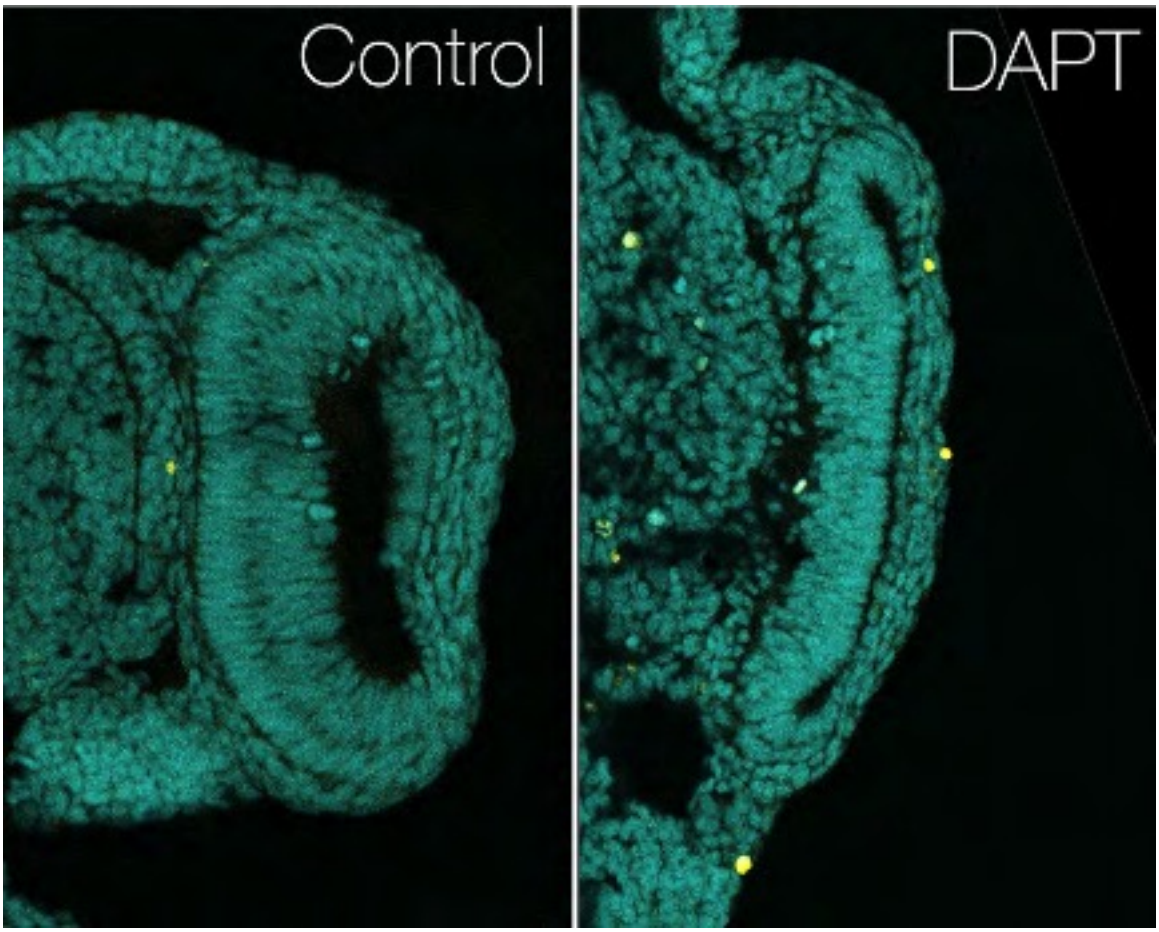

Figure 27: TUNEL staining of DAPT-treated embryos
Cross-section of 24 hour DAPT (20uM) and DMSO treated embryos. Embryos were treated at Stage 21 and fixed 3 hours post-treatment. Sytox-Green (cyan) and TUNEL (yellow).

interkinetic nuclear migration in any Lophotrochozoan neuroepithelium (Gibson, 2011). Nuclear migration has been described in the *Drosophila* eye disc but never related to the process occurring in vertebrate neuroepithelial tissue and is not tied to the cell cycle (Tomlinson, 1986). This work suggests a common mechanism governing differentiation and progenitor cell maintenance of photoreceptive neuroepithelial tissue by Notch that is shared across the Bilateria. An in depth understanding of nuclear migration as well as neuroepithelial formation in the Lophotrochozoa more broadly will provide a superior understanding of the shared Urbilaterian tool kit that was elaborated to generate such neural diversity.

Chapter 7: Conclusions and future directions

7.1: SUMMARY OF WORK

Our goal has been to establish the cephalopod eye as an accessible system to address questions regarding the evolution of nervous system novelty and complexity as well as gain insight into the nature of photoreception in the Urbiltarian ancestor. We have shown the potential of this system by identifying a compelling case of convergence in the genetic network underlying early formation of the cephalopod lens. These findings suggest a greater prevalence of homoplasy in the shared genetic networks underlying complex organs. A great amount of work remains to be done to better understand the nature of gene regulatory evolution and to understand why specific transcription factors may be suited to specific tasks.

Finally this study has also highlighted some of the cellular behaviors and characteristics that may be fundamental to nervous systems in the Bilateria. Building our understanding of the character of tissues and cells that are shared across species can give us greater insight into how complexity is built. Notch signaling enables the possibility of multiple neural cell types. The organization of neuroepithelia and the process of interkinetic nuclear migration may be the mechanism to execute this complexity. It will be necessary to explore gene and protein expression of the Notch pathway in greater detail in the cephalopod as well as other taxa to truly understand how these mechanisms contribute to this process and their character in the Urbilaterian ancestor. In all, this work

opens a whole new avenue of investigation regarding the evolution of complexity and the emergence of novelty.

7.2: FUTURE DIRECTIONS

7.2.1: Tool Building

After building a strong foundation for the study of cephalopod eye development, there remain two main tools that are necessary for the longevity of the system. First, to truly test molecular hypotheses it is necessary to be able to functionally manipulate gene expression or protein function. Fortunately, Crispr/Cas9 is proving to be a revolutionizing method, opening the door to F0 transgenics in traditionally non-model systems. Furthermore, new *in vivo* transfection systems, including lipofection and viral techniques, hold great promise for studying organogenesis. The second tool needed in cephalopod eye development is a broader more thorough assembly of molecular cell type markers in the retina. Until cells can be specifically identified by molecular markers, it will be difficult to analyze the effects of genetic perturbations.

Despite the remaining foundation-building tools that will be important to move the system forward, there remains a number of projects illuminated by this work that are easily accessible with the tools currently available.

7.2.2: Determine how Notch signaling may play a role in the generation of cell type diversity in the cephalopod eye

As discussed above, Notch signaling is necessary for proper neural differentiation across the Bilateria and is fundamental to promoting cell type diversity in neural tissues (Tomita, 1996; Go, 1998). Notch functions in vertebrate neurolepithelial tissues to maintain a progenitor pool as waves of specific cell-types differentiate sequentially. Recent work has identified that interkinetic nuclear migration is essential to the cell type diversity regulated by Notch signaling in the vertebrate retina (Del Bene, 2008). My dissertation work has shown that the cephalopod retina primordia is also a neuroepithelial tissue that undergoes interkinetic nuclear migration very similar to the vertebrate retina (Austin, 1995). In cephalopods, my work has also shown that Notch signaling causes premature cell-cycle exit in the retina, resulting in the loss of photoreceptor cells and the premature differentiation of retina cells into an unknown neural cell type. The future of this work will address whether cephalopods use similar mechanisms to promote cell-type diversity in their neurogenic tissues. A more thorough in-depth characterization of Notch pathway members in the cephalopod retina throughout development including all Notch, Delta, Jagged/Serrate, Hes, and Ash family members is necessary. A simple RNA-seq experiment of both Notch-inhibited and control retinas could also identify and analyze potential candidate gene response to Notch inhibition. This could then be used to compare the cephalopod network to what is known in other systems. A greater understanding of how Notch functions in neuroepithelia would provide a greater understanding of the Urbilaterian toolset that was elaborated upon to create neural diversity.

7.2.3: Determine the factors contributing to the morphogenetic movements involved in eye vesicle closure in the cephalopod *Doryteuthis pealleii*

As discussed above, the single-chambered eye of the squid is highly acute and morphologically independently evolved. The eye forms from an internalization of two retina placodes that appear early in development (Arnold, 1965). Eye morphogenesis occurs on the surface of the embryo in the cephalopod, making this an ideal system for *in vivo* imaging. With advances in microscopy, long-term, live-imaging protocols that can be employed to better understand the process of closure in the squid. This type of evolutionary *in vivo* cell biology could potentially identify unknown morphogenetic movements. The squid would be highly amenable to tracing cellular dynamics involved in vesicle closure, and likely a good candidate to perform targeted ablation experiments to reveal the physical forces involved. The molecular underpinnings of this process could be effectively addressed using drug treatments and *in vivo* transfection. My RNA-seq data identified possible involvement of cephalopod specific protocadherin molecules during closure stages that could be potentially involved in this process. This could be a unique effort to use the tools of *in vivo* cell biology to better understand evolutionary biological questions.

Appendix: Materials and Methods

A1: Animal Acquisition and Husbandry

Squid mops were acquired from the Marine Resources Center at the Marine Biological Laboratory, Woods Hole MA. Animals were housed in flow through sea tables at the MBL or in aquaria at the University of Texas at Austin at ambient temperatures

A2: Whole Embryo Transcriptome Library Prep

Two embryos from the same egg sack of each Stages 16-27 were prepared in TRIzol, phase separated and transferred to a QIAGEN RNeasy column. Extraction was completed according to manufacturer instructions. Libraries for each stage were prepared according to previously described methods in (Meyer, 2012). Libraries were combined at equal volume and sequenced using 454 technology at the University of Texas at Austin.

A3: RNA-seq Library Prep

Eye and optic lobes tissues were dissected and prepared in TRIzol, phase separated and transferred to a Qiagen RNeasy column. Extraction was completed according to manufacturer instructions. Libraries were prepared at the Vanderbilt VANGTAGE laboratory using poly(A) selection followed by TruSeq RNA-seq library production.

A4: Assembly, Annotation, Mapping and Statistical Analysis

454 raw reads were processed using custom Perl scripts as described previously (Meyer, 2009). Trimmed reads were then assembled using the Roche *De Novo* Assembler (Newbler v2.6). Annotation of the assembled transcriptome was performed using BLASTX and custom Perl scripts mapped against the Uniprot database. Illumina data was processed for quality and trimmed for adapter sequences using custom perl scripts. Reads were mapped to the 454-reference embryonic transcriptome as described previously (Meyer, 2012). Raw read and assembly statistics can be seen in Supplemental table 4.

A5: Time Course Clustering and Differential Gene Expression Analysis

Differential gene expression analysis and clustering was performed using the DESeq Bioconductor package version 1.10.1 run in R for Mac release 3.2.0 (Love, 2014). The data was exposed to log transformation and variance stabilizing transformation, analyzed for principal component analysis, variance and differential gene expression across stages. Analysis was performed on the whole data set and subsets of the dataset focusing on transcription factors and regulatory genes as identified by GO Terms GO:0006355 and GO:0003700. The likelihood ratio test was performed comparing Stage 19 to Stage 27 expression. A false discovery rate of 0.1 was used to assess differential gene expression over time and the heat maps were generated based on Pearson correlation using the heatmap.2 in the gplots package for R to generate hierarchical clustering of the dataset.

A6: Alignment and Trees

Sequence analysis was performed using the Geneious software package (Kearse, 2012). We tested orthology between *Doryteuthis pealeii* Pax6, Pax2, Six3, Six2, Notch, Hes, and Eya and known sequences using maximum likelihood analysis. Candidate sequences assembled in the transcriptome were identified through reciprocal blast using *Drosophila* orthologs as bait. Isotig sequences were translated into amino acid sequence and trimmed to include only the open reading frame. We searched for shared protein domains using the PFAM database, which identified hidden Markov models (HMM) to search the rp-15 proteome database through the HMMER server (Bateman, 2004; Finn, 2011). A broadly representative taxonomic subset of sequences was included in the final analysis. Other previously identified Lophotrochozoan sequences were also included in the analysis. For Eya, no PFAM HMM is available. A sampling of the related proteins was generated with Blast using *Drosophila* Eya as bait. A taxonomically representative sampling of these results was included in the tree. We performed multiple sequence alignment on the amino acid sequences using the E-INS-I strategy in MAFFT (Katoh, 2013). We performed maximum likelihood phylogenetic analysis and bootstrapping using PHYML (Guindon, 2010). We estimated support for a consensus tree from 1000 bootstrapped maximum likelihood trees for each phylogeny. Trees are shown unrooted (Fig. 10-15). Information regarding the sequences used in these trees can be found in Supplemental Table 2.

A7: Cloning and *In Situ* Probe Synthesis

RNA from a range of embryonic stages was reverse transcribed to create a cDNA library for cloning. Primers were designed from sequences identified in the embryonic transcriptome (Supplemental Table 1). Accession numbers for these sequences can be

found in Supplemental Table 3. Sequences were amplified, ligated into the pGEM-T-easy vector (Promega) and verified by Sanger sequencing. Plasmids were linearized and sense and anti-sense riboprobes were synthesized with digoxygenin labeled rNTPs (Roche) according to manufacturers instructions.

A8: *IN SITU* HYBRIDIZATION

Embryos were fixed overnight in 4% paraformaldehyde and filtered seawater. Embryos were transitioned into Hybridization buffer (Hyb) (20 ml Formamide, 10 ml 20x SSC, 40ul Heparin, .5 ml 20% Tween-20, 2 ml 20% SDS, 200 mg yeast t-RNA and water to 40 ml). Embryos incubated in Hyb at 65° Celsius overnight. Probe was heated to 85° Celsius and applied to embryos overnight. Embryos were washed in Hyb 3 times for 10 minutes and 2 times for 1 hour. Embryos were transitioned into half washes of 2x SSC for 20 minutes and 2 full washes of 3x SSC for 20 minutes. Embryos were washed 2 times in .2x SSC at room temperature for five minutes. Embryos were washed 3 times in PBS and Triton-X for five minutes. Embryos were incubated in Normal Goat Serum and PBS and Triton for 30 minutes and then incubated in alkaline-phosphatase-labeled anti-Digoxygenin fab fragments (Roche) at a 1:2000 dilution in PT-NGS overnight at 4° Celsius. Embryos were washed with PBS and Triton-X and the Alkaline Phosphatase reaction was performed as per manufacturers instructions. Embryos were washed in PT and stored in 4% paraformaldehyde and PBS. Dozens of embryos were examined at each stage.

A9: Fluorescent Staging Series

Embryos were fixed in 4% paraformaldehyde in filtered seawater overnight. Embryos were washed in Phosphate Buffered Saline solution (PBS) and .1% Triton-X (PT) and incubated in successive concentrations of PBS and sucrose: 25% for 1 hour and 35% sucrose overnight. Embryos were embedded in Tissue Freezing Medium and sectioned using a cryostat. Twelve-micron sections were sliced of each individual and eyes from three individuals were documented at each stage. Sections were stained with the nuclear stain Sytox diluted 1:1000 (5uM final concentration) and F-Actin stain Phalloidin at 1:300 dilution of the manufacturer's suggested stock concentration (2.2uM final concentration). After incubation, sections were mounted in Vectashield (Vector Labs) and visualized using confocal microscopy. Images are single focal planes isolated from Z-stack scans.

A10: BrdU Incorporation Assays

Embryos were exposed to dissolved 10mM BrdU in Pen-Step seawater (100 units/ml and 100 ug/ml respectively) for 3 hours and fixed immediately after exposure. Embryos were prepared and sectioned as described above. Once sectioned, slides were rehydrated in Phosphate Buffered Saline Solution (PBS) and incubated in 4N HCl fo 10 minutes at 37° Celsius. Sections were washed in PBS and blocked with 5% Normal Goat Serum. Sections were incubated in primary Rat anti-BrdU (Abcam ab6326) overnight at 4° C. Sections were washed in pbs and incubated in secondary antibody (Jackson ImmunoResearh 112-175-143) for 2 hours at room temperature. After secondary application, embryos were washed in pbs for 2 hours and then exposed to Sytox as

described above. Specimens were mounted in Vectasheild (Vector Labs) and imaged using confocal microscopy.

A11: TUNEL Cell Death Assays

Embryos were fixed and embedded and cryosectioned as described above. The TUNEL reaction was performed according to manufacturers instructions (*In Situ* Cell Death Detection Kit, TMR red ROCHE 12156792910). Sections were counter-stained with Sytox, mounted in Vectasheild and imaged using confocal microscopy. At least 3 individuals were examined for each stage.

A12: MicroCT

Hatchlings were fixed in 4% glutaraldehyde and 2% paraformaldehyde in seawater. Hatchlings were washed in PBS and stained with .1% iodine metal and .2% potassium iodide in water. Specimens were dehydrated overnight into ethanol and scanned using the Xradia micro CT Scanner at the University of Texas High-Resolution CT Facility.

A13: Lineage Tracing

A stock solution of 5ug/ul stock solution of CellTracker CM-DiI (Invitrogen) was made in Ethanol. This was diluted into vegetable oil to a final concentration of 0.5ug/ul. This solution was loaded into injection needles and cell populations were exposed to oil droplets until labeled. Embryos at Stage 18 were labeled and label location was documented (Arnold, 1965). Embryos were reared in individual wells of 12 well culture dishes on a bed of 1% agarose in filtered Pen-Strep seawater. Embryos were allowed to

grow until hatching stage, fixed in 4% PFA and documented in whole-mount. Specimens were embedded and cryosectioned as described above, counterstained with Sytox and imaged using confocal microscopy.

A13: DAPT TREATMENTS

Embryos were allowed to grow to experimental stages, dissected out of their chorion and incubated in a concentration of 20uM or 40uM DAPT solution in 1% DMSO and filtered Pen-Strep seawater. Embryos were kept in culture dishes as described above in groups of 7 or less. Experiments included over 20 embryos per exposure. Control embryos were incubated in 1% DMSO in filtered Pen-Strep seawater. Embryos were exposed for 24 hours and either fixed immediately, exposed to BrdU for 3 hours and fixed, or allowed to recover and grow to Stage 27 and fixed. At least 3 individuals were examined for each experiment.

Gene Name	Primers Sequence
Pax6	AGCAAGATTCTCGGAMGNTAYTAYGA
Pax6	TGCAAAAACGTCTGGRTARTGNGT
NF70	CGAATGGGGAAAAGAAACCTC
NF70	TGTCTGCGGTTTTCAGCGTC
Optix/Six3	TTCTGGGCAGCGGAAACTTC
Optix/Six3	AAGATAGTGGTGACATTGAACGGC
Sine Oculis/Six2	TTGTGGTCAAACCTGTGGCTTC
Sine Oculis/Six2	TGCGAGCACCTACACAAAAACG
Eyes Absent	AAGAGAACGGCTTCACCTGACC
Eyes Absent	GGAGGAGGTCATCATTGTCACTGC
Eyes Absent	TCGGTCACTTTGGGACTTTCGAATGG
Pax2	TGGCTGTGTTTTGAGAAGGGATAC
Pax2	GTAGCCACCCCAAAAGTTGTAGAG
Prospero	AGCGATGGGGAGAGCACAATAG
Prospero	ATGGATACTCGGCACTGTTGGTGG
Notch	CGAGGTCCAGATGGTTTCACAC
Notch	CGACATTATTCACAGATGCTGCC
Hes	TTCCTCCACCAACAGCAACAAG
Hes	GACACATAGCAACCATTTGAAGCG
Rhodopsin	TGCGGTATTATTGGTTGTGTCG
Rhodopsin	CACGGAACTTAGGATGAGATACGG

Table 1:
Primer sequences

Prospero Sequences				
Uniprot Entry	**Entry name**	**Protein names**	**Gene names**	**Organism**
P34522	HM26_CAEEL	Homeobox protein ceh-26	ceh-26 K12H4.1	Caenorhabditis elegans
K1RD84	K1RD84_CRAGI	Homeobox protein prospero	CGI_10022026	Crassostrea gigas (Pacific oyster) (Crassostrea angulata)
T1FZP0	T1FZP0_HELRO	Uncharacterized protein (Fragment)	HELRODRAFT_69065	Helobdella robusta (Californian leech)
T1G3T0	T1G3T0_HELRO	Uncharacterized protein	HELRODRAFT_79761	Helobdella robusta (Californian leech)
T1G8J3	T1G8J3_HELRO	Uncharacterized protein	HELRODRAFT_92637	Helobdella robusta (Californian leech)
V3ZWV3	V3ZWV3_LOTGI	Uncharacterized protein	LOTGIDRAFT_183824	Lottia gigantea (Giant owl limpet)
P29617	PROS_DROME	Homeobox protein prospero	pros CG17228	Drosophila melanogaster (Fruit fly)
D6WUC4	D6WUC4_TRICA	Prospero	pros TcasGA2_TC010596	Tribolium castaneum (Red flour beetle)
F1QAE1	F1QAE1_DANRE	Uncharacterized protein	prox1a	Danio rerio (Zebrafish) (Brachydanio rerio)
D2DHG1	D2DHG1_DANRE	Prospero-like protein Prox1b (Uncharacterized protein)	prox1b	Danio rerio (Zebrafish) (Brachydanio rerio)
Q92786	PROX1_HUMAN	Prospero homeobox protein 1 (Homeobox prospero-like protein PROX1) (PROX-1)	PROX1	Homo sapiens (Human)
P48437	PROX1_MOUSE	Prospero homeobox protein 1 (Homeobox prospero-like protein PROX1) (PROX-1)	Prox1	Mus musculus (Mouse)
F1RDL6	F1RDL6_DANRE	Uncharacterized protein	prox2	Danio rerio (Zebrafish) (Brachydanio rerio)
Q3B8N5	PROX2_HUMAN	Prospero homeobox protein 2 (Homeobox prospero-like protein PROX2) (PROX-2)	PROX2	Homo sapiens (Human)
Q8BII1	PROX2_MOUSE	Prospero homeobox protein 2 (Homeobox prospero-like protein PROX2) (PROX-2)	Prox2	Mus musculus (Mouse)
Q4H2W9	Q4H2W9_CIOIN	Transcription factor protein (Uncharacterized protein) (Fragment)	Ci-Prox-A prox-a	Ciona intestinalis (Transparent sea squirt) (Ascidia intestinalis)
Q4H2W8	Q4H2W8_CIOIN	Transcription factor protein (Uncharacterized protein)	Ci-Prox-B prox-b	Ciona intestinalis (Transparent sea squirt) (Ascidia intestinalis)
W4YJM0	W4YJM0_STRPU	Uncharacterized protein	Sp-Prox1	Strongylocentrotus purpuratus (Purple sea urchin)
CAY12633	C3W8S4_PLADU	Prospero related homeodomain protein	Prox	Platynereis drumerillii

Table 2:
Prospero sequences for ML phylogenetic trees

Pax Sequences				
Entry	**Entry name**	**Protein names**	**Gene names**	**Organism**
Q4H2Z5	Q4H2Z5_CIOIN	Transcription factor protein (Uncharacterized protein)	Ci-Pax1/9 pax1/9	Ciona intestinalis (Transparent sea squirt) (Ascidia intestinalis)
G5ED14	G5ED14_CAEEL	C04G2.7 (PAX protein)	egl-38 C04G2.7 CELE_C04G2.7	Caenorhabditis elegans
Q9VTX7	Q9VTX7_DROME	Eyegone, isoform A (Eyegone, isoform B) (Eyegone, isoform C)	eyg CG10488 Dmel_CG10488	Drosophila melanogaster (Fruit fly)
O01996	O01996_CAEEL	Y53C12C.1	eyg-1 CELE_Y53C12C.1 Y53C12C.1	Caenorhabditis elegans
P09082	GSB_DROME	Protein gooseberry (BSH9) (Protein gooseberry distal)	gsb GSB-D GSBB CG3388	Drosophila melanogaster (Fruit fly)
P09083	GSBN_DROME	Protein gooseberry-neuro (BSH4) (Protein gooseberry proximal)	gsb-n Gsb-p GSBA CG2692	Drosophila melanogaster (Fruit fly)
V4BBM7	V4BBM7_LOTGI	Uncharacterized protein (Fragment)	LOTGIDRAFT_69535	Lottia gigantea (Giant owl limpet)
V3ZQV3	V3ZQV3_LOTGI	Uncharacterized protein (Fragment)	LOTGIDRAFT_133720	Lottia gigantea (Giant owl limpet)
V3ZI38	V3ZI38_LOTGI	Uncharacterized protein (Fragment)	LOTGIDRAFT_135549	Lottia gigantea (Giant owl limpet)
V4AMZ8	V4AMZ8_LOTGI	Uncharacterized protein (Fragment)	LOTGIDRAFT_142778	Lottia gigantea (Giant owl limpet)
V4A9T6	V4A9T6_LOTGI	Uncharacterized protein	LOTGIDRAFT_161614	Lottia gigantea (Giant owl limpet)
H2Y2B4	H2Y2B4_CIOIN	Uncharacterized protein	pax1/9	Ciona intestinalis (Transparent sea squirt) (Ascidia intestinalis)
F1QRF4	F1QRF4_DANRE	Uncharacterized protein	pax1a	Danio rerio (Zebrafish) (Brachydanio rerio)
F1QJW7	F1QJW7_DANRE	Uncharacterized protein (Fragment)	pax1b	Danio rerio (Zebrafish) (Brachydanio rerio)
Q21272	Q21272_CAEEL	K07C11.1	pax-1 CELE_K07C11.1 K07C11.1	Caenorhabditis elegans
F6VTF7	F6VTF7_CIOIN	Uncharacterized protein	pax2/5/8-b	Ciona intestinalis (Transparent sea squirt) (Ascidia intestinalis)
F1R139	F1R139_DANRE	Uncharacterized protein	pax2b	Danio rerio (Zebrafish) (Brachydanio rerio)
Q21263	Q21263_CAEEL	K06B9.5a	pax-2 CELE_K06B9.5 K06B9.5	Caenorhabditis elegans
F6SH39	F6SH39_CIOIN	Uncharacterized protein	pax3/7	Ciona intestinalis (Transparent sea squirt) (Ascidia intestinalis)
F1Q9S0	F1Q9S0_DANRE	Uncharacterized protein (Fragment)	pax3b	Danio rerio (Zebrafish) (Brachydanio rerio)
G5ED66	G5ED66_CAEEL	F27E5.2	pax-3 CELE_F27E5.2 F27E5.2	Caenorhabditis elegans
F1R840	F1R840_DANRE	Uncharacterized protein (Fragment)	pax4	Danio rerio (Zebrafish) (Brachydanio rerio)
E7FB46	E7FB46_DANRE	Uncharacterized protein	pax5	Danio rerio (Zebrafish) (Brachydanio rerio)
Q9YHZ8	Q9YHZ8_DANRE	Pax-family transcription factor 6.2 (Uncharacterized protein)	pax6b pax6.2	Danio rerio (Zebrafish) (Brachydanio rerio)
F6PW95	F6PW95_CIOIN	Uncharacterized protein	pax6	Ciona intestinalis (Transparent sea squirt) (Ascidia intestinalis)
E7F0A6	E7F0A6_DANRE	Uncharacterized protein	pax7a	Danio rerio (Zebrafish) (Brachydanio rerio)
C0M005	C0M005_DANRE	Paired box protein 7b (Uncharacterized protein)	pax7b	Danio rerio (Zebrafish) (Brachydanio rerio)
F1Q9Q9	F1Q9Q9_DANRE	Uncharacterized protein (Fragment)	pax8	Danio rerio (Zebrafish) (Brachydanio rerio)
Q98865	Q98865_DANRE	Pax9a (Uncharacterized protein)	pax9 Pax9	Danio rerio (Zebrafish) (Brachydanio rerio)
O57416	O57416_DANRE	Transcription factor PAX3 (Uncharacterized protein)	pax3a pax3	Danio rerio (Zebrafish) (Brachydanio rerio)
P15863	PAX1_HUMAN	Paired box protein Pax-1 (HuP48)	PAX1 HUP48	Homo sapiens (Human)
P09084	PAX1_MOUSE	Paired box protein Pax-1	Pax1 Pax-1	Mus musculus (Mouse)
K1QYI7	K1QYI7_CRAGI	Paired box protein Pax-2-A	CGI_10024166	Crassostrea gigas (Pacific oyster) (Crassostrea angulata)
Q90268	PAX2A_DANRE	Paired box protein Pax-2a (No isthmus protein) (Pax[Zf-b])	pax2a noi pax2.1 paxzf-b	Danio rerio (Zebrafish) (Brachydanio rerio)
Q02962	PAX2_HUMAN	Paired box protein Pax-2	PAX2	Homo sapiens (Human)
P32114	PAX2_MOUSE	Paired box protein Pax-2	Pax2 Pax-2	Mus musculus (Mouse)
P23760	PAX3_HUMAN	Paired box protein Pax-3 (HuP2)	PAX3 HUP2	Homo sapiens (Human)
P24610	PAX3_MOUSE	Paired box protein Pax-3	Pax3 Pax-3	Mus musculus (Mouse)
O43316	PAX4_HUMAN	Paired box protein Pax-4	PAX4	Homo sapiens (Human)
P32115	PAX4_MOUSE	Paired box protein Pax-4	Pax4 Pax-4	Mus musculus (Mouse)
Q02548	PAX5_HUMAN	Paired box protein Pax-5 (B-cell-specific transcription factor) (BSAP)	PAX5	Homo sapiens (Human)
Q02650	PAX5_MOUSE	Paired box protein Pax-5 (B-cell-specific transcription factor) (BSAP)	Pax5 Pax-5	Mus musculus (Mouse)
K1QWY6	K1QWY6_CRAGI	Paired box protein Pax-6	CGI_10020873	Crassostrea gigas (Pacific oyster) (Crassostrea angulata)
K1QCD5	K1QCD5_CRAGI	Paired box protein Pax-6	CGI_10027695	Crassostrea gigas (Pacific oyster) (Crassostrea angulata)
P26630	PAX6_DANRE	Paired box protein Pax-6 (Pax[Zf-a])	pax6a pax[zf-a] paxzf-a si:dkeyp-46c10.1	Danio rerio (Zebrafish) (Brachydanio rerio)
O18381	PAX6_DROME	Paired box protein Pax-6 (Protein eyeless)	ey pax6 CG1464	Drosophila melanogaster (Fruit fly)
P26367	PAX6_HUMAN	Paired box protein Pax-6 (Aniridia type II protein) (Oculorhombin)	PAX6 AN2	Homo sapiens (Human)
P63015	PAX6_MOUSE	Paired box protein Pax-6 (Oculorhombin)	Pax6 Pax-6 Sey	Mus musculus (Mouse)
K1RJL2	K1RJL2_CRAGI	Paired box protein Pax-7	CGI_10026438	Crassostrea gigas (Pacific oyster) (Crassostrea angulata)
P23759	PAX7_HUMAN	Paired box protein Pax-7 (HuP1)	PAX7 HUP1	Homo sapiens (Human)
P47239	PAX7_MOUSE	Paired box protein Pax-7	Pax7 Pax-7	Mus musculus (Mouse)
K1R993	K1R993_CRAGI	Paired box protein Pax-8	CGI_10012686	Crassostrea gigas (Pacific oyster) (Crassostrea angulata)
Q06710	PAX8_HUMAN	Paired box protein Pax-8	PAX8	Homo sapiens (Human)
Q00288	PAX8_MOUSE	Paired box protein Pax-8	Pax8 Pax-8	Mus musculus (Mouse)
P55771	PAX9_HUMAN	Paired box protein Pax-9	PAX9	Homo sapiens (Human)
P47242	PAX9_MOUSE	Paired box protein Pax-9	Pax9 Pax-9	Mus musculus (Mouse)
P23757	POXM_DROME	Paired box pox-meso protein (Paired box mesodermal protein)	Poxm POX-M CG9610	Drosophila melanogaster (Fruit fly)
P23758	POXN_DROME	Paired box pox-neuro protein (Paired box neuronal protein)	Poxn pox-n CG8246	Drosophila melanogaster (Fruit fly)
P06601	PRD_DROME	Segmentation protein paired	prd CG6716	Drosophila melanogaster (Fruit fly)
O16117	O16117_DROME	Shaven, isoform A (Sparkling protein)	sv spa CG11049 Dmel_CG11049	Drosophila melanogaster (Fruit fly)
Q8T0M4	Q8T0M4_DROME	CG10704-PA (GH22493p)	toe CG10704 Dmel_CG10704	Drosophila melanogaster (Fruit fly)
Q9V490	Q9V490_DROME	GH14454p (Twin of eyeless, isoform A)	toy CG11186 Dmel_CG11186	Drosophila melanogaster (Fruit fly)
G5EDS1	G5EDS1_CAEEL	F14F3.1a (Variable abnormal-3)	vab-3 CELE_F14F3.1 F14F3.1	Caenorhabditis elegans
Q8MUR8	Q8MUR8_EUPSC	Pax6		Euprymna scolopes

Table 3:
Pax sequences for ML phylogenetic trees

Six Sequences				
Entry	**Entry name**	**Protein names**	**Gene names**	**Organism**
E9PGG2	ANHX_HUMAN	Anomalous homeobox protein	ANHX	Homo sapiens (Human)
Q23175	HM32_CAEEL	Homeobox protein ceh-32	ceh-32 W05E10.3	Caenorhabditis elegans
Q94166	HM33_CAEEL	Homeobox protein ceh-33	ceh-33 C10G8.7	Caenorhabditis elegans
Q94165	HM34_CAEEL	Homeobox protein ceh-34	ceh-34 C10G8.6	Caenorhabditis elegans
T1G0W2	T1G0W2_HELRO	Uncharacterized protein	HELRODRAFT_72129	Helobdella robusta (Californian leech)
T1G2I3	T1G2I3_HELRO	Uncharacterized protein (Fragment)	HELRODRAFT_76318	Helobdella robusta (Californian leech)
T1G701	T1G701_HELRO	Uncharacterized protein	HELRODRAFT_88222	Helobdella robusta (Californian leech)
T1G7F5	T1G7F5_HELRO	Uncharacterized protein (Fragment)	HELRODRAFT_89655	Helobdella robusta (Californian leech)
T1G8C7	T1G8C7_HELRO	Uncharacterized protein	HELRODRAFT_92182	Helobdella robusta (Californian leech)
T1EGZ9	T1EGZ9_HELRO	Uncharacterized protein (Fragment)	HELRODRAFT_124011	Helobdella robusta (Californian leech)
T1EJ85	T1EJ85_HELRO	Uncharacterized protein (Fragment)	HELRODRAFT_142999	Helobdella robusta (Californian leech)
T1EJC9	T1EJC9_HELRO	Uncharacterized protein (Fragment)	HELRODRAFT_143898	Helobdella robusta (Californian leech)
T1FH69	T1FH69_HELRO	Uncharacterized protein	HELRODRAFT_181629	Helobdella robusta (Californian leech)
T1FKB2	T1FKB2_HELRO	Uncharacterized protein	HELRODRAFT_183929	Helobdella robusta (Californian leech)
V4AHM7	V4AHM7_LOTGI	Uncharacterized protein	LOTGIDRAFT_115798	Lottia gigantea (Giant owl limpet)
V3ZUB0	V3ZUB0_LOTGI	Uncharacterized protein	LOTGIDRAFT_129577	Lottia gigantea (Giant owl limpet)
V3Z5W5	V3Z5W5_LOTGI	Uncharacterized protein	LOTGIDRAFT_179424	Lottia gigantea (Giant owl limpet)
A9JPG3	A9JPG3_TRICA	Optix protein (Sine oculis-related homeobox 3)	Optix optix TcasGA2_TC000361	Tribolium castaneum (Red flour beetle)
K1P313	K1P313_CRAGI	Protein sine oculis	CGI_10014640	Crassostrea gigas (Pacific oyster) (Crassostrea angulata)
D6WIY0	D6WIY0_TRICA	Sine oculis	So TcasGA2_TC030468	Tribolium castaneum (Red flour beetle)
F6PRL5	F6PRL5_CIOIN	Uncharacterized protein	six45	Ciona intestinalis (Transparent sea squirt) (Ascidia intestinalis)
H2XLH4	H2XLH4_CIOIN	Uncharacterized protein	six12	Ciona intestinalis (Transparent sea squirt) (Ascidia intestinalis)
Q6DHF9	SIX1A_DANRE	Homeobox protein six1a (Homeobox protein six1b) (Sine oculis homeobox homolo	six1a six1b	Danio rerio (Zebrafish) (Brachydanio rerio)
Q6NZ04	SIX1B_DANRE	Homeobox protein six1b (Homeobox protein six1a) (Sine oculis homeobox homolo	six1b six1 six1a	Danio rerio (Zebrafish) (Brachydanio rerio)
Q9BTH1	Q9BTH1_DANRE	Homeobox protein six2.1 (Sine oculis homeobox homolog 2.1) (Six2.1 protein) (Un	six2a six2.1	Danio rerio (Zebrafish) (Brachydanio rerio)
F6VVA7	F6VVA7_CIOIN	Uncharacterized protein (Fragment)	six36	Ciona intestinalis (Transparent sea squirt) (Ascidia intestinalis)
Q6PCA5	Q6PCA5_DANRE	Sine oculis homeobox homolog 3a (Uncharacterized protein)	six3a	Danio rerio (Zebrafish) (Brachydanio rerio)
O73709	O73709_DANRE	Homeobox protein Six6 (Sine oculis homeobox homolog 3b) (Six3) (Uncharacterize	six3b six3 six6	Danio rerio (Zebrafish) (Brachydanio rerio)
A4IG26	A4IG26_DANRE	Sine oculis homeobox homolog 4.2 (Uncharacterized protein)	six4a six4.2	Danio rerio (Zebrafish) (Brachydanio rerio)
Q5TYZ4	Q5TYZ4_DANRE	Uncharacterized protein	six4b	Danio rerio (Zebrafish) (Brachydanio rerio)
G3V2N2	G3V2N2_HUMAN	Homeobox protein SIX4 (Fragment)	SIX4	Homo sapiens (Human)
D6WFW3	D6WFW3_TRICA	Sine oculis-related homeobox 4	six4 TcasGA2_TC003852	Tribolium castaneum (Red flour beetle)
F6NWW8	F6NWW8_DANRE	Uncharacterized protein	six5 six4.3	Danio rerio (Zebrafish) (Brachydanio rerio)
Q7T3G8	Q7T3G8_DANRE	Sine oculis-related homeobox 6a (Uncharacterized protein)	six6a	Danio rerio (Zebrafish) (Brachydanio rerio)
Q5TYZ2	Q5TYZ2_DANRE	Sine oculis-related homeobox 6b (Uncharacterized protein)	six6b	Danio rerio (Zebrafish) (Brachydanio rerio)
O93282	O93282_DANRE	Homeobox protein Six7 (Sine oculis homeobox homolog 7) (Uncharacterized protei	six7	Danio rerio (Zebrafish) (Brachydanio rerio)
F6PAI1	F6PAI1_DANRE	Uncharacterized protein	six9	Danio rerio (Zebrafish) (Brachydanio rerio)
K1PJH4	K1PJH4_CRAGI	Homeobox protein SIX1	CGI_10009922	Crassostrea gigas (Pacific oyster) (Crassostrea angulata)
Q15475	SIX1_HUMAN	Homeobox protein SIX1 (Sine oculis homeobox homolog 1)	SIX1	Homo sapiens (Human)
Q62231	SIX1_MOUSE	Homeobox protein SIX1 (Sine oculis homeobox homolog 1)	Six1	Mus musculus (Mouse)
Q9NPC8	SIX2_HUMAN	Homeobox protein SIX2 (Sine oculis homeobox homolog 2)	SIX2	Homo sapiens (Human)
Q62232	SIX2_MOUSE	Homeobox protein SIX2 (Sine oculis homeobox homolog 2)	Six2	Mus musculus (Mouse)
K1QUB8	K1QUB8_CRAGI	Homeobox protein SIX3	CGI_10027570	Crassostrea gigas (Pacific oyster) (Crassostrea angulata)
O95343	SIX3_HUMAN	Homeobox protein SIX3 (Sine oculis homeobox homolog 3)	SIX3	Homo sapiens (Human)
Q52KB8	Q52KB8_MOUSE	Homeobox protein SIX3 (Six3 protein)	Six3	Mus musculus (Mouse)
K1RZS7	K1RZS7_CRAGI	Homeobox protein SIX4	CGI_10022945	Crassostrea gigas (Pacific oyster) (Crassostrea angulata)
Q9UIU6	SIX4_HUMAN	Homeobox protein SIX4 (Sine oculis homeobox homolog 4)	SIX4	Homo sapiens (Human)
Q61321	SIX4_MOUSE	Homeobox protein SIX4 (Sine oculis homeobox homolog 4) (Skeletal muscle-specifi	Six4 Arec3	Mus musculus (Mouse)
Q8N196	SIX5_HUMAN	Homeobox protein SIX5 (DM locus-associated homeodomain protein) (Sine oculis h	SIX5 DMAHP	Homo sapiens (Human)
P70178	SIX5_MOUSE	Homeobox protein SIX5 (DM locus-associated homeodomain protein homolog) (Sin	Six5 Dmahp	Mus musculus (Mouse)
O95475	SIX6_HUMAN	Homeobox protein SIX6 (Homeodomain protein OPTX2) (Optic homeobox 2) (Sine	SIX6 OPTX2 SIX9	Homo sapiens (Human)
Q9QZ28	SIX6_MOUSE	Homeobox protein SIX6 (Optic homeobox 2) (Sine oculis homeobox homolog 6) (Si	Six6 Optx2 Six9	Mus musculus (Mouse)
W4YNK2	W4YNK2_STRPU	Uncharacterized protein	Sp-Six1/2	Strongylocentrotus purpuratus (Purple sea urchin)
W4YNK3	W4YNK3_STRPU	Uncharacterized protein	Sp-Six4	Strongylocentrotus purpuratus (Purple sea urchin)
W4YSW9	W4YSW9_STRPU	Uncharacterized protein	Sp-Six3	Strongylocentrotus purpuratus (Purple sea urchin)
O17894	O17894_CAEEL	F56A12.1	unc-39 CELE_F56A12.1 F56A12.1	Caenorhabditis elegans
A7S598	A7S598_NEMVE	Predicted protein (Fragment)	v1g56637	Nematostella vectensis (Starlet sea anemone)
A7S005	A7S005_NEMVE	Predicted protein	v1g99489	Nematostella vectensis (Starlet sea anemone)
A7SPN4	A7SPN4_NEMVE	Predicted protein	v1g126214	Nematostella vectensis (Starlet sea anemone)
A7ST96	A7ST96_NEMVE	Predicted protein	v1g130873	Nematostella vectensis (Starlet sea anemone)
A7SZ27	A7SZ27_NEMVE	Predicted protein (Fragment)	v1g138693	Nematostella vectensis (Starlet sea anemone)
A7S425	A7S425_NEMVE	Predicted protein	v1g206468	Nematostella vectensis (Starlet sea anemone)
V5NS22	V5NS22_EUPSC	Six		Euprymna scolopes

Table 4:
Six sequences for ML phylogenetic trees

Notch Sequences				
Entry	**Entry name**	**Protein names**	**Gene names**	**Organism**
O35185	BHE40_MOUSE	Class E basic helix-loop-helix protein 40 (bHLHe40) (Class B basic helix-loop-helix pr	Bhlhe40 Bhlhb2 Clast5 Stra13	Mus musculus (Mouse)
Q99PV5	BHE41_MOUSE	Class E basic helix-loop-helix protein 41 (bHLHe41) (Class B basic helix-loop-helix pr	Bhlhe41 Bhlhb3 Dec2	Mus musculus (Mouse)
O14503	BHE40_HUMAN	Class E basic helix-loop-helix protein 40 (bHLHe40) (Class B basic helix-loop-helix pr	BHLHE40 BHLHB2 DEC1 SHARP2 STRA13	Homo sapiens (Human)
Q9C0J9	BHE41_HUMAN	Class E basic helix-loop-helix protein 41 (bHLHe41) (Class B basic helix-loop-helix pr	BHLHE41 BHLHB3 DEC2 SHARP1	Homo sapiens (Human)
A1Z7S7	A1Z7S7_DROME	CG8027 (EC 2.7.-.-) (FI02838p)	CG8027-RA CG8027 Dmel_CG8027	Drosophila melanogaster (Fruit fly)
Q9VGZ5	Q9VGZ5_DROME	Clockwork orange, isoform A	cwo CG17100 Dmel_CG17100	Drosophila melanogaster (Fruit fly)
Q26263	DPN_DROME	Protein deadpan	dpn CG8704	Drosophila melanogaster (Fruit fly)
Q6NY50	Q6NY50_DANRE	BHLH protein DEC1 (Bhlhe40 protein) (Uncharacterized protein)	bhlhe40 bhlhb2 DEC1	Danio rerio (Zebrafish) (Brachydanio rerio)
Q2PGD2	Q2PGD2_DANRE	BHLH protein DEC2 (Basic helix-loop-helix domain containing, class B, 3 like) (Dec2)	bhlhe41 bhlhb3l DEC2 DKEY-66C4.5-001	Danio rerio (Zebrafish) (Brachydanio rerio)
F6ZDG1	F6ZDG1_CIOIN	Uncharacterized protein (Fragment)		Ciona intestinalis (Transparent sea squirt) (Ascidia intestinalis)
F7AFG0	F7AFG0_CIOIN	Uncharacterized protein (Fragment)		Ciona intestinalis (Transparent sea squirt) (Ascidia intestinalis)
F7AFG7	F7AFG7_CIOIN	Uncharacterized protein (Fragment)		Ciona intestinalis (Transparent sea squirt) (Ascidia intestinalis)
F7AZ47	F7AZ47_CIOIN	Uncharacterized protein	n	Ciona intestinalis (Transparent sea squirt) (Ascidia intestinalis)
K1PK27	K1PK27_CRAGI	N-acetylglucosamine-1-phosphotransferase subunits alpha/beta	CGI_10013374	Crassostrea gigas (Pacific oyster) (Crassostrea angulata)
Q5RGJ8	GNPTA_DANRE	N-acetylglucosamine-1-phosphotransferase subunits alpha/beta (EC 2.7.8.17) (Glcl	gnptab gnpta si:ch211-234f20.3 zgc:122985	Danio rerio (Zebrafish) (Brachydanio rerio)
Q69ZN6	GNPTA_MOUSE	N-acetylglucosamine-1-phosphotransferase subunits alpha/beta (EC 2.7.8.17) (Glcl	Gnptab Gnpta Kiaa1208	Mus musculus (Mouse)
Q3T906	GNPTA_HUMAN	N-acetylglucosamine-1-phosphotransferase subunits alpha/beta (EC 2.7.8.17) (Glcl	GNPTAB GNPTA KIAA1208	Homo sapiens (Human)
T1G0U1	T1G0U1_HELRO	Uncharacterized protein	HELRODRAFT_72015	Helobdella robusta (Californian leech)
T1G236	T1G236_HELRO	Uncharacterized protein	HELRODRAFT_75318	Helobdella robusta (Californian leech)
T1G620	T1G620_HELRO	Uncharacterized protein	HELRODRAFT_85704	Helobdella robusta (Californian leech)
T1G9M2	T1G9M2_HELRO	Uncharacterized protein	HELRODRAFT_98385	Helobdella robusta (Californian leech)
T1FLN6	T1FLN6_HELRO	Uncharacterized protein	HELRODRAFT_184646	Helobdella robusta (Californian leech)
V4AWV7	V4AWV7_LOTGI	Uncharacterized protein (Fragment)	LOTGIDRAFT_67089	Lottia gigantea (Giant owl limpet)
V4A3Y9	V4A3Y9_LOTGI	Uncharacterized protein (Fragment)	LOTGIDRAFT_74634	Lottia gigantea (Giant owl limpet)
V4CNC5	V4CNC5_LOTGI	Uncharacterized protein (Fragment)	LOTGIDRAFT_97309	Lottia gigantea (Giant owl limpet)
V4ALY1	V4ALY1_LOTGI	Uncharacterized protein (Fragment)	LOTGIDRAFT_116653	Lottia gigantea (Giant owl limpet)
V4ADJ5	V4ADJ5_LOTGI	Uncharacterized protein	LOTGIDRAFT_153818	Lottia gigantea (Giant owl limpet)
V3ZUW0	V3ZUW0_LOTGI	Uncharacterized protein	LOTGIDRAFT_168395	Lottia gigantea (Giant owl limpet)
V3Z2B4	V3Z2B4_LOTGI	Uncharacterized protein	LOTGIDRAFT_168397	Lottia gigantea (Giant owl limpet)
V4BA37	V4BA37_LOTGI	Uncharacterized protein	LOTGIDRAFT_171867	Lottia gigantea (Giant owl limpet)
V4BGJ2	V4BGJ2_LOTGI	Uncharacterized protein (Fragment)	LOTGIDRAFT_184955	Lottia gigantea (Giant owl limpet)
V3ZJE0	V3ZJE0_LOTGI	Uncharacterized protein	LOTGIDRAFT_209713	Lottia gigantea (Giant owl limpet)
V4AQQ8	V4AQQ8_LOTGI	Uncharacterized protein	LOTGIDRAFT_238796	Lottia gigantea (Giant owl limpet)
F1QCA7	F1QCA7_DANRE	Uncharacterized protein	notch1b	Danio rerio (Zebrafish) (Brachydanio rerio)
P46530	NOTC1_DANRE	Neurogenic locus notch homolog protein 1 (Notch 1) [Cleaved into: Notch 1 extrac	notch1a notch	Danio rerio (Zebrafish) (Brachydanio rerio)
Q01705	NOTC1_MOUSE	Neurogenic locus notch homolog protein 1 (Notch 1) (Motch A) (mT14) (p300) [Cle	Notch1 Motch	Mus musculus (Mouse)
F1R9H8	F1R9H8_DANRE	Uncharacterized protein	notch2	Danio rerio (Zebrafish) (Brachydanio rerio)
O35516	NOTC2_MOUSE	Neurogenic locus notch homolog protein 2 (Notch 2) (Motch B) [Cleaved into: Notc	Notch2	Mus musculus (Mouse)
F1QZF2	F1QZF2_DANRE	Uncharacterized protein	notch3	Danio rerio (Zebrafish) (Brachydanio rerio)
Q61982	NOTC3_MOUSE	Neurogenic locus notch homolog protein 3 (Notch 3) [Cleaved into: Notch 3 extrac	Notch3	Mus musculus (Mouse)
P31695	NOTC4_MOUSE	Neurogenic locus notch homolog protein 4 (Notch 4) [Cleaved into: Transforming p	Notch4 Int-3 Int3	Mus musculus (Mouse)
P46531	NOTC1_HUMAN	Neurogenic locus notch homolog protein 1 (Notch 1) (hN1) (Translocation-associat	NOTCH1 TAN1	Homo sapiens (Human)
Q04721	NOTC2_HUMAN	Neurogenic locus notch homolog protein 2 (Notch 2) (hN2) [Cleaved into: Notch 2 e	NOTCH2	Homo sapiens (Human)
Q9UM47	NOTC3_HUMAN	Neurogenic locus notch homolog protein 3 (Notch 3) [Cleaved into: Notch 3 extrac	NOTCH3	Homo sapiens (Human)
Q99466	NOTC4_HUMAN	Neurogenic locus notch homolog protein 4 (Notch 4) (hNotch4) [Cleaved into: Notc	NOTCH4 INT3	Homo sapiens (Human)
K1S0U1	K1S0U1_CRAGI	Neurogenic locus Notch protein	CGI_10004834	Crassostrea gigas (Pacific oyster) (Crassostrea angulata)
K1PPU8	K1PPU8_CRAGI	Neurogenic locus Notch protein	CGI_10013186	Crassostrea gigas (Pacific oyster) (Crassostrea angulata)
P07207	NOTCH_DROME	Neurogenic locus Notch protein [Cleaved into: Processed neurogenic locus Notch p	N CG3936	Drosophila melanogaster (Fruit fly)
X1WEZ2	X1WEZ2_DANRE	Uncharacterized protein	notchl	Danio rerio (Zebrafish) (Brachydanio rerio)
Q9VJ16	Q9VJ16_DROME	CG10446-PA (GH26014p)	Side CG10446 Dmel_CG10446	Drosophila melanogaster (Fruit fly)
W4YEF0	W4YEF0_STRPU	Uncharacterized protein	Sp-Notch	Strongylocentrotus purpuratus (Purple sea urchin)

Table 5:
Notch sequences for ML phylogenetic trees

Hes Sequences				
Entry	**Entry name**	**Protein names**		**Gene names**
A3KQ56	A3KQ56_DANRE	Her1 protein (Uncharacterized protein)	her1	Danio rerio (Zebrafish) (Brachydanio rerio)
O14503	BHE40_HUMAN	Class E basic helix-loop-helix protein 40 (bHLHe40) (Class B basic helix-loop-helix pr	BHLHE40 BHLHB2 DEC1 SHARP2 STRA13	Homo sapiens (Human)
O35185	BHE40_MOUSE	Class E basic helix-loop-helix protein 40 (bHLHe40) (Class B basic helix-loop-helix pr	Bhlhe40 Bhlhb2 Clast5 Stra13	Mus musculus (Mouse)
Q9C0J9	BHE41_HUMAN	Class E basic helix-loop-helix protein 41 (bHLHe41) (Class B basic helix-loop-helix pr	BHLHE41 BHLHB3 DEC2 SHARP1	Homo sapiens (Human)
Q99PV5	BHE41_MOUSE	Class E basic helix-loop-helix protein 41 (bHLHe41) (Class B basic helix-loop-helix pr	Bhlhe41 Bhlhb3 Dec2	Mus musculus (Mouse)
Q26263	DPN_DROME	Protein deadpan	dpn CG8704	Drosophila melanogaster (Fruit fly)
P13097	ESM7_DROME	Enhancer of split m7 protein (E(spl)m7)	HLHm7 CG8361	Drosophila melanogaster (Fruit fly)
P13098	ESM8_DROME	Enhancer of split m8 protein (E(spl)m8)	E(spl) m8 CG8365	Drosophila melanogaster (Fruit fly)
Q01069	ESMB_DROME	Enhancer of split mbeta protein (E(spl)mbeta) (HLH-mbeta) (Split locus enhancer pr	HLHmbeta CG14548	Drosophila melanogaster (Fruit fly)
Q01070	ESMC_DROME	Enhancer of split mgamma protein (E(spl)mgamma) (Split locus enhancer protein m	HLHmgamma CG8333	Drosophila melanogaster (Fruit fly)
Q01071	ESMD_DROME	Enhancer of split mdelta protein (E(spl)mdelta) (HLH-mdelta) (Split locus enhancer	HLHmdelta CG8328	Drosophila melanogaster (Fruit fly)
F1Q965	F1Q965_DANRE	Uncharacterized protein (Fragment)	her8.2	Danio rerio (Zebrafish) (Brachydanio rerio)
F1QJ81	F1QJ81_DANRE	Uncharacterized protein (Fragment)	her8a	Danio rerio (Zebrafish) (Brachydanio rerio)
F1RDU0	F1RDU0_DANRE	Uncharacterized protein (Fragment)	her3	Danio rerio (Zebrafish) (Brachydanio rerio)
F6QRK3	F6QRK3_CIOIN	Uncharacterized protein (Fragment)	hey	Ciona intestinalis (Transparent sea squirt) (Ascidia intestinalis)
F6TXK6	F6TXK6_CIOIN	Uncharacterized protein	e(spl)/hairy-b	Ciona intestinalis (Transparent sea squirt) (Ascidia intestinalis)
F7A592	F7A592_CIOIN	Uncharacterized protein	e(spl)/hairy-c	Ciona intestinalis (Transparent sea squirt) (Ascidia intestinalis)
P14003	HAIR_DROME	Protein hairy	h CG6494	Drosophila melanogaster (Fruit fly)
Q6QB00	HELT_DANRE	Hairy and enhancer of split-related protein helt (HES/HEY-like transcription factor)	helt zgc:109704	Danio rerio (Zebrafish) (Brachydanio rerio)
A6NFD8	HELT_HUMAN	Hairy and enhancer of split-related protein HELT (HES/HEY-like transcription factor	HELT	Homo sapiens (Human)
Q7TS99	HELT_MOUSE	Hairy and enhancer of split-related protein HELT (HES/HEY-like transcription factor	Helt Hesl Mgn	Mus musculus (Mouse)
Q14469	HES1_HUMAN	Transcription factor HES-1 (Class B basic helix-loop-helix protein 39) (bHLHb39) (Ha	HES1 BHLHB39 HL HRY	Homo sapiens (Human)
P35428	HES1_MOUSE	Transcription factor HES-1 (Hairy and enhancer of split 1)	Hes1 Hes-1	Mus musculus (Mouse)
Q9Y543	HES2_HUMAN	Transcription factor HES-2 (Class B basic helix-loop-helix protein 40) (bHLHb40) (Ha	HES2 BHLHB40	Homo sapiens (Human)
O54792	HES2_MOUSE	Transcription factor HES-2 (Hairy and enhancer of split 2)	Hes2	Mus musculus (Mouse)
Q9HCC6	HES4_HUMAN	Transcription factor HES-4 (hHES4) (Class B basic helix-loop-helix protein 42) (bHLH	HES4 BHLHB42	Homo sapiens (Human)
Q5TA89	HES5_HUMAN	Transcription factor HES-5 (Class B basic helix-loop-helix protein 38) (bHLHb38) (Ha	HES5 BHLHB38	Homo sapiens (Human)
P70120	HES5_MOUSE	Transcription factor HES-5 (Hairy and enhancer of split 5)	Hes5 Hes-5	Mus musculus (Mouse)
Q8AXV6	HEY1_DANRE	Hairy/enhancer-of-split related with YRPW motif protein 1	hey1	Danio rerio (Zebrafish) (Brachydanio rerio)
Q9Y5J3	HEY1_HUMAN	Hairy/enhancer-of-split related with YRPW motif protein 1 (Cardiovascular helix-lo	HEY1 BHLHB31 CHF2 HERP2 HESR1 HRT1	Homo sapiens (Human)
Q9WV93	HEY1_MOUSE	Hairy/enhancer-of-split related with YRPW motif protein 1 (Hairy and enhancer of s	Hey1 Herp2 Hesr1 Hrt1	Mus musculus (Mouse)
Q9I9L0	HEY2_DANRE	Hairy/enhancer-of-split related with YRPW motif protein 2 (Protein gridlock)	hey2 grl zgc:136746	Danio rerio (Zebrafish) (Brachydanio rerio)
Q9UBP5	HEY2_HUMAN	Hairy/enhancer-of-split related with YRPW motif protein 2 (Cardiovascular helix-lo	HEY2 BHLHB32 CHF1 GRL HERP HERP1 HRT2	Homo sapiens (Human)
Q9QUS4	HEY2_MOUSE	Hairy/enhancer-of-split related with YRPW motif protein 2 (HES-related repressor p	Hey2 Chf1 Herp Herp1 Hesr2 Hrt2	Mus musculus (Mouse)
Q7KM13	HEY_DROME	Hairy/enhancer-of-split related with YRPW motif protein	Hey Hesr-1 CG11194	Drosophila melanogaster (Fruit fly)
Q8AXV5	HEYL_DANRE	Hairy/enhancer-of-split related with YRPW motif-like protein	heyl si:dkey-148n22.1	Danio rerio (Zebrafish) (Brachydanio rerio)
Q9NQ87	HEYL_HUMAN	Hairy/enhancer-of-split related with YRPW motif-like protein (hHeyL) (Class B basic	HEYL BHLHB33 HRT3	Homo sapiens (Human)
Q9DBX7	HEYL_MOUSE	Hairy/enhancer-of-split related with YRPW motif-like protein (Hairy and enhancer o	Heyl Hesr3 Hrt3	Mus musculus (Mouse)
K1PP05	K1PP05_CRAGI	Transcription factor HES-1-B	CGI_10019616	Crassostrea gigas (Pacific oyster) (Crassostrea angulata)
K1PZ92	K1PZ92_CRAGI	Transcription factor HES-1	CGI_10014039	Crassostrea gigas (Pacific oyster) (Crassostrea angulata)
K1QKA1	K1QKA1_CRAGI	Hairy/enhancer-of-split related with YRPW motif protein 1	CGI_10018323	Crassostrea gigas (Pacific oyster) (Crassostrea angulata)
K1QQK8	K1QQK8_CRAGI	Hairy and enhancer of split-related protein HELT	CGI_10022440	Crassostrea gigas (Pacific oyster) (Crassostrea angulata)
K1R9L1	K1R9L1_CRAGI	Transcription factor HES-1	CGI_10017446	Crassostrea gigas (Pacific oyster) (Crassostrea angulata)
Q9VGZ5	Q9VGZ5_DROME	Clockwork orange, isoform A	cwo CG17100 Dmel_CG17100	Drosophila melanogaster (Fruit fly)
Q9VJ16	Q9VJ16_DROME	CG10446-PA (GH26014p)	Side CG10446 Dmel_CG10446	Drosophila melanogaster (Fruit fly)
V3Z2B4	V3Z2B4_LOTGI	Uncharacterized protein	LOTGIDRAFT_168397	Lottia gigantea (Giant owl limpet)
V3ZJE0	V3ZJE0_LOTGI	Uncharacterized protein	LOTGIDRAFT_209713	Lottia gigantea (Giant owl limpet)
V3ZUW0	V3ZUW0_LOTGI	Uncharacterized protein	LOTGIDRAFT_168395	Lottia gigantea (Giant owl limpet)
V4A3Y9	V4A3Y9_LOTGI	Uncharacterized protein (Fragment)	LOTGIDRAFT_74634	Lottia gigantea (Giant owl limpet)
V4ADJ5	V4ADJ5_LOTGI	Uncharacterized protein	LOTGIDRAFT_153818	Lottia gigantea (Giant owl limpet)
V4ALY1	V4ALY1_LOTGI	Uncharacterized protein (Fragment)	LOTGIDRAFT_116653	Lottia gigantea (Giant owl limpet)
V4AWV7	V4AWV7_LOTGI	Uncharacterized protein (Fragment)	LOTGIDRAFT_67089	Lottia gigantea (Giant owl limpet)
V4BA37	V4BA37_LOTGI	Uncharacterized protein	LOTGIDRAFT_171867	Lottia gigantea (Giant owl limpet)
V4CNC5	V4CNC5_LOTGI	Uncharacterized protein (Fragment)	LOTGIDRAFT_97309	Lottia gigantea (Giant owl limpet)
W4XTR1	W4XTR1_STRPU	Uncharacterized protein	Sp-Hairy	Strongylocentrotus purpuratus (Purple sea urchin)
W4XTR2	W4XTR2_STRPU	Uncharacterized protein	Sp-Hairy2/4	Strongylocentrotus purpuratus (Purple sea urchin)
W4Y187	W4Y187_STRPU	Uncharacterized protein	Sp-Hey	Strongylocentrotus purpuratus (Purple sea urchin)
W4YIV6	W4YIV6_STRPU	Uncharacterized protein	Sp-Hey4	Strongylocentrotus purpuratus (Purple sea urchin)
W4Z0H3	W4Z0H3_STRPU	Uncharacterized protein	Sp-HesC	Strongylocentrotus purpuratus (Purple sea urchin)

Table 6:
Hes sequences for ML phylogenetic trees

Eya Sequences				
Entry	**Entry name**	**Protein names**	**Gene names**	**Organism**
A9VB82	A9VB82_MONBE	Predicted protein	29484	Monosiga brevicollis (Choanoflagellate)
A8J031	A8J031_CHLRE	Predicted protein	CHLREDRAFT_191069	Chlamydomonas reinhardtii (Chlamydomonas smithii)
P97480	EYA3_MOUSE	Eyes absent homolog 3 (EC 3.1.3.48)	Eya3	Mus musculus (Mouse)
O08575	EYA2_MOUSE	Eyes absent homolog 2 (EC 3.1.3.48)	Eya2 Eab1	Mus musculus (Mouse)
Q9Z191	EYA4_MOUSE	Eyes absent homolog 4 (EC 3.1.3.48)	Eya4	Mus musculus (Mouse)
O82162	O82162_ARATH	At2g35320/T4C15.1 (EYA-like protein) (Similar to eyes absent protein) (Tyrosine-sp	EYA At2g35320 At2g35320/T4C15.1	Arabidopsis thaliana (Mouse-ear cress)
O17670	O17670_CAEEL	Eyes absent homolog (EC 3.1.3.48)	eya-1 C49A1.4 CELE_C49A1.4	Caenorhabditis elegans
F6HTB0	F6HTB0_VITVI	Putative uncharacterized protein	VIT_02s0012g01000	Vitis vinifera (Grape)
F6UD40	F6UD40_CIOIN	Eyes absent homolog (EC 3.1.3.48)	LOC101243276	Ciona intestinalis (Transparent sea squirt) (Ascidia intestinalis)
O95677	EYA4_HUMAN	Eyes absent homolog 4 (EC 3.1.3.48)	EYA4	Homo sapiens (Human)
D0MQA0	D0MQA0_PHYIT	Eyes absent family protein	PITG_00231	Phytophthora infestans (strain T30-4) (Potato late blight fungus)
C3Y1E5	C3Y1E5_BRAFL	Eyes absent homolog (EC 3.1.3.48)	BRAFLDRAFT_83679	Branchiostoma floridae (Florida lancelet) (Amphioxus)
A8XU56	A8XU56_CAEBR	Eyes absent homolog (EC 3.1.3.48)	eya-1 Cbr-eya-1 cbr-eya-1 CBG18807 CBG_18807	Caenorhabditis briggsae
A7SG20	A7SG20_NEMVE	Eyes absent homolog (EC 3.1.3.48) (Fragment)	v1g116873	Nematostella vectensis (Starlet sea anemone)
O00167	EYA2_HUMAN	Eyes absent homolog 2 (EC 3.1.3.48)	EYA2 EAB1	Homo sapiens (Human)
Q05201	EYA_DROME	Developmental protein eyes absent (EC 3.1.3.48) (Protein Clift)	eya cli CG9554	Drosophila melanogaster (Fruit fly)
Q99504	EYA3_HUMAN	Eyes absent homolog 3 (EC 3.1.3.48)	EYA3	Homo sapiens (Human)
A3KQ54	A3KQ54_DANRE	Eyes absent homolog (EC 3.1.3.48)	eya3	Danio rerio (Zebrafish) (Brachydanio rerio)
Q66HX1	Q66HX1_DANRE	Eyes absent homolog (EC 3.1.3.48)	eya2 zgc:92279	Danio rerio (Zebrafish) (Brachydanio rerio)
C5YZG4	C5YZG4_SORBI	Putative uncharacterized protein Sb09g002540	Sb09g002540 SORBIDRAFT_09g002540	Sorghum bicolor (Sorghum) (Sorghum vulgare)
I1H1W7	I1H1W7_BRADI	Uncharacterized protein	BRADI1G51790	Brachypodium distachyon (Purple false brome) (Trachynia distachya)
P97767	EYA1_MOUSE	Eyes absent homolog 1 (EC 3.1.3.16) (EC 3.1.3.48)	Eya1	Mus musculus (Mouse)
B3S2N8	B3S2N8_TRIAD	Eyes absent homolog (EC 3.1.3.48)	TRIADDRAFT_58093	Trichoplax adhaerens (Trichoplax reptans)
E9QGF5	E9QGF5_DANRE	Eyes absent homolog (EC 3.1.3.48)	eya4	Danio rerio (Zebrafish) (Brachydanio rerio)
Q99502	EYA1_HUMAN	Eyes absent homolog 1 (EC 3.1.3.16) (EC 3.1.3.48)	EYA1	Homo sapiens (Human)
F1QNU4	F1QNU4_DANRE	Eyes absent homolog (EC 3.1.3.48)	eya1	Danio rerio (Zebrafish) (Brachydanio rerio)
W4YDN9	W4YDN9_STRPU	Eyes absent homolog (EC 3.1.3.48)	Sp-Eya	Strongylocentrotus purpuratus (Purple sea urchin)
G4VPW6	G4VPW6_SCHMA	Eyes absent homolog (EC 3.1.3.48)	Smp_173090	Schistosoma mansoni (Blood fluke)
V5NSK2	V5NSK2_EUPSC	Eyes absent homolog		Euprymna scolopes
Q7Q8A3	Q7Q8A3_ANOGA	Eyes absent homolog (EC 3.1.3.48) (Fragment)	AgaP_AGAP008726	Anopheles gambiae (African malaria mosquito)
V5NSK2	V5NSK2_EUPSC	Eyes absent homolog		Euprymna scolopes

Table 7:
Eya sequences for ML phylogenetic trees

References

Allen RD, Metuzals J, Tasaki I, Brady ST, and Gilbert SP (1982). Fast axonal transport in squid giant axon. *Science*, **218**(4577), 1127-1129.

Albertin CB, Simakov O, Mitros T, Wang ZY, Pungor JR, Edsinger-Gonzales E, ... and Rokhsar DS (2015). The octopus genome and the evolution of cephalopod neural and morphological novelties. *Nature*, *524*(7564), 220-224.

Arendt D (2003) Evolution of eyes and photoreceptor cells *International Journal of Developmental Biology* **47** (563).

Arnold JM (1965). Normal embryonic stages of the squid, Loligo pealii (Lesueur). *Biological Bulletin*, 24-32.

Arnold JM (1966). On the occurrence of microtubules in the developing lens of the squid Loligo pealii. *Journal of ultrastructure research*, *14*(5), 534-539.

Arnold JM (1967). Fine structure of the development of the cephalopod lens. *Journal of ultrastructure research*, *17*(5), 527-543.

Arnold JM and Williams-Arnold LD (1976). The egg cortex problem as seen through the squid eye. *American Zoologist*, *16*(3), 421-446.

Bao, S., Fischbach, K. F., Corbin, V., & Cagan, R. L. (2010). Preferential adhesion maintains separation of ommatidia in the Drosophila eye. *Developmental biology*, *344*(2), 948-956.

Baratte, S., Andouche, A., & Bonnaud, L. (2007). Engrailed in cephalopods: a key gene related to the emergence of morphological novelties. *Development genes and evolution*, *217*(5), 353-362.

Bassett, E. A., & Wallace, V. A. (2012). Cell fate determination in the vertebrate retina. *Trends in neurosciences*, *35*(9), 565-573.

Bateman A, Coin L, Durbin R, et al. (2004). The Pfam protein families database. *Nucleic acids research*, *32*(suppl 1), D138-D141.

Baye LM and Link BA (2008). Nuclear migration during retinal development. *Brain research*, *1192*, 29-36.

Bibliowicz J, Tittle RK, & Gross JM (2011). Towards a better understanding of human eye disease: insights from the zebrafish, Danio rerio. *Progress in molecular biology and translational science*, *100*, 287.

Blair SS (1999) Eye development: Notch lends a handedness *Current Biology,* **9:** R356-R360

Bonini NM (1997). Surviving Drosophila eye development. *Cell death and differentiation*, *4*(1), 4-11.

Boycott, B. B. (1961). The functional organization of the brain of the cuttlefish Sepia officinalis. *Proceedings of the Royal Society of London B: Biological Sciences*, *153*(953), 503-534.

Brady ST, Lasek RJ, and Allen RD (1982) Fast axonal transport in extruded axoplasm from squid giant axon. *Science* **218**(4577) 1129-1131.

Buresi A, Baratte S, Da Silva C, and Bonnaud L (2012). orthodenticle/otx ortholog expression in the anterior brain and eyes of Sepia officinalis (Mollusca, Cephalopoda). *Gene Expression Patterns*, *12*(3), 109-116.

Charlton-Perkins M, Brown NL, Cook TA (2011) The lens in focus: a comparison of lens development in *Drosophila* and vertebrates. Molecular Genetics and Genomics **286** (3-4) 189-213.

Cook T, Pichaud F, Sonneville R, Papatsendko D, Desplan C (2003) Distinction between color photoreceptor cell fate is controlled by Prospero in *Drosophila* **4**:853-864

Cvekl A, Ashery-Padan R (2014) The cellular and molecular mechanisms of vertebrate lens development. *Development* **141**: 4432-4447.

Dyer MA, Livesey FJ, Cepko CL, Oliver G (2003) Prox1 function controls progenitor cell proliferation and horizontal cell genesis in the mammalian retina *Nature Genetics* **34**:53-58.

Fernald RD (2004) Eyes: Variety, Development and Evolution. Brain Behav Evol; 64:141-147

Fernald RD (2006). Casting a genetic light on the evolution of eyes. *Science*, *313*(5795), 1914-1918.

Finn RD, Clements J, & Eddy SR (2011). HMMER web server: interactive sequence similarity searching. *Nucleic acids research*, gkr367.

Gehring WJ, Ikeo K (1999) Pax 6: mastering eye morphogenesis and eye evolution, *Trends in Genetics*, **15** (9) 371-377.

Gehring WJ (1996) The master control gene for morphogenesis and evolution of the eye. *Genes to Cells* **1** 1265-2443.

Gehring WJ (2005) THE WILHEMINE E. KEY 2004 INVITATIONAL LECTURE: New Perspectives on Eye Development and the Evolution of Eyes and Photoreceptors *J Hered 96 (3): 171-184*.

Geling A, Steiner H, Willem M, Bally-Cuif L, & Haass C (2002). A γ-secretase inhibitor blocks Notch signaling in vivo and causes a severe neurogenic phenotype in zebrafish. *EMBO reports*, *3*(7), 688-694.

Gilbert D L, Adelman W J, and Arnold JM (1990). *Squid as experimental animals*. Springer Science & Business Media.

Go MJ, Eastman DS, and Artavanis-Tsakonas S (1998). Cell proliferation control by Notch signaling in Drosophila development. *Development*, *125*(11), 2031-2040.

Grasso FW (2014). 5 The octopus with two brains: how are distributed and central representations integrated in the octopus central nervous system?. *Cephalopod Cognition*, 94.

Guindon S, Dufayard JF, Lefort V, Anisimova M, Hordijk W, and Gascuel O. (2010). New algorithms and methods to estimate maximum-likelihood phylogenies: assessing the performance of PhyML 3.0. *Systematic biology*, *59*(3), 307-321.

Gunhaga, L. (2011). The lens: a classical model of embryonic induction providing new insights into cell determination in early development. *Philosophical Transactions of the Royal Society B: Biological Sciences*, *366*(1568), 1193-1203.

Halder G, Callaerts P, Gehring WJ (1995) New perspectives on eye evolution *Current Opinion in Genetics & Development*, **5** (5), 602-609.

Hartmann B, Lee PN, Kang YY, Tomarev S, De Couet HG, and Callaerts P (2003). Pax6 in the sepiolid squid Euprymna scolopes: evidence for a role in eye, sensory organ and brain development. *Mechanisms of development*, *120*(2), 177-183.

Hodgkin AL, Katz B (1949) The effect of sodium ions on the electrical activity of the giant axon of the squid. *The Journal of Physiology*. **108**(1), 37-77

Hodgkin AL, Huxley AF (1952) Currents carried by sodium and potassium ions through the membrane of the giant axon of *Loligo*. *The Journal of Physiology*. **116**(4), 449-472

Hodgkin AL, and Huxley AF (1952). The dual effect of membrane potential on sodium conductance in the giant axon of Loligo. *The Journal of physiology*, **116**(4), 497-506.

Hodgkin AL, Huxley AF & Katz B (1952). Measurement of current-voltage relations in the membrane of the giant axon of Loligo. *The Journal of physiology*, **116**(4), 424.

Jacobson L (2005). Essential fish habitat source document: longfin inshore squid, Loligo pealeii, life history and habitat characteristics. *NOAA Technical memorandum, NMFS-NE*, *193*.

Katoh K and Standley DM (2013). MAFFT multiple sequence alignment software version 7: improvements in performance and usability. *Molecular biology and evolution*, **30**(4), 772-780.

Kingston, A. C., Wardill, T. J., Hanlon, R. T., & Cronin, T. W. (2015). An unexpected diversity of photoreceptor classes in the Longfin squid, Doryteuthis pealeii. *PloS one*, *10*(9), e0135381.

Kearse M, Moir R, Wilson A, et al. (2012). Geneious Basic: an integrated and extendable desktop software platform for the organization and analysis of sequence data. *Bioinformatics*, *28*(12), 1647-1649.

Kumar, J. P. (2010). 1 Retinal Determination: The Beginning of Eye Development. *Current topics in developmental biology*, *93*, 1.

Kumar JP (2010) Chapter one - Retinal Determination: The Beginning of Eye Development, In: Ross L. Cagan and Thomas A. Reh, Editor(s), *Current Topics in Developmental Biology*, Academic Press (93) 1-28

Lamb, T. D., Collin, S. P., & Pugh, E. N. (2007). Evolution of the vertebrate eye: opsins, photoreceptors, retina and eye cup. *Nature Reviews Neuroscience*, *8*(12), 960-976.

Land MF, and Fernald RD (1992) The Evolution of Eyes. *Annual Review of Neuroscience*, **15**: 1 -29. 1992.

Lang RA (1997). Apoptosis in mammalian eye development: lens morphogenesis, vascular regression and immune privilege. *Cell death and differentiation*, *4*(1), 12-20.

Lapan SW & Reddien PW (2012). Transcriptome analysis of the planarian eye identifies ovo as a specific regulator of eye regeneration. *Cell reports*, *2*(2), 294-307.

Layden MJ and Martindale MQ (2014). Non-canonical Notch siganaling represents and ancestral mechanism to regulate neural differentiation. *Evodevo,* 5(1), 30.

Lee PN, Callaerts P, de Couet HG, & Martindale MQ (2003). Cephalopod Hox genes and the origin of morphological novelties. *Nature*, *424*(6952), 1061-1065.

Livesey FJ, and Cepko CL (2001). Vertebrate neural cell-fate determination: lessons from the retina. *Nature Reviews Neuroscience*, **2**(2), 109-118.

Love MI, Huber W, and Anders S (2014). Moderated estimation of fold change and dispersion for RNA-seq data with DESeq2. *Genome Biol*, *15*(12), 550.

Marthy HJ (1973). An experimental study of eye development in the cephalopod Loligo vulgaris: determination and regulation during formation of the primary optic vesicle. *Journal of embryology and experimental morphology*, *29*(2), 347-361.

Meyer E, Aglyamova GV, Wang S, et al. (2009). Sequencing and de novo analysis of a coral larval transcriptome using 454 GSFlx. *BMC genomics*, *10*(1), 219.

Meyer E, Logan TL, and Juenger TE (2012). Transcriptome analysis and gene expression atlas for Panicum hallii var. filipes, a diploid model for biofuel research. *The Plant Journal*, *70*(5), 879-890.

Naef, A. (1928). Die Cephalopoden (Embryologie). *Fauna Flora Golf Neapel*, *35*(2), 1-357.

Navet S, Andouche A, Baratte S, and Bonnaud L (2009). Shh and Pax6 have unconventional expression patterns in embryonic morphogenesis in Sepia officinalis (Cephalopoda). *Gene Expression Patterns*, *9*(7), 461-467.

Nilsson DE (2004). Eye evolution: a question of genetic promiscuity. *Current opinion in neurobiology*, *14*(4), 407-414.

Nilsson DE (2013). Eye evolution and its functional basis. *Visual Neuroscience*. **30** (1-2):5-20.

Oakley TH, Speiser DI (2015). How complexity originates: The evolution of animal eyes. *bioRxiv,* 017129.

Ohata S, Aoki R, Kinoshita S, Yamaguchi M, Tsuruoka-Kinoshita S, Tanaka H, ... & Okamoto H (2011). Dual roles of Notch in regulation of apically restricted mitosis and apicobasal polarity of neuroepithelial cells. *Neuron*, *69*(2), 215-230.

Oigo H, Ochi H, Reza HM, Yasuda K (2012) Transcription factors involved in lens development from the preplacodal ectoderm. *Developmental Biology* **363**: 333-347

Piatigorsky J (2003). Gene sharing, lens crystallins and speculations on an eye/ear evolutionary relationship. *Integrative and comparative biology*, *43*(4), 492-499.

Piatigorsky J (2007). *Gene sharing and evolution: The diversity of protein functions* (p.1). Cambridge MA: Harvard University Press.

Peyer SM, Pankey MS, Oakley TH, and McFall-Ngai MJ (2014). Eye-specification genes in the bacterial light organ of the bobtail squid Euprymna scolopes, and their expression in response to symbiont cues. *Mechanisms of development*, *131*, 111-126.

Quiring R, Walldorf U, Kloter U, and Gehring WJ. (1994) Homology of the eyeless gene of Drosophila to the Small eye gene in mice and Aniridia in humans. *Science* **265** (5173), 785-789.

von Salvini-Plawen L, Mayr E (1977) On the evolution of photoreceptors and eyes. *Evol. Biol. 10, 207–263*

Schnitzler CE, Pang K, Powers ML, et al. Genomic organization, evolution, and expression of photoprotein and opsin genes in *Mnemiopsis leidyi*: a new view of ctenophore photocytes. *BMC Biology*. 2012.

Schwarz, F Cercconi G, Bernier N, et al. (2000) Spatial specification of mammalian eye territories by reciprocal transcriptional repression of Pax2 and Pax6 *Development* **127**: 4325-4334.

Shigeno S, Parnaik R, Albertin CB, and Ragsdale CW (2015). Evidence for a cordal, not ganglionic, pattern of cephalopod brain neurogenesis. *Zoological Letters*, *1*(1), 1-13.

Simakov, O., Marletaz, F., Cho, S. J., Edsinger-Gonzales, E., Havlak, P., Hellsten, U., ... & Rokhsar, D. S. (2013). Insights into bilaterian evolution from three spiralian genomes. *Nature*, *493*(7433), 526-531.

Szaro BG, Pan HC, Wa J, and Battey J (1991). Squid low molecular weight neurofilament proteins are a novel class of neurofilament protein. A nuclear lamin-like core and multiple distinct proteins formed by alternative RNA processing. *Journal of Biological Chemistry*, *266*(23), 15035-15041.

Tomarev SI, Callaerts P, Kos L et al. (1997) Squid Pax-6 and eye development. *Proceedings of the National Academy of Sciences* **94** (6) 2421-2426.

Tomarev SI (1997). Pax-6, Eyes absent, and Prox 1in eye development. *Int. J. Dev. Biol*, *41*, 835-842.

Tomita, K, Ishibashi M, Nakahara K, Ang SL, Nakanishi S, Guillemot F, and Kageyama R (1996). Mammalian hairy and Enhancer of split homolog 1 regulates differentiation of retinal neurons and is essential for eye morphogenesis. *Neuron*, **16**(4), 723-734.

Tomlinson A, and Ready DF (1987). Neuronal differentiation in the Drosophila ommatidium. *Developmental biology*, *120*(2), 366-376.

Vale RD, Schnapp BJ, Reese TS and Sheetz MP (1985a). Movement of organelles along filaments dissociated from the axoplasm of the squid giant axon. *Cell*, **40**(2), 449-454.

Vale RD, Schnapp BJ, Reese TS, and Sheetz MP (1985b). Organelle, bead, and microtubule translocations promoted by soluble factors from the squid giant axon. *Cell*, **40**(3), 559-569.

Wagner GP (2014) *Homology, Genes, and Evolutionary Innovation* (Princeton Univ Press, Princeton).

West JA, Sivak JG, Pasternak J, and Piatigorsky J (1994). Immunolocalization of S-crystallins in the developing squid (Loligo opalescens) lens. *Developmental dynamics*, *199*(2), 85-92.

West JA, Sivak JG, and Doughty MJ (1995). Microscopical evaluation of the crystalline lens of the squid (Loligo opalescens) during embryonic development. *Experimental eye research*, *60*(1), 19-35.

Wollesen T, McDougall C, Degnan BM, and Wanninger A (2014). POU genes are expressed during the formation of individual ganglia of the cephalopod central nervous system. *EvoDevo*, *5*(1), 41.

Yamamoto, M. (1985a). Ontogeny of the visual system in the cuttlefish, Sepiella japonica. I. Morphological differentiation of the visual cell. *Journal of Comparative Neurology*, *232*(3), 347-361.

Yamamoto, M., Takasu, N., & Uragami, I. (1985b). Ontogeny of the visual system in the cuttlefish, Sepiella japonica. II. Intramembrane particles, histofluorescence, and electrical responses in the developing retina. *Journal of Comparative Neurology*, *232*(3), 362-371.

Yamamoto M, Shimazaki Y, and Shigeno S (2003). Atlas of the embryonic brain in the pygmy squid, Idiosepius paradoxus. *Zoological science*, *20*(2), 163-179.

Yoshida MA, Yura K, and Ogura A (2014). Cephalopod eye evolution was modulated by the acquisition of Pax-6 splicing variants. *Scientific reports*, *4*.

Young JZ (1962a). The retina of cephalopods and its degeneration after optic nerve section. *Philosophical Transactions of the Royal Society B: Biological Sciences*, *245*(718), 1-18.

Young JZ (1962b). The optic lobes of Octopus vulgaris. *Philosophical Transactions of the Royal Society B: Biological Sciences*, *245*(718), 19-58.

Young JZ (1971). Anatomy of the Nervous System of Octopus vulgaris.
Nixon, M., & Young, J. Z. (2003). *The brains and lives of cephalopods*. Oxford University Press.

Zonana HV (1961) Fine Structure of the squid Retina. *Bulletin of the Johns Hopkins Hospital*, **109**: 185-205